NASA CONTRACTOR
REPORT

NASA CR-150114

DETERMINATION OF BURNING AREA AND PORT VOLUME IN COMPLEX BURNING REGIONS OF A SOLID ROCKET MOTOR

By J. A. Kingsbury
Northrop Services, Inc.
P. O. Box 1484
Huntsville, Alabama 35807

February 1977

Prepared for

NASA - GEORGE C. MARSHALL SPACE FLIGHT CENTER
Marshall Space Flight Center, Alabama 35802

TECHNICAL REPORT STANDARD TITLE PAGE

1 REPORT NO.	2 GOVERNMENT ACCESSION NO.	3 RECIPIENT'S CATALOG NO.
NASA CR-150114		

4 TITLE AND SUBTITLE	5 REPORT DATE
Determination of Burning Area and Port Volume in Complex Burning Regions of a Solid Rocket Motor	February 1977
	6 PERFORMING ORGANIZATION CODE
7. AUTHOR(S)	8. PERFORMING ORGANIZATION REPORT #
J. A. Kingsbury	TR-1726
9 PERFORMING ORGANIZATION NAME AND ADDRESS	10. WORK UNIT NO.
Northrop Services, Inc. P. O. Box 1484 Huntsville, Alabama 35807	11. CONTRACT OR GRANT NO. NAS8-31644
12 SPONSORING AGENCY NAME AND ADDRESS	13 TYPE OF REPORT & PERIOD COVERED
National Aeronautics and Space Administration Washington, D. C. 20546	Contractor Report
	14 SPONSORING AGENCY CODE

15. SUPPLEMENTARY NOTES

This work was done under the sponsorship of the Marshall Space Flight Center, Science and Engineering Directorate. Technical Coordinator: J. R. Redus.

16. ABSTRACT

An analysis of the geometry of the burning in both star-cylindrical port interface regions and regions of partially inhibited slots is presented. Some characteristic parameters are defined and illustrated. Methods are proposed for calculating burning areas which functionally depend only on the total distance burned. According to this method, several points are defined where abrupt changes in geometry occur, and these are tracked throughout the burn. Equations are developed for computing port perimeter and port area at pre-established longitudinal positions. Some common formulas and some newly developed formulas are then used to compute burning surface area and port volume. Some specific results are presented for the solid rocket motor committed to the Space Shuttle project.

17. KEY WORDS	18. DISTRIBUTION STATEMENT
	Unclassified-Unlimited H. E. Thomason Dir, Systems Anal & Integration Lab

19. SECURITY CLASSIF. (of this report)	20. SECURITY CLASSIF. (of this page)	21. NO. OF PAGES	22 PRICE
Unclassified	Unclassified	114	NTIS

FOREWORD

This report presents work performed by Northrop Services, Inc., Huntsville, Alabama, while under contract to the Science and Engineering Directorate, Marshall Space Flight Center (NAS8-31644). This task was conducted in response to the requirements of Schedule Order No. 1.7.5, Amendment 1, Task No. 3. Technical contact for this effort was Mr. J. R. Redus, EL24.

ACKNOWLEDGEMENT

Contributions to the development of this geometry model were made by Mr. J. C. Winkler, whose patience and assistance were invaluable to the author.

TABLE OF CONTENTS

LIST OF ILLUSTRATIONS

LIST OF ILLUSTRATIONS (Concluded)

Section I

INTRODUCTION

This document represents the culmination of a theoretical investigation into the geometry changes taking place during the burning of a solid rocket motor--especially in the regions of atypical burning surfaces. The final destination of these results is intended to be the Boeing developed SRB-II solid rocket performance prediction model, and is thus a method of freeing that model from excessive geometric input and a reliance on tables of burn area as a function of burn distance. It is, however, a general geometric codification and can be of valuable use in other models as well.

The performance of a solid rocket motor (SRM) with a given propellant, that is, its internal pressure-time history, is largely dependent upon its internal geometry. Since the propellant itself is a solid, several basic shapes can be selected for the interior port. The naming for each configuration is based on the geometrical figure inscribed by the port on a plane taken perpendicular to the motor (longitudinal) axis. Figure 1-1 presents the basic shapes in common use today, along with the name and abbreviation (if one exists) associated with each.

In response to the particular circumstances surrounding the SRM committed to the Space Shuttle program, it was decided that a slotted cone and cylindrically perforated (CP) grain combination would suffice. The internal pressure in the SRM is directly dependent on the total amount of propellant surface area exposed to active burning. The star (here, the terms slotted cone and star are used interchangeably) configuration at the head end (Figure 1-2) will allow a large surface area to be exposed at ignition, producing a rapid build-up of internal pressure and thus a high thrust. Since the propellant there will burn so rapidly, it is the general case that this particular region is consumed long before the rest of the propellant in the motor. The CP section then takes over as the prime gas generating region, not too long after ignition.

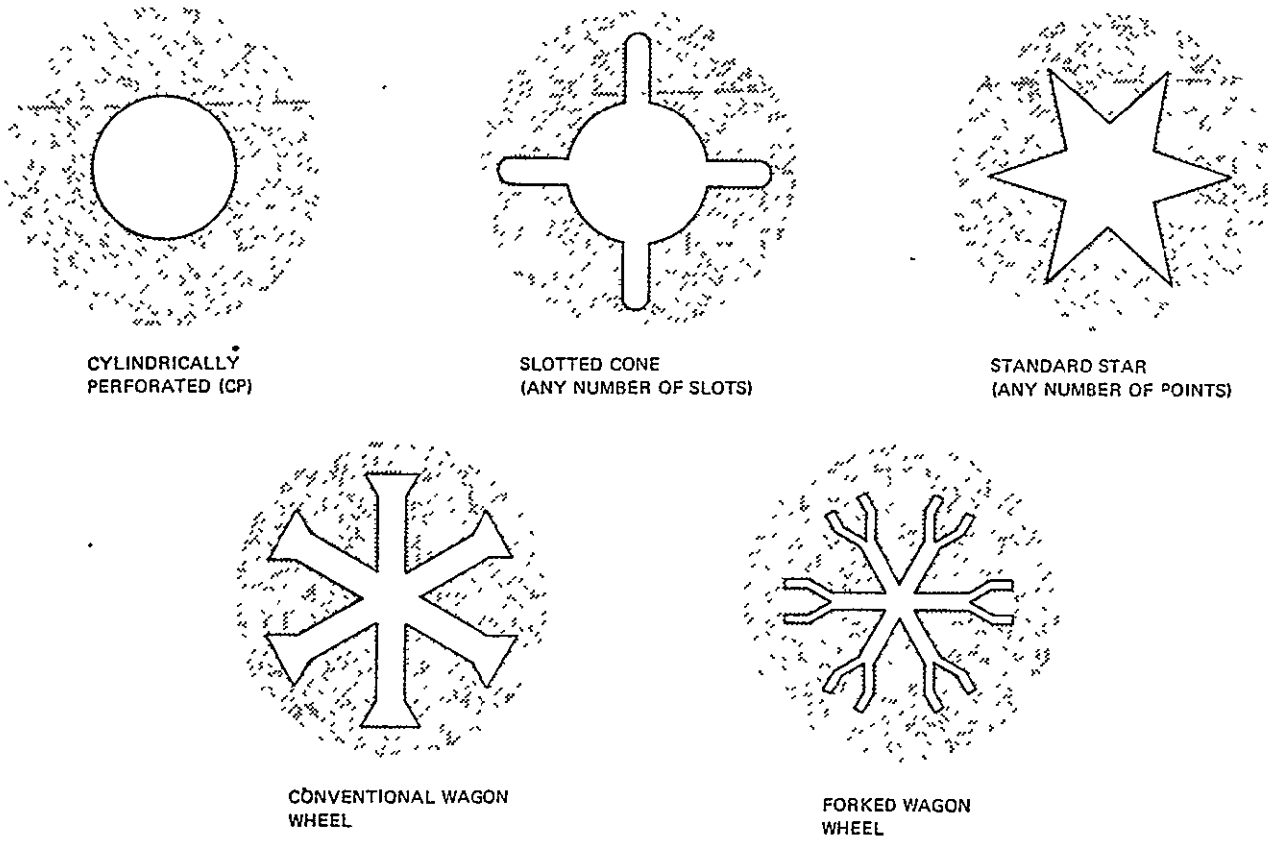

Figure 1-1. PORT CONFIGURATIONS IN COMMON USE

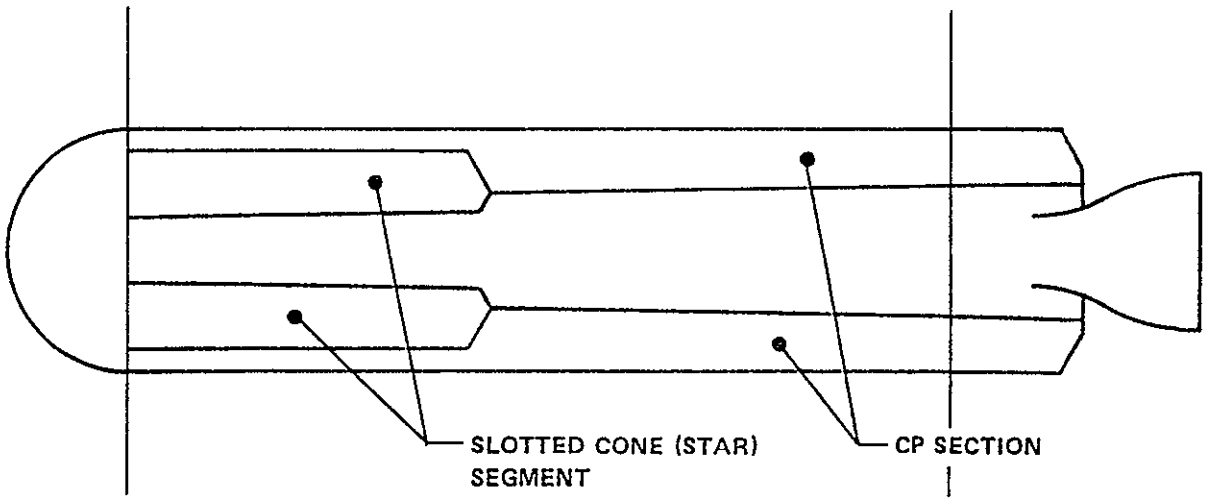

Figure 1-2. CONFIGURATION LOCATION

The analytical model described here was specifically constructed for the slotted cone and cylindrically perforated combination of cross sectional geometry. The number of slots in the slotted cone remains variable. Modeling a standard star is based only on proper variable assignments and is handled in the same way as the slotted cone. For this reason, as indicated above, the two will be called "star", because there is no analytic difference.

Typical surface area traces for a slotted cone region and a CP region are given in Figure 1-3.

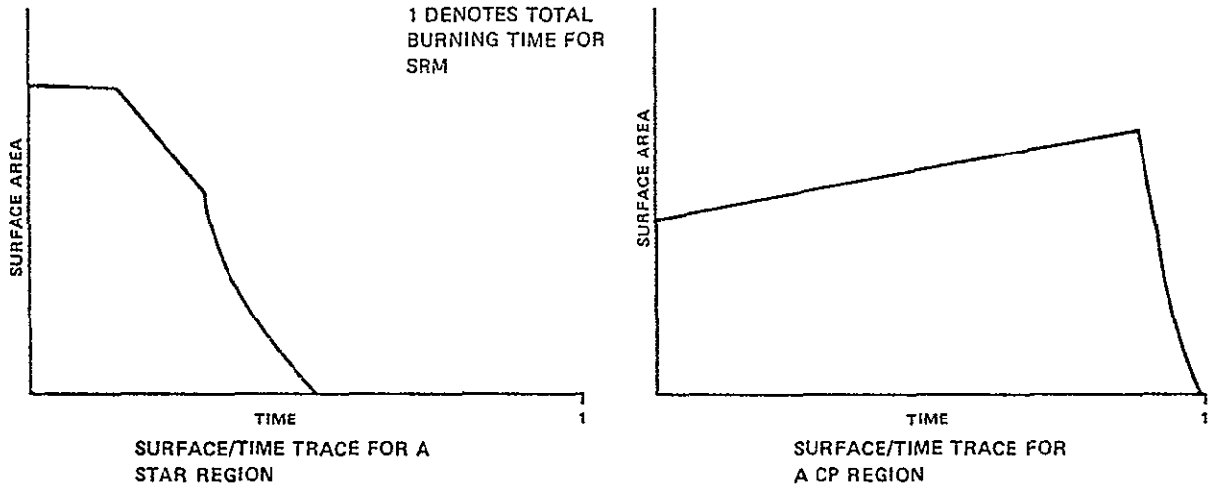

Figure 1-3. SURFACE AREA VERSUS TIME TRACES IN DIFFERENT MOTOR SEGMENTS

Notice that the star segment is regressive, that is, the exposed surface area decreases rapidly with time. Hence, its influence during the burn diminishes. Just the opposite is true of the CP region. Its burning surface increases during the burn, and its influence becomes great. For this reason, the burning in a CP region is termed progressive. In passing, it is pointed out that the pressure trace is directly related to a summation of the two traces in Figure 1-3.

Large SRM's, such as those on the Space Shuttle, require casting the propellant in several sections, called casting segments; and these, in turn, are joined together (usually at the launch site) to form the motor. The gaps

in the propellant caused by the joining of these casting segments are called slots. These slots present new surfaces to the burning.

In order to "program" the burning of a solid rocket motor to conform to a given thrust-time history, these slots may or may not have to be inhibited to some degree to eliminate or control these new burning surfaces. A non-burning ablative material can be placed against the propellant bounding a slot to control these otherwise bothersome areas. If no burning is wanted in this region, the propellant is covered completely with the inhibitor. If some burning is needed, the inhibitor can be built up to leave an annulus-shaped region bare to the burning (Figure 1-4). In such a region, burning not only takes place radially, but also longitudinally.

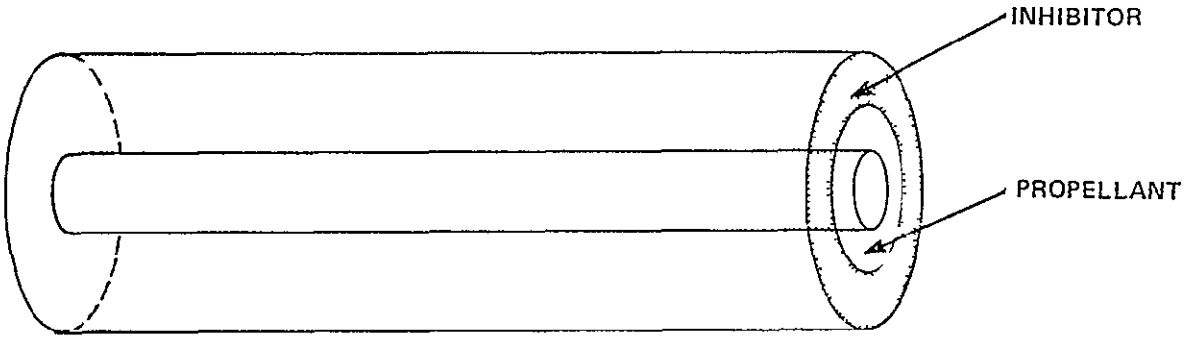

Figure 1-4. INITIAL PROPELLANT FACE IN A PARTIALLY INHIBITED SLOT

In most regions of an SRM, burning takes place in the radially outward direction. Special regions do exist in some motors where the burning takes place not only radially outward, but possibly in other directions as well. The just described slot burning is an example. These are the regions in which special care must be taken with any model. The two- and sometimes three-dimensional regression of the grain leads to a complex geometrical configuration. It is for these configurations that this geometric model was developed.

The following discussion progresses along well defined lines. Each region of a motor (exclusive of the head dome region and the aft dome region) will be handled in turn in its own paragraph. The general progress is from the simple to the difficult, in hopes that both geometrical intuition and analytical sophistication can be fostered.

The first three sections of the analytical model deal, respectively, with the CP, star, and partially inhibited slot regions. The final, and by far the most involved, section describes the region of transition between the star and CP segments, where burning proceeds in three dimensions. A section of verbal description and general mathematics precedes the analytic model, and more mathematics of a less influential nature is presented in two appendixes. Continuity can be maintained by passing over the mathematics section if the equations in later sections are to be accepted without argument.

Some results for the Shuttle-committed SRM grain design are given in Appendix C.

Section II

SOLID ROCKET GEOMETRY

This section gives a verbal description of the burning of the propellant in an SRM. Also included is an extensive description dealing specifically with the mathematical methods which will be used to model the grain regression. The notions of increment dividing planes and reference planes are introduced, and the philosophical differences between the two are explored.

Care should be taken to absorb paragraph 2.4 which deals with the volume and surface area formulas used within the model. Those formulas, along with many others within the body of this work, have been developed from information taken from References 1 and 2 (see, however, Appendix A).

2.1 ATYPICAL GEOMETRY AND GRAIN REGRESSION

Any portion of the grain which is not interior to a CP or star segment is likely to develop an atypical (complex) geometry during the burn. These areas are characterized by the fact that the geometry makes a radical change; for example, a portion of the CP becoming star shaped. In this sense, regions of complex geometry occur in the grain surrounding a partially inhibited slot and in the region of transition between star and CP. The portion of the motor which is uniformly star shaped does not, for example, constitute a region of complex geometry, since a six pointed star remains that until the burning has consumed the entire region.

Even though the star section is not, per se, a region of atypical geometry, the region has been mathematically modeled here in order to be compatible with the three-dimensional burning taking place in the star to CP transition region. This also requires a new modeling of the burning in the CP region. In so doing, the entire surface of the grain can be handled with analytical methods, through functions depending only on total distance burned.

Figure 2-1 shows the geometry changes which can take place in different regions of the motor. Together with those shown, the transition between star

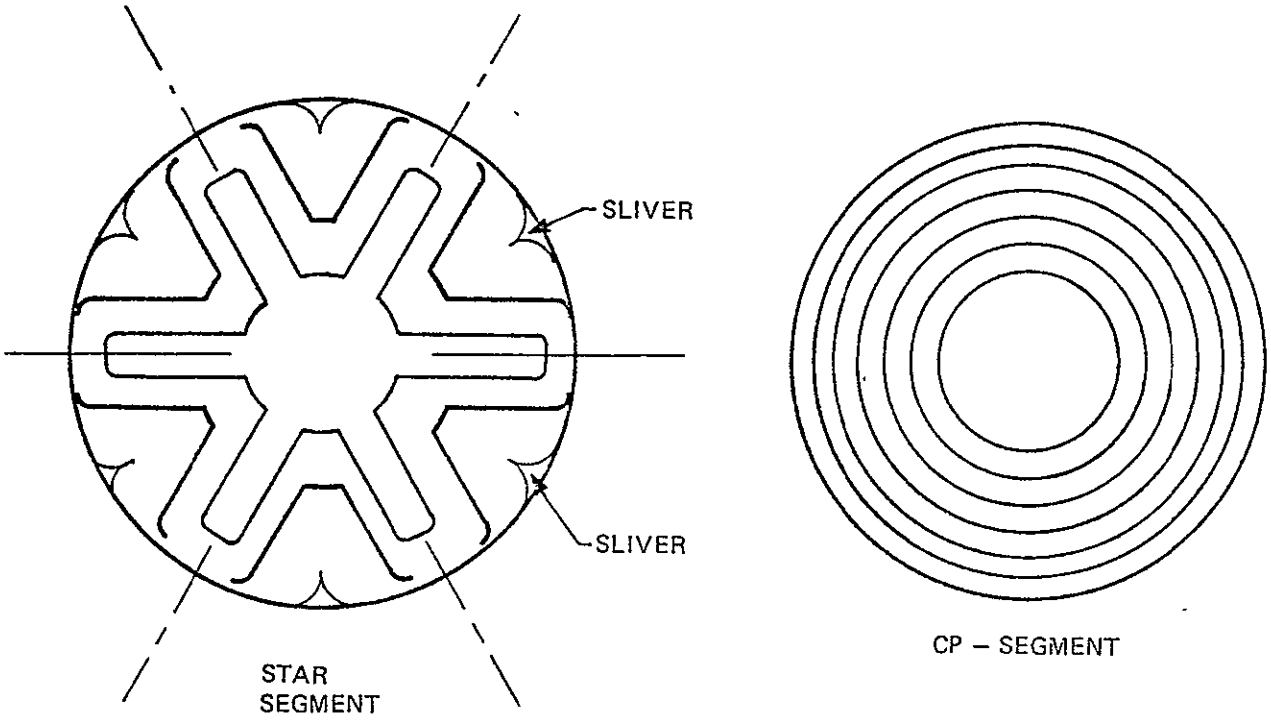

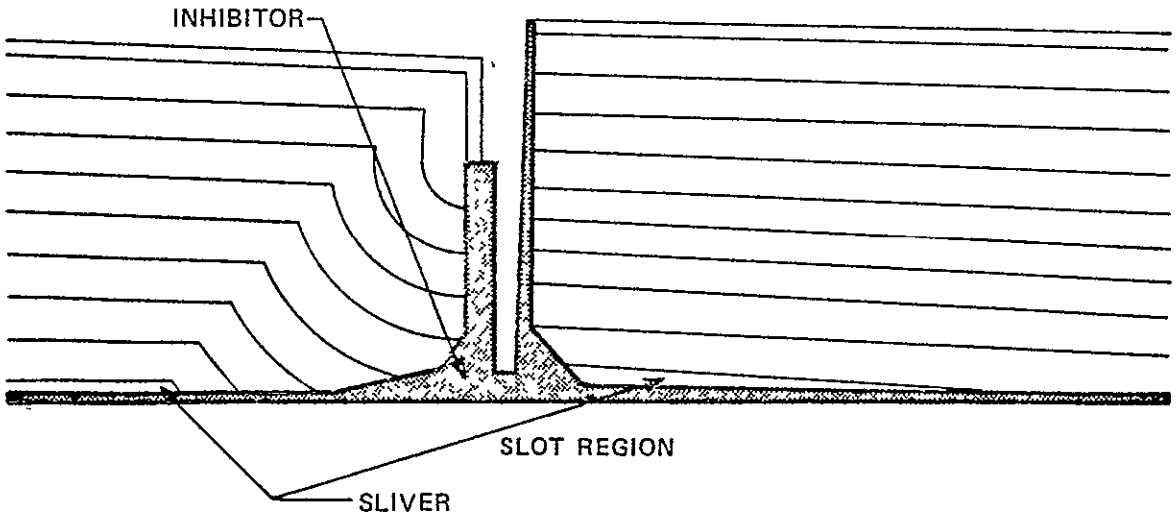

Figure 2-1. GRAIN REGRESSIONS IN DIFFERENT PORT CONFIGURATIONS

and CP segments offers a challenging exercise in planar renditions of spacial regressions. Some three-dimensional offerings are given later in the theoretical modeling of that region (Section V). Three basic assumptions govern the burning and produce renditions like those in Figure 2-1:

1. Propellant burning during ignition and steady state occurs along the outward normal at each point of the port-grain interface.
2. Initial arcs of propellant reaching into the port progress to points.
3. Outward angles progress to arcs.

The first assumption provides the vehicle for the analytical description, while the second two provide means by which analytical discontinuities, whether real or potential, may be handled.

Pencil and paper grain regressions are made by taking the original cross-sectional configuration and drawing curves toward the case wall at equal distances from the initial curve. It is not unreasonable, then, to have assumptions like 2 and 3 above.

Before turning to the analytical description itself, it will be of interest in later theoretics to go through some general, but useful, developments. The next section is devoted to this.

2.2 GENERAL MATHEMATICS

It will be of interest further on to have a few general notions adequately developed. The information contained in this subsection will be called when needed by appropriate names posted in this paragraph. This paragraph may be passed over without disruption of reading continuity, except for the definitions herein presented.

Two mathematical notions share equally in importance in this geometry model. The first is in response to seeking what happens when families of concentric circles intersect families of parallel lines, and the second is a method for analytically describing familiar shapes in space.

Consider first the situation appearing in Figure 2-2. On the one hand, there is a circle centered at point (a, b) in the x-y Cartesian coordinate system, and on the other, a straight line, whose equation is given.

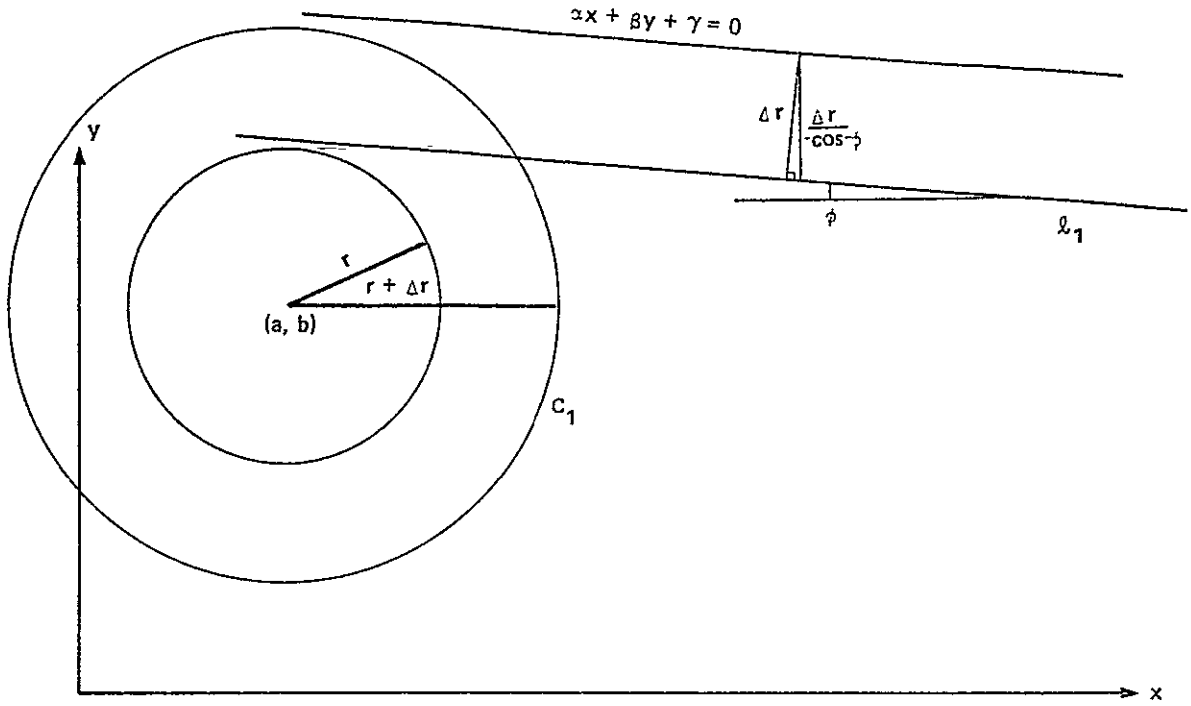

Figure 2-2. DEFINITION OF A CIRCLE-LINE PAIR

Assume that the radius of the circle grows at a specified rate, while the original line moves in the direction of the circle center at the same rate. A circle-line pair is defined to be the circle centered at (a, b) with radius $r + \Delta r$ along with the line which has moved Δr distance from the original line, in the direction indicated. In this respect, the circle C_1 and the line ℓ_1 of Figure 2-2 represent a circle-line pair. The distance Δr is taken to be any real number such that $\Delta r \geq -r$.

Considering only the points of intersection (if extant) of circle-line pairs for all $\Delta r \geq -r$, what is the functional analog of this curve? (Clearly a curve results because of the continuous nature of the movement.)

The original circle has equation

$$(x - a)^2 + (y - b)^2 = r^2 \quad .$$

and the original line has equation

$$\alpha x + \beta y + \gamma = 0.$$

Suppose, at one point, the radius of the circle has grown to $r + \Delta r$. The new circle has equation

$$(x - a)^2 + (y - b)^2 = (r + \Delta r)^2 \quad .$$

If ϕ represents the angle of inclination of the line with respect to the x-axis (that is, $\phi = \arctan(\alpha/\beta)$), then the new line has equation

$$\alpha x + \beta y + \gamma + \Delta r/\cos\phi = 0$$

Thinking of the above two equations as equations in three variables (x, y, Δr), one variable in the circle equation can be eliminated using the line equation. For example, eliminate Δr. Solving the line for this quantity, obtain

$$\Delta r = -(\alpha x + \beta y + \gamma)\cos\phi$$

or

$$\Delta r = -(\bar{\alpha} x + \bar{\beta} y + \bar{\gamma})$$

where $\bar{\alpha} = \alpha\cos\phi$, and so on. Substitute this value into the circle to obtain

$$(x - a)^2 + (y - b)^2 = (r - (\bar{\alpha} x + \bar{\beta} y + \bar{\gamma}))^2 \quad .$$

Expanding and rearranging the form

$$(1 - \bar{\alpha}^2)\, x^2 - 2\overline{\alpha\beta}\, xy + (1 - \bar{\beta}^2)\, y^2 - 2(a - r\bar{\alpha} + \overline{\alpha\gamma})\, x$$
$$- 2(b - r\bar{\beta} + \overline{\beta\gamma})\, y + a^2 + b^2 - r^2 + 2r\bar{\gamma} - \bar{\gamma}^2 = 0 \quad \ldots \quad (2\text{-}1)$$

is obtained. If these assignments are made:

$$A = 1 - \bar{\alpha}^2 \qquad D = -2(a - r\bar{\alpha} + \overline{\alpha\gamma})$$

$$B = -2\overline{\alpha\beta} \qquad E = -2(b - r\bar{\beta} + \overline{\beta\gamma})$$

$$C = 1 - \bar{\beta}^2 \qquad F = a^2 + b^2 - r^2 + 2r\bar{\gamma} - \bar{\gamma}^2$$

the equation has the form

$$Ax^2 + Bxy + Cy^2 + Dx + Ey + F = 0 \quad .$$

Notice that this is the general second degree equation. It then represents either a hyperbola, a parabola, or an ellipse, depending on $B^2 - 4AC > 0$, $= 0$, or < 0, respectively. But

$$B^2 - 4AC = 4\,\bar{\alpha}^2\,\bar{\beta}^2 - 4(1 - \bar{\alpha}^2)\,(1 - \bar{\beta}^2)$$

or

$$B^2 - 4AC = 4\,(\bar{\alpha}^2 + \bar{\beta}^2 - 1)$$

The conditions on $B^2 - 4AC$ are then translated into conditions on the line coefficients $\bar{\alpha}$ and $\bar{\beta}$. These results are summarized as:

Hyperbola: $B^2 - 4AC > 0$

$$\bar{\alpha}^2 + \bar{\beta}^2 > 1$$

Parabola: $B^2 - 4AC = 0$

$$\bar{\alpha}^2 + \bar{\beta}^2 = 1$$

Ellipse: $B^2 - 4AC < 0$

$$\bar{\alpha}^2 + \bar{\beta}^2 < 1$$

The family of points arising from the intersection of circle-line pairs represents a general second order polynomial in two variables. Specifically, this second order equation is a hyperbola, parabola, or ellipse depending only on the location of the pair $(\bar{\alpha}, \bar{\beta})$ with respect to the unit circle--"outside," "on," or "inside" can be translated as "hyperbola," "parabola," or "ellipse," respectively.

These particular shapes play important supportive roles during the modeling of a burning SRM. It will be remembered that the initial grain surface, for the most part, is piecewise linear. At abrupt angular changes, burning causes arcs to emerge, which grow at the burning rate. These circular arcs, then, are adjacent to linear regions of grain surface; and during burning, the point of intersection of the grain surface with the formed circular arc causes one of these second-degree equations to become "law of motion," used to track that point of intersection. Predictions can then be made as to the location of a circle-line pair intersection at important times, such as end of burn. For that reason, such second-degree formulas will be termed "burn-back" curves--a burn-back parabola, burn-back hyperbola, or burn-back ellipse.

Now, turn to the other major notion--that of finding an analytical formula for familiar geometric objects in three space. Here, a powerful method of

advanced calculus* is used to obtain specific equations. The method ultimately rests only on the fact that in space, there are two planes which intersect at right angles.

Two examples will serve to illustrate the method. The first develops the equation of a specific torus in space; the other develops the equation of a cylinder in space which leans into the first octant with specified angles of inclination.

EXAMPLE 1: TORUS

In an x-y-z Cartesian coordinate system (Figure 2-3), assume that a circle centered at (a,b,0) of radius r is revolved about the line x = c. The circle $(x - a)^2 + (y - b)^2 = r^2$ is called the base curve; the other is called the generator curve. The generator is a circle centered at (c,b,0) of radius a - c. Revolve the circle as described to obtain a shape like that in Figure 2-4.

The base circle can be expressed as a multiple valued function of y as

$$x = f(y) = \pm \sqrt{r^2 - (y-b)^2} + a$$

Choose a point P_o with coordinates ($x_o = f(y_o)$, y_o, 0) on the base circle. Choose an arbitrary point P_1 (x,y,z) on the circle that P_o makes when revolved about x = c. Since the revolution takes place parallel to the x-z plane, then $y_o = y_1$; x_1, and z_1 satisfy the circle equation

$$(x_1 - c)^2 + z_1^2 = (x_o - c)^2$$

Substituting appropriate quantities, obtain:

$$(x_1 - c)^2 + z_1^2 = (f(y_o) - c)^2$$

$$(x_1 - c)^2 + z_1^2 = (f(y_1) - c)^2$$

$$(x_1 - c)^2 + z_1^2 = \left(\pm \sqrt{r^2 - (y_1 - b)^2} + a - c \right)^2$$

See Reference 2, Pages 615-620.

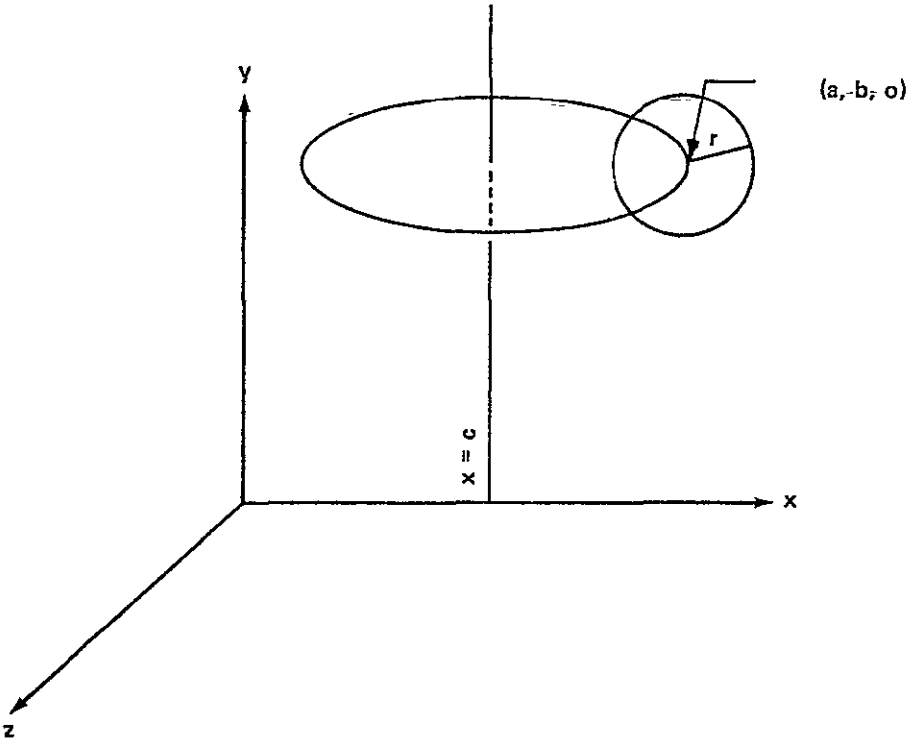

Figure 2-3. GENERATION OF A TORUS

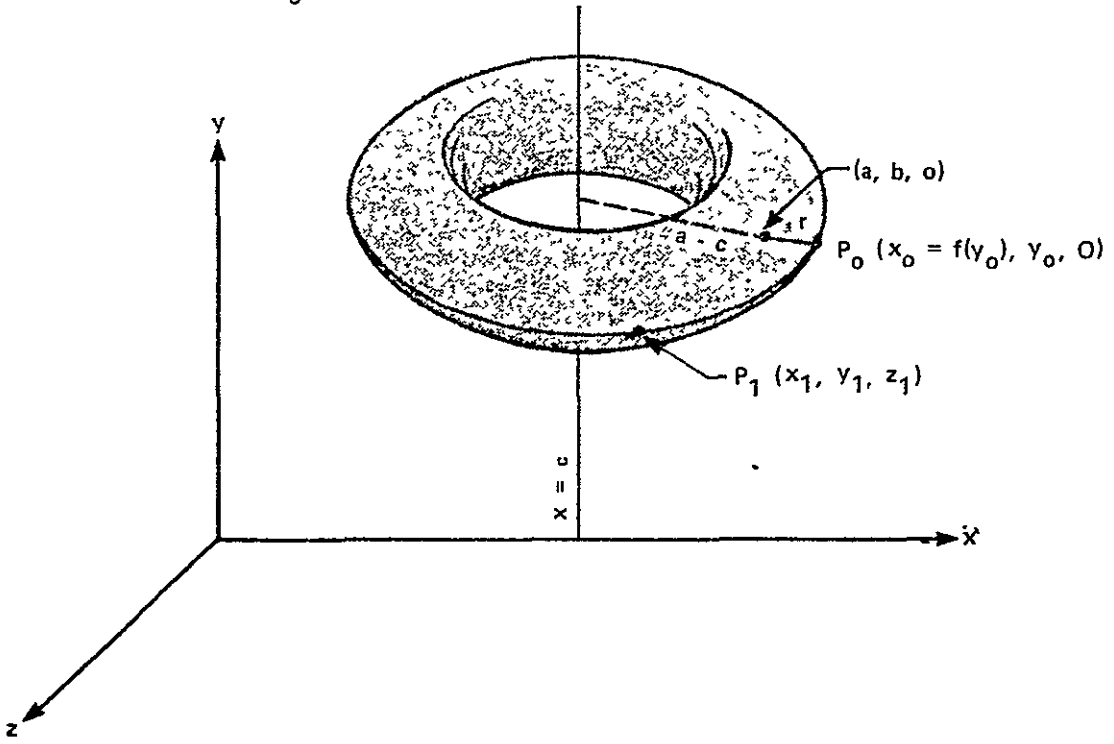

Figure 2-4. GENERATED TORUS

There is nothing magical about the subscripts, and they can be dropped to obtain

$$(x - c)^2 + z^2 = (\pm \sqrt{r^2 - (y - b)^2} + a - c)^2$$

which is the appropriate formula for the torus. Choice of the + or - sign separately yields the upper and lower regions, respectively. In summary, the equation of a torus with generator curve, circle centered at (c,b,0) radius a - c and base curve: circle centered at (a,b,0) with radius r, is given by

$$(x - c)^2 + z^2 = (\pm \sqrt{r^2 - (y - b)^2} + a - c)^2$$

EXAMPLE 2: AN OFFSET CYLINDER

Consider a cylinder as drawn in Figure 2-5, whose centerline rests in the x-z plane.

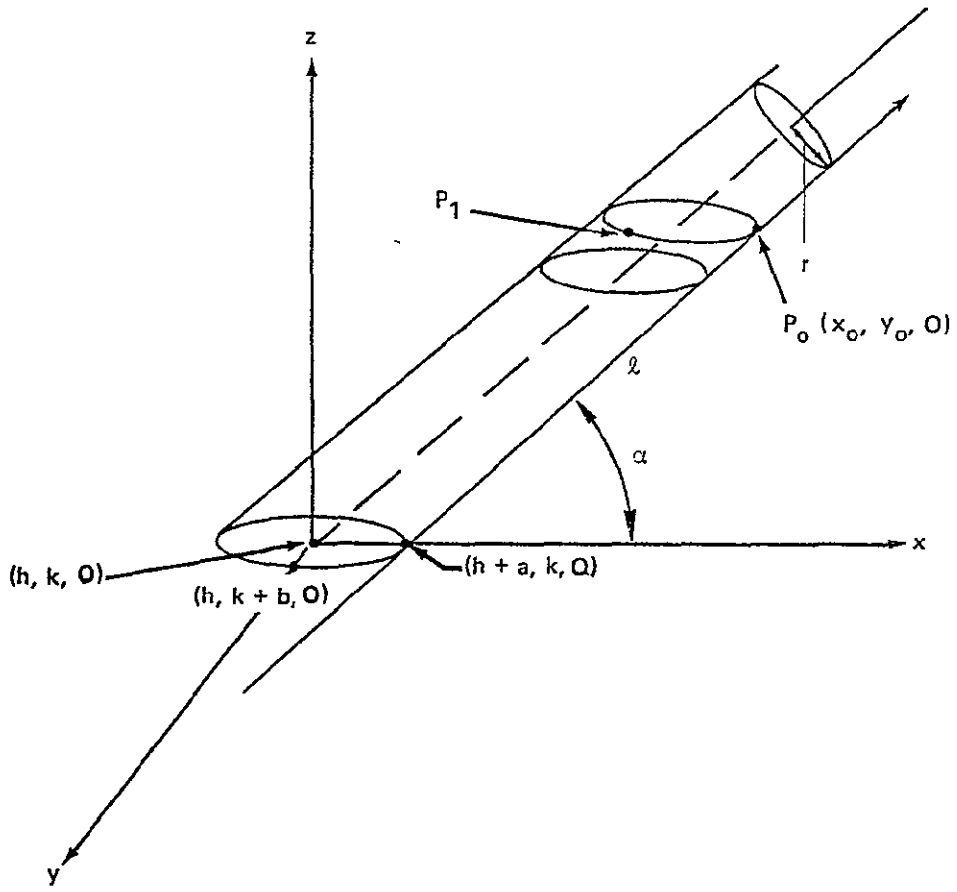

Figure 2-5. GENERATION OF AN ASKEW CYLINDER

This cylinder will be described first, then the figure will be rotated into the first octant to obtain final resultant offset.

Using the same methods as in the last example, the base curve is a straight line indicated by ℓ, while the generator curve (the generator curve must be in the x-y plane in Figure 2-5) is an ellipse given by

$$\frac{(x - h)^2}{a^2} + \frac{(y - k)^2}{b^2} = 1$$

and has the following attributes:

$a = r/\sin\alpha$

$b = r$

$e = \cos\alpha$, e = eccentricity

Next, choose a point P_o $(x_o, y_o, 0)$ on the base curve. The base curve has equation

$$\begin{cases} x = x_o + t\cos\alpha \\ y = y_o = b\sqrt{1 - \left(\frac{x_o - h}{a}\right)^2} + k \quad \ldots, \text{ all real numbers, } t. \\ z = t\sin\alpha \end{cases}$$

Since x and z are the only two equations containing t, t can be eliminated as

$$x = x_o + t\cos\alpha$$

$$z = t\sin\alpha$$

$$t = z/\sin\alpha = \frac{x - x_o}{\cos\alpha}$$

so that

$$(x - x_o)\sin\alpha = z\cos\alpha$$

or

$$z = (x - x_o)\tan\alpha$$

But

$$x_o = a\sqrt{1 - \left(\frac{y_o - k}{b}\right)^2} + h, \; y = y_o$$

so

$$z = (x - a\sqrt{1 - \left(\frac{y - k}{b}\right)^2} - h)\ \tan\alpha$$

or

$$\left(\frac{y - k}{b}\right)^2 + \left(\frac{z\cot\alpha}{a} - \frac{x - h}{a}\right)^2 = 1 \ \ldots$$

Notice that when $z = 0$, there is the cross section (trace)

$$\left(\frac{y - k}{b}\right)^2 + \left(\frac{x - h}{a}\right)^2 = 1$$

which is the generator line. When $\alpha = 90°$, then the right circular cylinder is obtained, given by

$$(y - k)^2 + (x - h)^2 = a^2 = b^2$$

Taking a plane parallel to the x-y plane at $z = c$, there is

$$\left(\frac{y - k}{b}\right)^2 + \left(\frac{x - h - c\cot\alpha}{a}\right)^2 = 1$$

which is an ellipse centered at $(h + c\cot\alpha, k, c)$ with eccentricity as described.

Hence, the above formula is truly that of the described cylinder. Next, twist the cylinder in the positive y-direction to move it into the first octant (Figure 2-6).

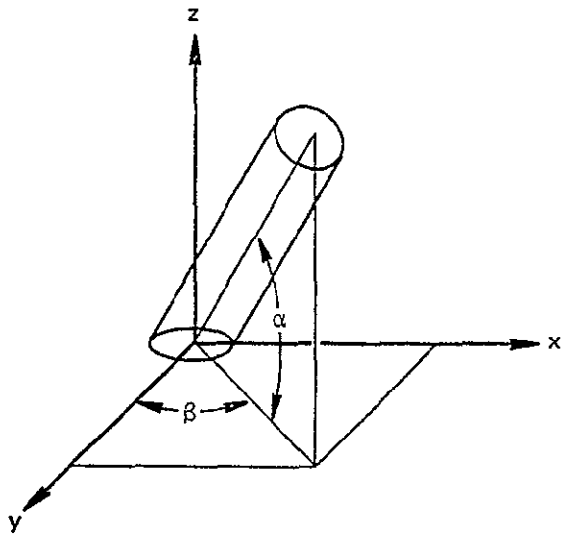

Figure 2-6. AN OFFSET CYLINDER

It is easy to see that equation (2-1) must be updated to the form

$$\left(\frac{y - (k + z\cos\beta\cot\alpha)}{b}\right)^2 + \left(\frac{x - (h + z\sin\beta\cot\alpha)}{a}\right)^2 = 1 \qquad (2\text{-}2)$$

Notice if $\alpha = 90°$, there is

$$\left(\frac{y - k}{b}\right)^2 + \left(\frac{x - h}{a}\right)^2 = 1 \qquad a = b$$

If $\beta = 90°$,

$$\left(\frac{y - k}{b}\right)^2 + \left(\frac{x - (h + z\cot\alpha)}{a}\right)^2 = 1$$

and all things reduce to the last case. The trace in the plane $z = c$ yields

$$\left(\frac{y - (k + c\cos\beta\cot\alpha)}{b}\right)^2 + \left(\frac{x - (h + c\sin\beta\cot\alpha)}{a}\right)^2 = 1$$

which is an ellipse centered at

$$(h + c\sin\beta\cot\alpha,\ k + c\cos\beta\cot\alpha,\ c)$$

namely, a rigid translation of the generator curve to that point.

In summary, it can be stated that the equation of a cylinder skewed from the y-z plane by angle β, and from the x-y plane by angle α, and having radius r must have equation

$$\left(\frac{y - (k + z\cos\beta\cot\alpha)}{b}\right)^2 + \left(\frac{x - (h + z\sin\beta\cot\alpha)}{a}\right)^2 = 1$$

where

$$b = r \qquad a = r/\sin\alpha.$$

For an application of both the cylinder and the torus equation, see the section on modeling the transition region, Section V.

2.3 REFERENCE PLANES AND INCREMENT DIVIDING PLANES

Initial geometry is conveyed to the model by way of a number of reference planes. These are simply planes positioned perpendicular to the centerline of the motor at user-defined intervals. They convey such information as the position along the motor axis from a given reference, initial port radius,

and other data to specify the distinctions between star and CP. These planes are also used to convey insulation thicknesses by specifying the radius from the centerline to the case wall.

Since only a few reference planes are needed to adequately define an internal geometry, it is then the general case in a large motor that these planes are wide apart. An internal ballistics solution using only the reference planes, then, cannot have needed accuracy, so a shrinkage of the world view is necessary. This is accomplished by the device of the increment dividing plane (IDP).

In order to space geometric data closer together than is possible using a small number of reference planes, the increment dividing planes are introduced. Since these are set at positions in the motor by the code, an otherwise lengthy and necessarily redundant list of reference plane geometry input constants is reduced to a bare and necessary minimum.

The increment dividing plane becomes the major vehicle to transmit geometric data to the code. The values at any increment dividing plane include those at reference planes with the addition that on this level, total burn distance is tracked. The increment dividing plane is not a static notion, as is the reference plane, and some increment dividing planes actually change position to track radical changes in geometry.

Information is conveyed to the increment dividing plane level by first positioning each IDP at reasonable intervals between reference planes, making sure that each reference plane position is also occupied by an increment dividing plane. Other values are transmitted to the increment dividing plane using linear interpolation of like variables of the two-reference plane bounding a given IDP and the position of the IDP. At this point, attention is called to the necessity of adequately placing a sufficient number of reference planes along the motor axis to convey important changes in taper and in insulation thickness. The interior grain configuration is guaranteed to change linearly in the areas mentioned, so the prior level of generality is maintained by the use of linear interpolation routines.

After the increment dividing planes have been set and geometry input has been conveyed to this level, the reference planes are discarded, and only serve the code as a repository of information. The dynamic changes in geometry are calculated on the increment dividing plane level, and the reference plane concept is reduced to one of only transmitting initial data. No calculations are ever made on the reference plane level.

Since the planes are perpendicular to the centerline of the motor, the ideas of port fuel perimeter and port area make sense. These are calculated and tracked at each increment dividing plane. With this information at two adjacent IDP's, using volume and surface area formulas yet to be described, the port volume and burning propellant surface area can be calculated. These values represent the ultimate reason for the existence of this model, since these values are, in turn, fed to the internal ballistics calculations, and these govern the regression of the grain.

2.4 VOLUME AND SURFACE AREA FORMULAS

This paragraph describes the philosophy and use of the volume and surface area formulas used in this geometric code. Before turning to these, however, the restriction necessary on the model is restated, since the formulas depend on this.

It is assumed at the onset that the regression of the grain occurs normal to the propellant surface at any time. With this assumption, and the fact that initial surfaces vary piecewise linearly along the motor axis, it would seem that the best formulas are the family of cone frustum mensuration formulas. With these formulas, grain linearity between increment dividing planes is tacitly assumed. (Notice that linearity between dividing planes is stated and not reference planes. The burning itself may cause a nonlinear burning surface to emerge, which is approximated by a piecewise linear surface, with changes in taper taking place at IDP's. This will admit a better approximation than one between reference planes.)

However, in certain areas of complex geometry, even frustum formulas are not adequate, so a new volume formula is introduced which is particularly suited to the analytic nature of this code.

Consider, first, the two frustum formulas of volume and surface area (see Figure 2-7 for definition of nomenclature).

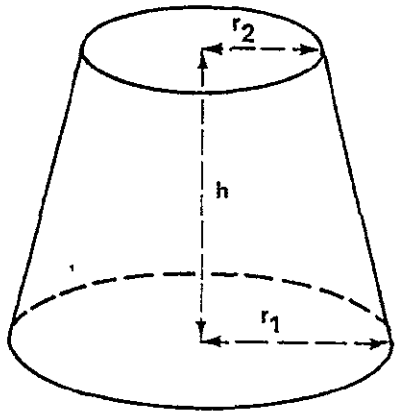

Figure 2-7. A CONE FRUSTUM

Surface area (lateral)

$$S = \pi(r_1 + r_2)\sqrt{(r_1 - r_2)^2 + h^2}$$

Volume

$$V = \frac{1}{3}\pi h(r_1^2 + r_2^2 + r_1 r_2).$$

From the geometric routines, port perimeter and port area are determined. Consequently, with these known, the surface area and volume equations should be compatible with that knowledge. A digression is made here to render these formulas so compatible.

Surface Area

$$S = \pi(r_1 + r_2)\sqrt{(r_1 - r_2)^2 + h^2}$$

$$= (\pi r_1 + \pi r_2)\sqrt{(r_1 - r_2)^2 \frac{4\pi^2}{4\pi^2} + h^2 \frac{4\pi^2}{4\pi^2}}$$

manipulations will yield

$$S = \frac{1}{4\pi}(2\pi r_1 + 2\pi r_2)\sqrt{(2\pi r_1 - 2\pi r_2)^2 + 4\pi^2 h^2}\ .$$

But $2\pi r_1 = P_1$, $2\pi r_2 = P_2$ — the perimeters at top and bottom — (Figure 2-7) so

$$S = \frac{1}{4\pi} (P_1 + P_2) \sqrt{(P_1 - P_2)^2 + (2\pi h)^2} .$$

Volume

$$V = \frac{1}{3} \pi h (r_1^2 + r_2^2 + r_1 r_2)$$

$$= \frac{1}{3} h \left(\pi r_1^2 + \pi r_2^2 + \sqrt{(\pi r_1^2)(\pi r_2^2)} \right) .$$

If $A_1 = \pi r_1^2$, $A_2 = \pi r_2^2$, the port areas at top and bottom, then the volume formula can be written as

$$V = \frac{1}{3} h \left(A_1 + A_2 + \sqrt{A_1 A_2} \right).$$

With these equations in proper form, attention is turned for the moment to the irregular geometry occurring in the transition from star to CP. The grain itself may vary nonlinearly in this section, so that frustum formulas may yield only approximations to the true values. This can be circumvented in the case of volume in the following way:

A general prismatoid is defined to be a solid whose area, A_z, at a section parallel to and distant z from a fixed plane can be expressed as a polynomial in z of degree not higher than three. If B_1 is the area of a lower base, B_2 the area at an upper base, and M the area at the midsection, then

$$V = \frac{1}{6} h (B_1 + 4M + B_2).$$

Examples of general prismatoids include cones, cylinders, spheres, and spheroids.

This particular formula presents a powerful tool for the calculation of the volume in an irregular, nonlinear region. It is a generalization of the frustum formula just given, but does not depend on linearity. It does, however, need the extra calculations for M, the area of a midsection, and for this reason, the general prismatoid formula is used only when necessary.

Unfortunately, there is no such generalization for the surface area formula. Instead, the formula for a cone frustum is used repeatedly where the interval between IDP's is broken into several (equal) smaller subintervals. This

piecewise linear approximation is as close to true values as is computationally feasible and expedient. It must be remembered that values of port area and port perimeter are available at any position along the motor centerline by virtue of the functional nature of the geometry (it depends only on total burn distance); and so the breaking up of the interval for surface area or volume is only an exercise in function evaluation.

The formulas for surface area and volume are different still in the regions of partially inhibited slots. There, the volumes and surface areas are described analytically through use of the calculus and surfaces and volumes of revolution. This will be handled in the section on partially inhibited slots (Section IV).

Section III

NORMAL GEOMETRY

Although the homogenous CP and star regions of the motor are not regions of complicated geometry, and very efficient codes already exist for their modeling, this section offers still another mathematical interpretation of the burning in these sections. This was considered expedient to facilitate computational continuity at the interfaces between these regions and those of atypical geometry.

Included in this section are paragraphs dealing with specific computational quantities in the CP and star regions, in that order. The idea of a burn-back parabola is introduced in the star paragraph, and extensive use is made of this simple but powerful notion.

The star algorithm presented here is not in its final and most usable form, and will be further updated in the section on the transition region, Section V.

3.1 CP BURNING

Consider the view presented in Figure 3-1, that is, a segment of propellant between two increment-dividing planes, I and I+1, which is totally within

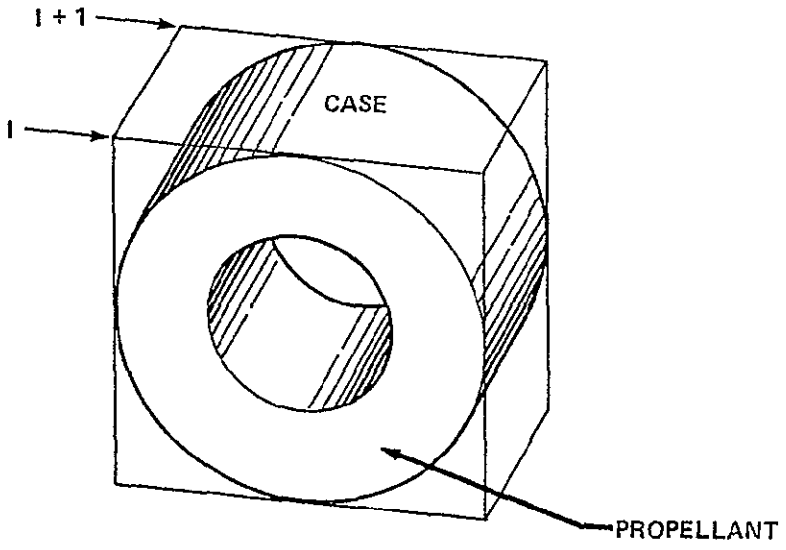

Figure 3-1. A SECTION OF PROPELLANT IN A CP SEGMENT

the CP region of the motor, and will not change its cross-sectional geometric shape. The port volume contained between the two planes is called a mass addition region.

In the general case, the initial port radii at the two positions are dissimilar, so that the region between the planes forms a cone frustum.

Further restricting the view, consider only the cross section at plane I (Figure 3-2). The initial port radius is r, and burn distance is s_b. The port fuel perimeter and port area at plane I (Figure 3-1) are given at this burn distance by

$$\text{Perimeter} = P_I = 2\pi(r + s_b)$$

$$\text{Area} = A_I = \pi(r + s_b)^2.$$

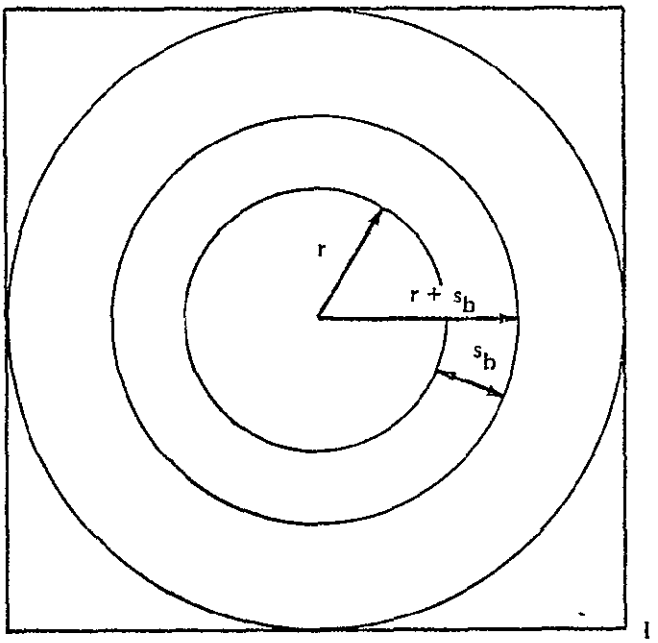

Figure 3-2. AN ANALYTICAL VIEW OF A CP CROSS SECTION

If the same quantities have been established at plane I+1, then

$$\text{Surface Area} = SA = \frac{(P_I + P_{I+1}) \sqrt{(P_I - P_{I+1})^2 + (2\pi h)^2}}{4\pi}$$

and

$$\text{Volume} = V = \frac{1}{3} h \left(A_I + A_{I+1} + \sqrt{A_I A_{I+1}}\right)$$

where h is the known distance between the two planes.

Further refinements to this rather simple model have been made for purposes of flexibility and accuracy. The first is to consider the port not in an overall view of 2π radians, but on a sector basis.

If work is done in this mode, the number of sectors, n, is input to the program; and an angle, α, is calculated as $2\pi/n$. Then the perimeter and area equations become

$$P_I = \alpha(r + s_b)$$

$$A_I = \frac{\alpha}{2} (r + s_b)^2$$

and the same frustrum formulas can be used to establish the surface area and volume of the mass addition region.

The other addition to the model constitutes a way to treat the final burnout in the mass addition region. In this respect, consider the situation presented in Figure 3-3. Notice that the burning has caused complete grain consumption at plane I; while grain remains at plane I+1. The propellant involved in this region has, of course, a linear surface. In Figure 3-3, only the propellant is shown--the case and insulation have been omitted.

The situation in Figure 3-3 leads to an abstraction like that in Figure 3-4, which shows a cross section taken through the centerline perpendicular to planes I and I+1. Figure 3-5 is a further abstraction for the purpose of analysis and nomenclature.

The slope of the grain, M_G, is given by

$$M_G = \frac{(r + s_b) - (r' + s_b')}{D}$$

where D is the undirected distance between plane I and I+1.

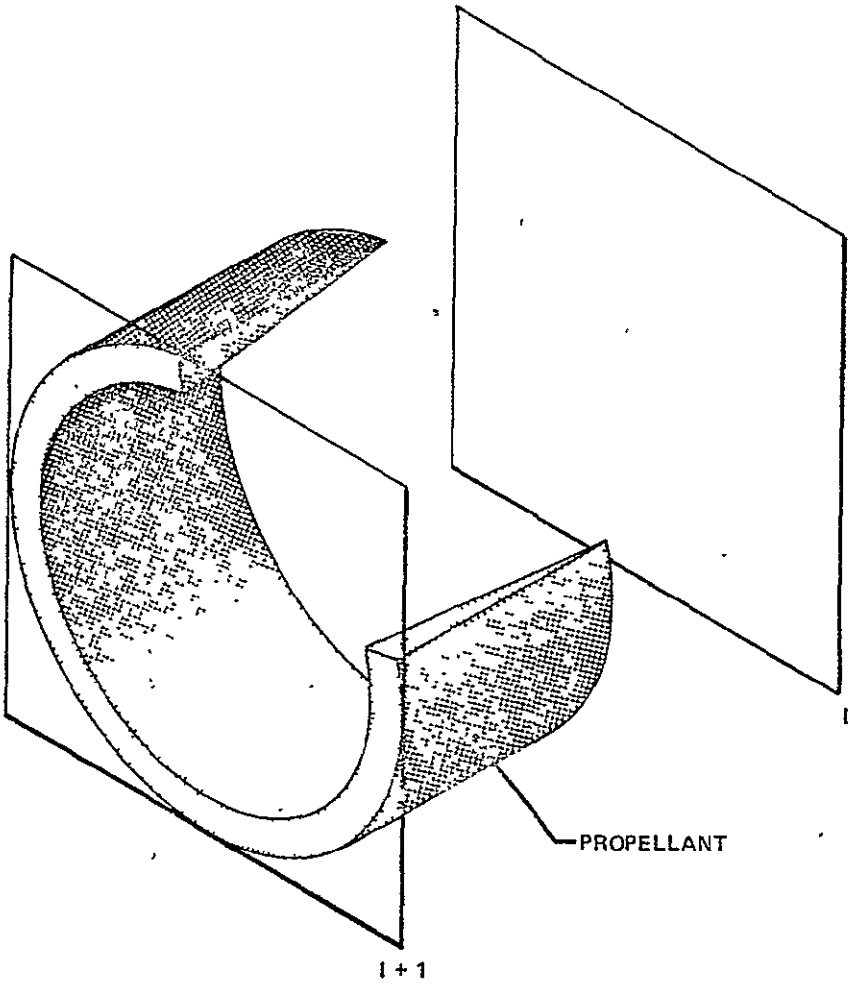

Figure 3-3. PARTIAL BURNOUT IN A CP REGION

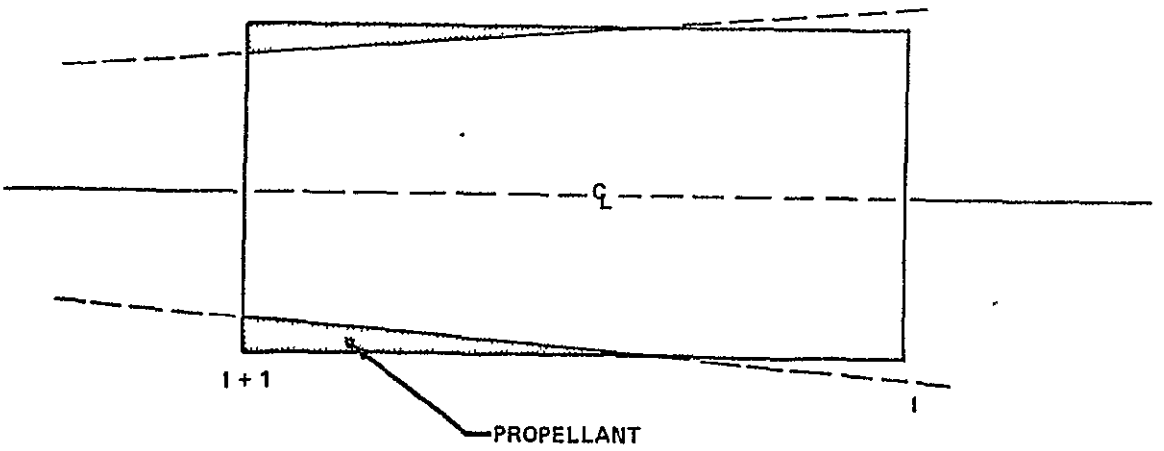

Figure 3-4. AN ANALYTICAL VIEW OF A CP BURNOUT

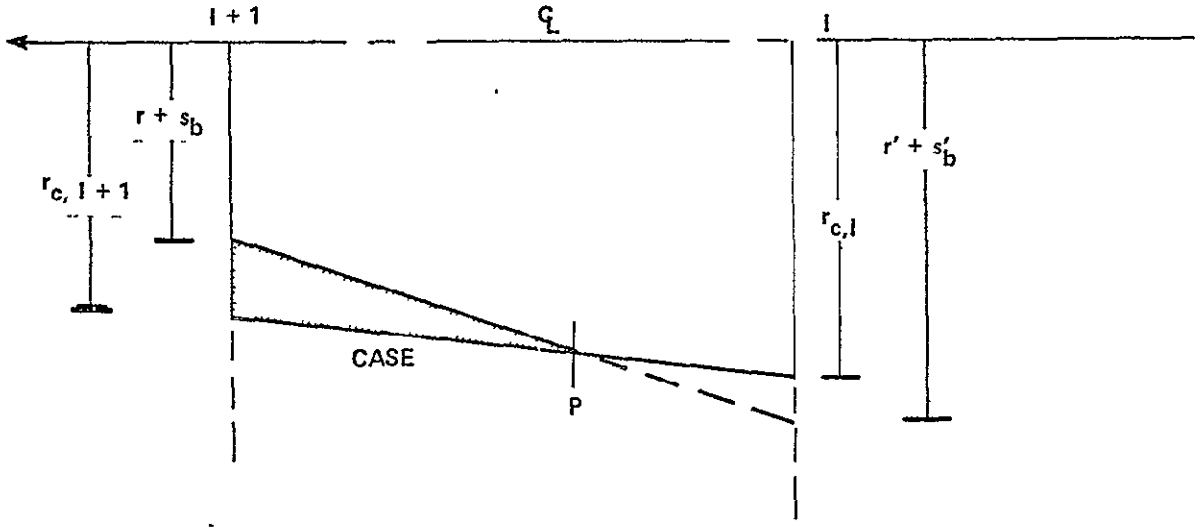

Figure 3-5. DEFINITIONS OF TERMS USED TO DETERMINE A CP BURNOUT

The slope of the case, M_c, is likewise given by

$$M_c = \frac{r_{c,I+1} - r_{c,I}}{D}$$

An exercise in the use of the laws of cosines yields the position of point P relative to the foretangent plane as

$$\text{Position of P} = \text{Position of I} + \frac{r_{c,I} - r' + s'_b}{M_G - M_c}$$

At point P, the port perimeter is maximal, and the port area is maximal. The volume of the mass addition region is given by calculating two volumes, from I to P and from P to I+1; and the surface area is given by using the frustum surface area formula for the region between P and plane I+1. Burnout occurring from the other direction is handled by the same formula.

The above two additions to the CP burning routine make that routine a general, self-contained code useful in asymmetrical grain studies and without need for augmenting routines to calculate mensuration quantities for a partially burned-out mass addition region.

3.2 STAR BURNING

Attention is now turned to the star segment of the motor (Figure 1-2). Consider the situation shown in Figure 3-6. A regression of the grain is shown in Figure 3-7. It is evident (Figure 3-6) from the symmetry involved that only one-half of one star peak need be modeled. The port fuel perimeter and the port area for the whole cross section are then integer multiples of those quantities involved in the restricted view.

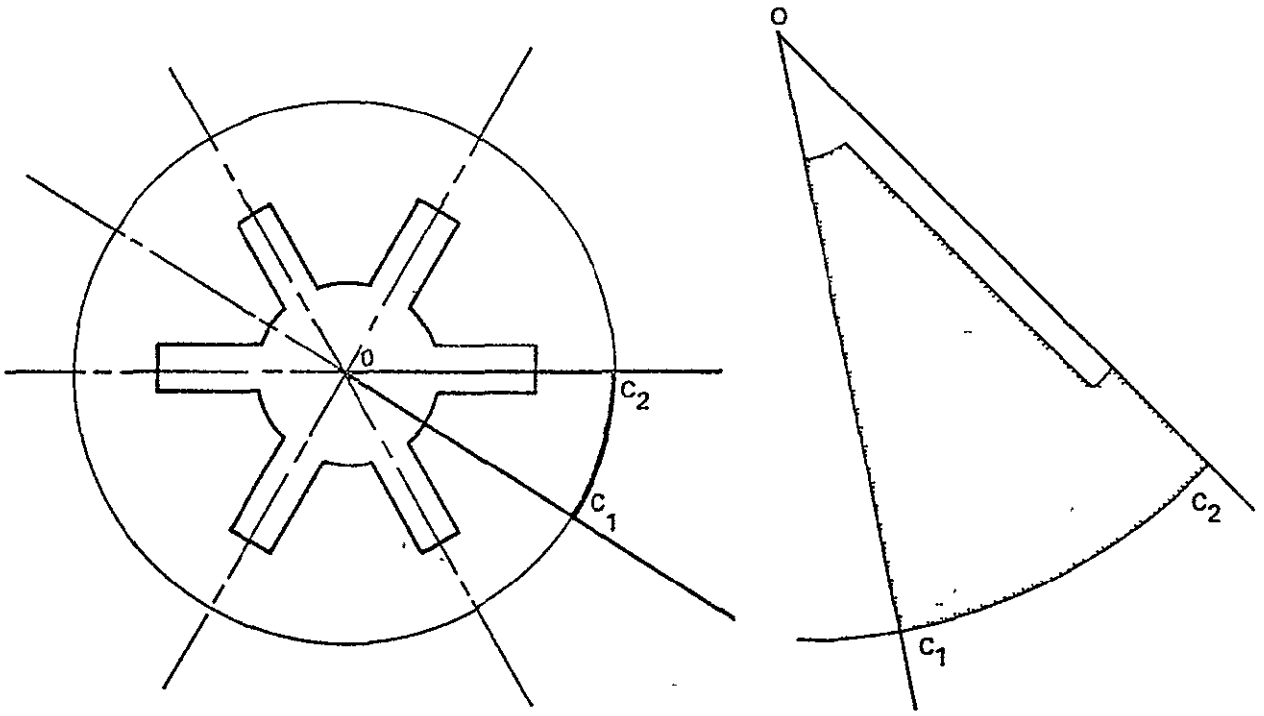

Figure 3-6. STAR CROSS SECTIONS AND SECTOR DEFINITIONS

The cross section shown in Figure 3-6 is taken perpendicular to the centerline so that the vertex of angle $\measuredangle C_1OC_2$ lies on the motor axis. The valley side is, in the general case, slanted. Line ℓ (Figure 3-7) is constructed perpendicular to the valley side through the fillet center represented by point Q.

In Figure 3-7, the actual calculation of port fuel perimeter and port area can take place on an even more restricted view. In particular, four areas of distinct geometry present themselves. These areas are:

1. The concave portion of the star peak
2. The linear portion of the valley side
3. The arced portion of the valley side, emmanating from the fillet circle.
4. The linear valley floor.

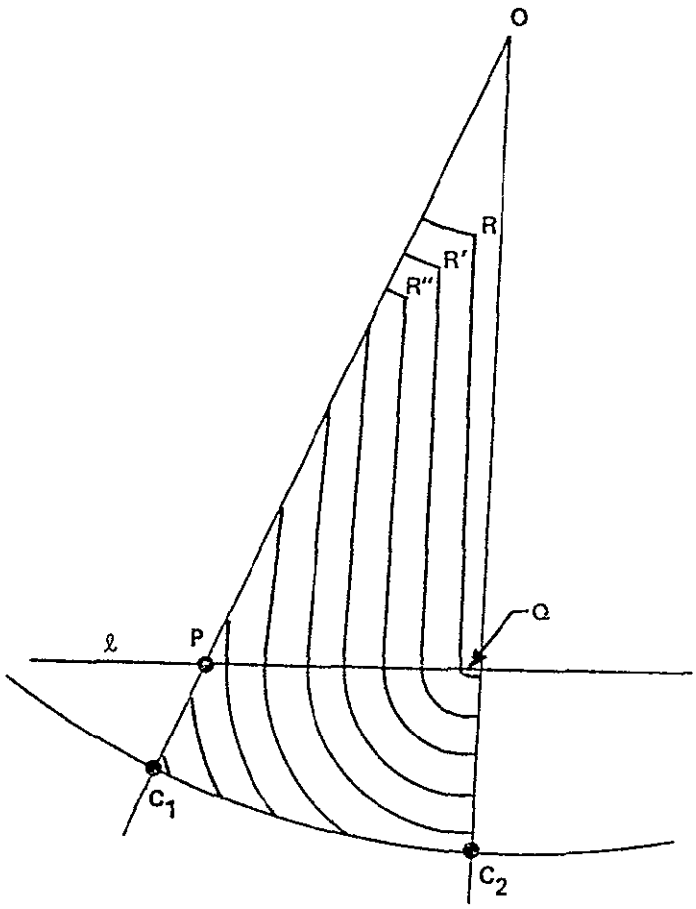

Figure 3-7. GRAIN REGRESSION IN A STAR SECTOR

The discussion now covers the delineation of these four subregions and the calculation of the pertinent quantities in each. This is done by tracking a few points along predetermined paths. In effect, the assumption of perpendicular burning establishes these paths and makes such an analysis rather simple.

The specific points that will be tracked are shown in Figure 3-8. The figure represents two times during the burn, the initial perimeter and one

after a distance s_b has been burned. Note that the four points P_1 through P_4 are at initial positions, and P_1' through P_4' are at terminal positions. The regions for which these points are vertices comprise the sections referred to above.

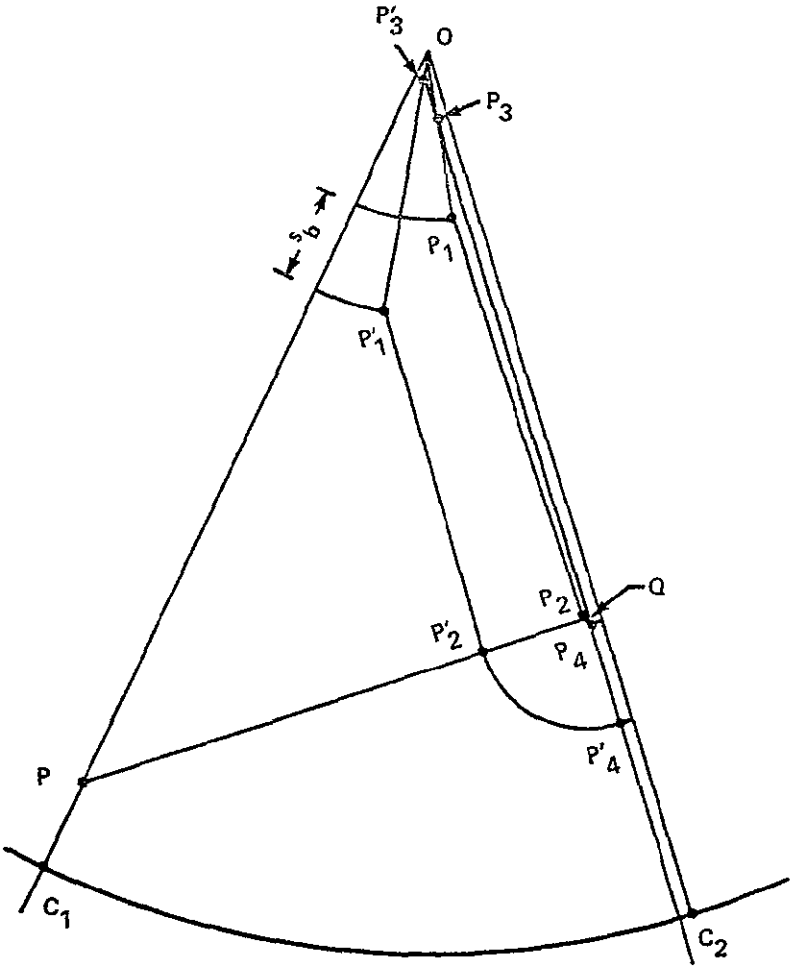

Figure 3-8. NOMENCLATURE USED TO DEFINE THE BURNING IN A STAR SECTOR

It is the general case where line $\overline{P_1 P_2}$ in Figure 3-8 is not parallel to the valley centerline, $\overline{OC_2}$. Because of the distances involved in large SRM's, special care must be taken in any analytical routine to use the existing value of angle $\measuredangle P_1P_2P$. In particular, as seen in the following discussion, the length $P_1' P_2'$ varies trigonometrically with this angle; and at the beginning of the burn, when a large length of side exists, even this diminutive quantity can have substantial effects.

It is also seen that the position of P_2 varies directly with this small angle. In Figure 3-8, point P is calculated and serves as an internal reference to the program. A small change in the angle mentioned will show itself in the positioning of P.

Some definitions are appropriate here, before progressing to actual theoretical development. The point O of Figure 3-8 is on the motor centerline, and points O, C_1, C_2 determine the plane of the cross section made perpendicular to the motor axis. Points C_1 and C_2 rest on the case wall. The line $\overline{OC}_1$ is the centerline of the star peak, and the line $\overline{OC}_2$ is the centerline of the star valley.

Notice that the star peak is concave in nature, the valley sides slope, and that at the bottom of the valley, both a small fillet and a linear length exist. The valley side is assumed tangent to the fillet as is the line at the trough floor. The judicious choice of values for these constraints permits the modeling of both a true star or a slotted cone.

Order can be obtained by imposing a coordinate system, as is done in Figure 3-9, where a Cartesian system is selected over a polar system because this leads ultimately to a simplification of certain important formulas. One of these is the notion of a burn-back parabola.

As the burn progresses, notice (Figure 3-7) that the concave portion of the star peak proceeds down the star centerline while, at the same rate, the valley side progresses along line QP in direction P. If ϕ represents the angle of inclination of the star valley side with the x-axis, then the linear equation representing this side can be expressed as

$$y = -x\tan\phi + (\tan\phi\sin\phi + \cos\phi)\ s_b + C$$

where s_b represents the distance burned, and

$$C = r_4 + r_f \cos\phi + (r_2 + r_f \sin\phi)\ \tan\phi)$$

where r_f is the fillet radius in the trough,

r_4 is the length of line on the trough floor,

and r_2 as indicated in Figure 3-9, is the valley floor radius, minus the fillet radius.

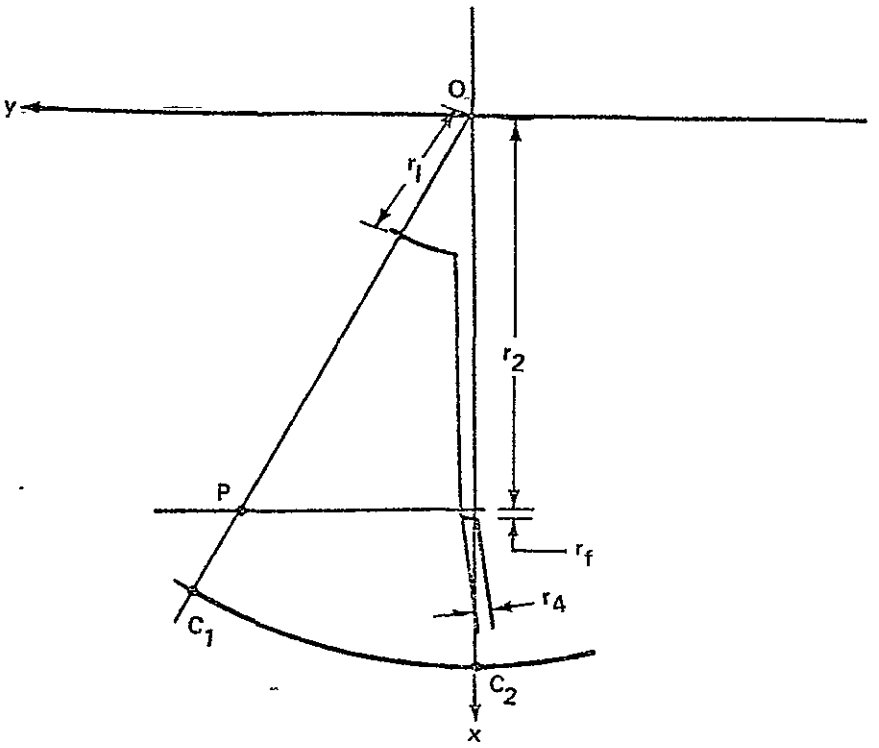

Figure 3-9. QUANTITY DEFINITIONS IN A STAR SECTOR

At any time before the annihilation of the concave star peak, the equation of this star peak is given by the circle equation as:

$$x^2 + y^2 = (r_1 + s_b)^2.$$

The intersection of the star valley with the concave region of the star peak is the point R, (R′ and R′′) in Figure 3-7 for various distances burned, s_b, s_b', s_b''. The means to predict where the concave portion annihilates is now at our disposal.

Placing the line equation in a form so that the coefficients of s_b in both the line and the circle equations, above, are identical, we have

$$\frac{y + x\tan\phi - C}{\tan\phi\sin\phi + \cos\phi} = s_b$$

Now, in accordance with subsection 2.2

$$\overline{\alpha} = \frac{\tan\phi}{\tan\phi\sin\phi + \cos\phi} = \sin\phi$$

$$\bar{\beta} = \frac{1}{\tan\phi\sin\phi + \cos\phi} = \cos\varphi$$

$$\bar{\gamma} = - C\cos\phi$$

$$\bar{\alpha}^2 + \bar{\beta}^2 = 1,$$

and point R of Figure 3-7 tracks out a parabola as it passes through R′ and R″ to intercept the star peak centerline. A parabola of this sort--that tracks a particular point--will be called a burn-back parabola. The burn-back parabola is pictured in Figure 3-10 for the case just worked.

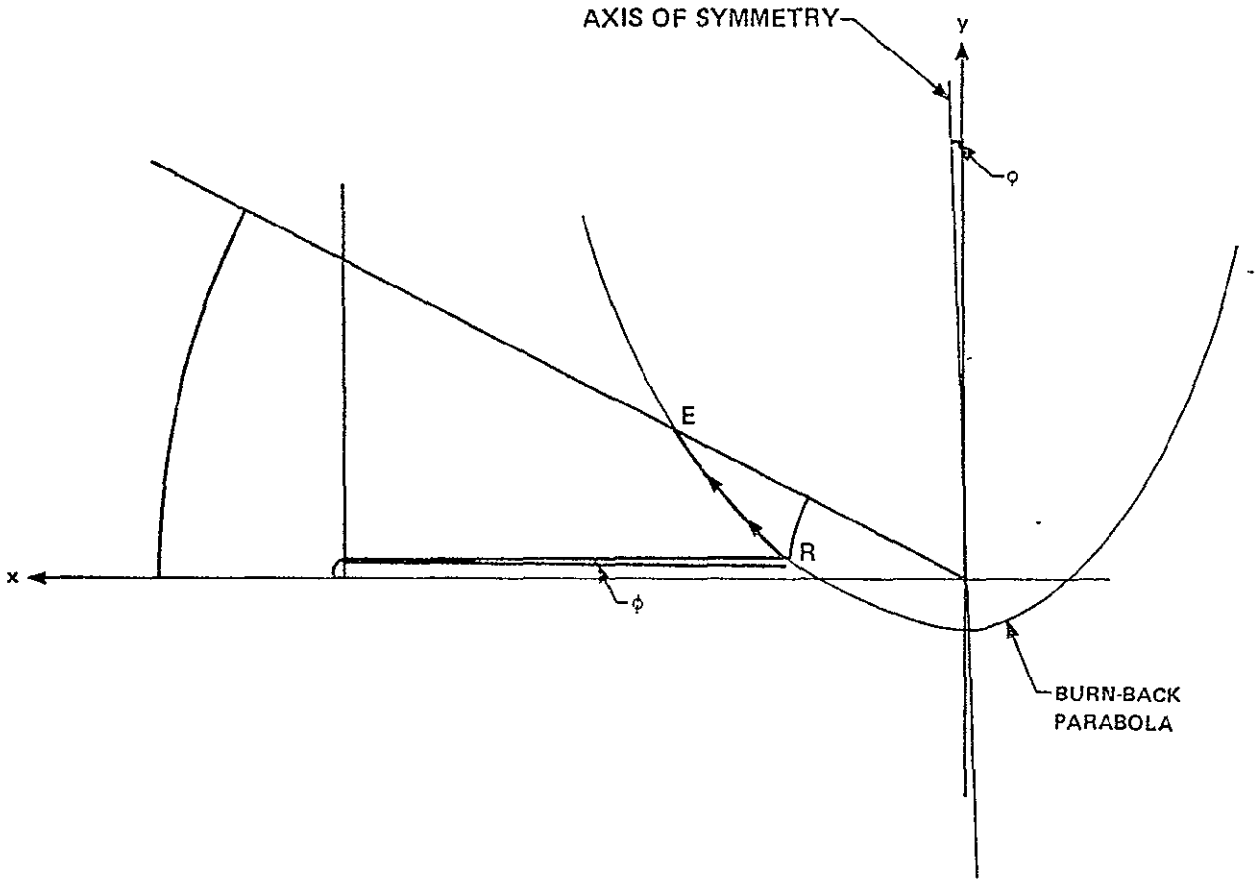

Figure 3-10. A BURN-BACK PARABOLA IN A STAR SECTOR

Furthermore, since $\bar{\alpha}$, $\bar{\beta}$, and $\bar{\gamma}$ are all known from the line equation, the burn-back parabola has the form

$$Ax^2 + Bxy + Cy^2 + Dx + Ey + F = 0$$

where

$$A = 1 - \bar{\alpha}^2 \qquad C = 1 - \bar{\beta}^2 \qquad E = -2\bar{\beta}(\bar{\gamma} + r_1)$$

$$B = -2\bar{\alpha}\,\bar{\beta} \qquad D = -2\bar{\alpha}(\bar{\gamma} + r_1) \qquad F = -(\bar{\gamma} + r_1)^2$$

with $B^2 - 4AC = 0$ (guaranteed). In descriptive form, the parabola is one with focus at (0,0) and axis of symmetry the line $Y = x\cot\phi$.

Now, the solution alluded to above--that of a point where the burn-back parabola intersects the star peak centerline at E (Figure 3-10)--is the simultaneous solution of the parabola equation with the equation of the star peak centerline. That equation is given by

$$y = x\tan\psi$$

where $\psi = \pi/n$, n = number of star points.
Substituting this expression into the burn-back parabola yields

$$Ax^2 + Bx\,(x\tan\psi) + C(x\tan\psi)^2 + Dx + E\,(x\tan\psi) + F = 0$$

Manipulations result in the solution in terms of x as

$$x = (r_1 - r_f - r_2\sin\phi - r_4\cos\phi)\left[\frac{\sin(\phi + \psi) \pm 1}{\cos^2(\phi + \psi)}\right]\cos\psi$$

where choice of sign is dictated by the fact that x is to be positive.

Since the burn-back parabola is in essence a function of three variables (x,y,s_b), the same parabola can be expressed in terms of x and s_b instead of x and y. Doing this, and knowing s_b, the x-coordinate of point R can be evaluated. Hence, there is all the information necessary to know the exact position of R during that part of the burn in which the concave portion of the star peak is extant.

In the manner of the above exposition, the burn-back parabola in terms of x and s_b can be obtained as

$$Ax^2 + B\,xs_b + Cs_b^2 + Dx + Es_b + F = 0 \qquad B^2 - 4AC = 0$$

where the letters A-F here have no relationship with those above. In fact,

$$A = \sec^2\phi \qquad D = -2\tan\phi\,(r_4 + r_f/\cos\phi + r_2\tan\phi)$$

$$B = -2\sin\phi\sec^2\phi \qquad E = 2\,((r_4 + r_f/\cos\phi + r_2\tan\phi)/\cos\phi - r_1)$$

$$C = \tan^2\phi \qquad F = (r_4 + r_f/\cos\phi + r_2\tan\phi)^2 - r_1^2$$

Note that indeed $B^2 - 4AC = 0$ since

$B^2 - 4AC = -4\sin^2\phi\sec^4\phi - 4\sec^2\phi\tan^2\phi$ and $\tan^2\phi = \sin^2\phi\sec^2\phi$

Knowing s_b at any time yields

$$x = \frac{-(Bs_b + D) + \sqrt{(2BD - 4AE)\,s_b + D^2 - 4AF}}{2A}$$

where the plus sign was chosen to keep x positive.

Referencing Figure 3-11, once point R has been placed on the burn-back parabola, then the quantities of port area and port perimeter can be calculated. This is done in four segments, as indicated. Knowing the coordinates of R, then angle η can be determined. This angle bounds region I. The port perimeter contribution from this section is given by

$$\eta\,(r_1+s_b)$$

and the port area in this section as

$$\frac{1}{2}\,\eta\,(r_1 + s_b)^2.$$

Angle $\angle RSU$ is known to be $\pi/n-\eta$, since line US is parallel with line OZ, the valley centerline. Consequently, point S is known as the simultaneous solution of the set

$$\begin{cases} y = r_4 \\ y = x\tan(\angle RSU) \end{cases}$$

To derive the contributions from region II, U is taken as a fixed point, and V is marked off $s_b + r_f$ distance from U along line $\overline{UP}$. Hence, V is known, and lengths of line segments $\overline{RS}$, $\overline{SU}$, $\overline{UV}$, and $\overline{VR}$ are caluclated. The port perimeter in this section is length $\overline{VR}$. The Bretschneider-Heron formula for the area of the general quadrilateral gives the port area contribution from this section (Appendix A).

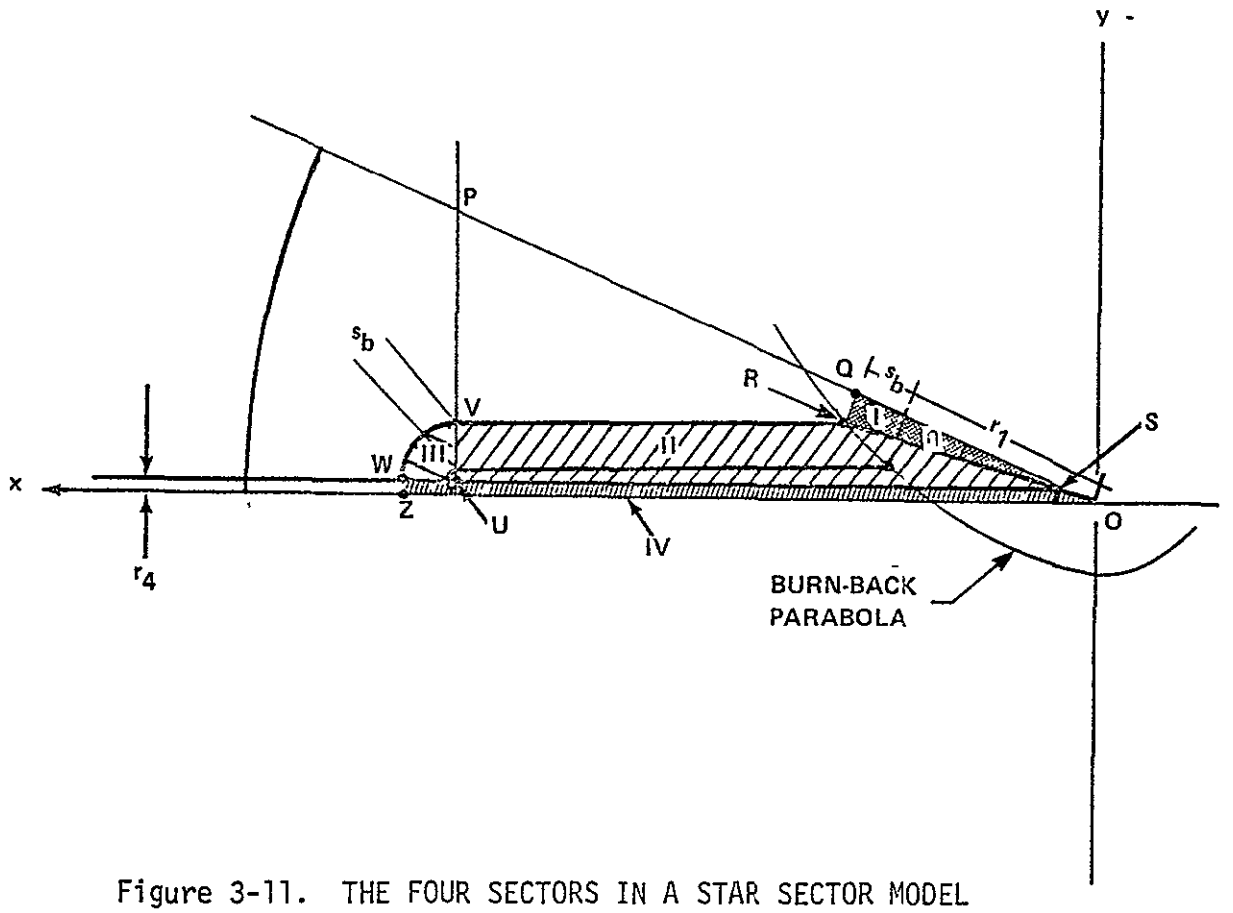

Figure 3-11. THE FOUR SECTORS IN A STAR SECTOR MODEL

Angle ∠VUW is $\pi/2 - \phi$, so both the port perimeter and port area in region III are known. Length $\overline{WZ}$ is simply r_4, so the port perimeter and the port area contribution in region IV are known, using Bretschneider's formula.

The above calculations yield the total value of port perimeter as

$$\text{perimeter} = \eta(r_1 + s_b) + \overline{VR} + (\pi/2 - \phi)\ (r_f + s_b) + r_4.$$

A similar summation gives the port area.

After the concave region of the star peak has been completely consumed, a situation like that in Figure 3-12 appears.

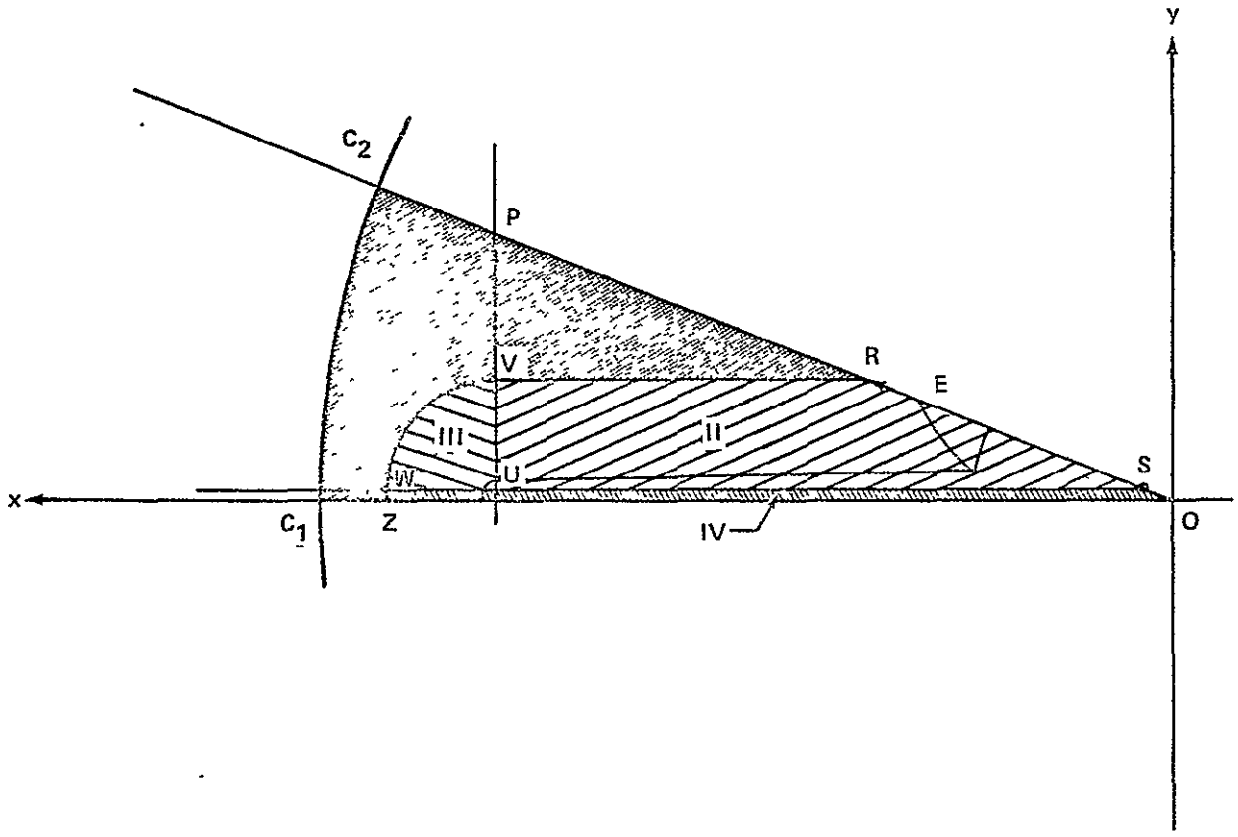

Figure 3-12. A STAR SECTOR AFTER CONCAVE PEAK CONSUMPTION

Appearing is an analogy to that in Figure 3-11, yet η=0 (that is, region I has become degenerate) so that there is no need for calculating mensuration quantities in that section. The difference does manifest itself, though, in the calculation of the positioning of point R. It is now receding down the peak centerline, off the burn-back parabola, at an accelerated rate. Hence, when R reaches E along the path indicated, R is thereafter positioned as the simultaneous solution of the star valley side and the peak centerline.

The valley side and the peak centerline are represented by the set

$$\begin{cases} y = -x\tan\phi + s_b/\cos\phi + C \\ y = x\tan\psi \end{cases}$$

where C, as before, is $r_4 + r_2\tan\phi + r_f/\cos\phi$. This indicates that R has coordinate representation as:

$$R = \left(\frac{1}{\tan\psi + \tan\phi}\ (s_b/\cos\phi + C),\ \frac{\tan\psi}{\tan\psi + \tan\phi}\ (s_b/\cos\phi + C)\right) .$$

With R known, calculations proceed from region II through IV to obtain port perimeter and port area. This procedure is maintained until R reaches point P or V reaches point P, as they both reach point P simultaneously.

While R is progressing from E to P, burn-out in the star valley has occurred, so that $\overline{WZ}$ no longer contributes to the port perimeter and no longer is there a circular sector of $\pi/2-\phi$ radians. Point W (Figure 3-13) is tracked up the case wall, away from C_1 to C_2, as the simultaneous solution of the two circle equations

$$x^2 + y^2 = c_1^2$$

$$(x - r_2)^2 + (y - r_4)^2 = (s_b + r_f)^2$$

The decrement of the sector angle can then be tracked and the perimeter measured.

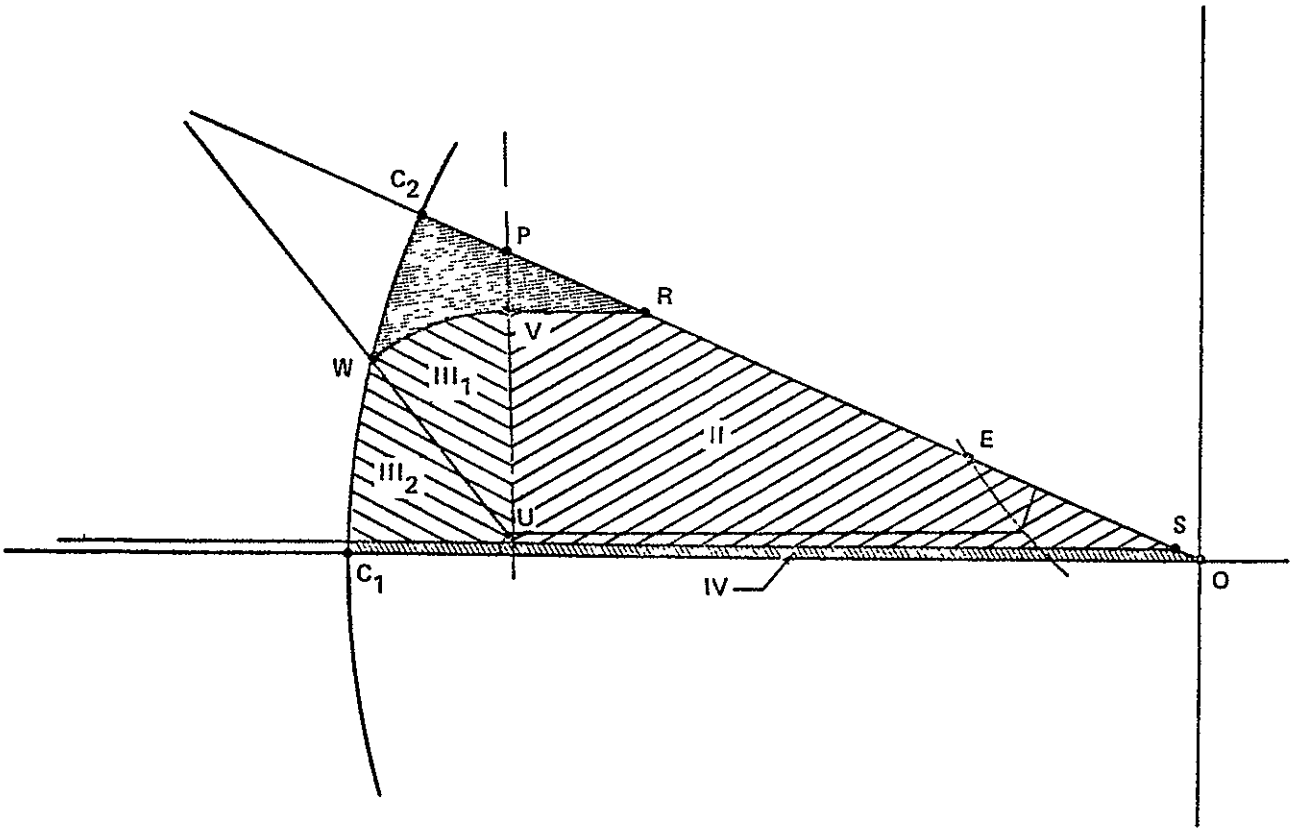

Figure 3-13. A STAR SECTOR WITH VALLEY FLOOR BURNED OUT

In Figure 3-13, angle ∢WUV can be measured and, consequently, mensuration quantity contributions from area III_1 calculated. In area III_2, a bit more work is necessary to obtain the port area contribution (Appendix A).

When R passes P, then Figure 3-14 represents what fuel remains in the sector. Again, angle ∢WUR can be calculated, since W is known in the method above, and R now is the simultaneous solution of the line and circle:

$$y = x\tan\psi$$

$$(x - r_2)^2 + (y - r_4)^2 = (s_b + r_f)^2$$

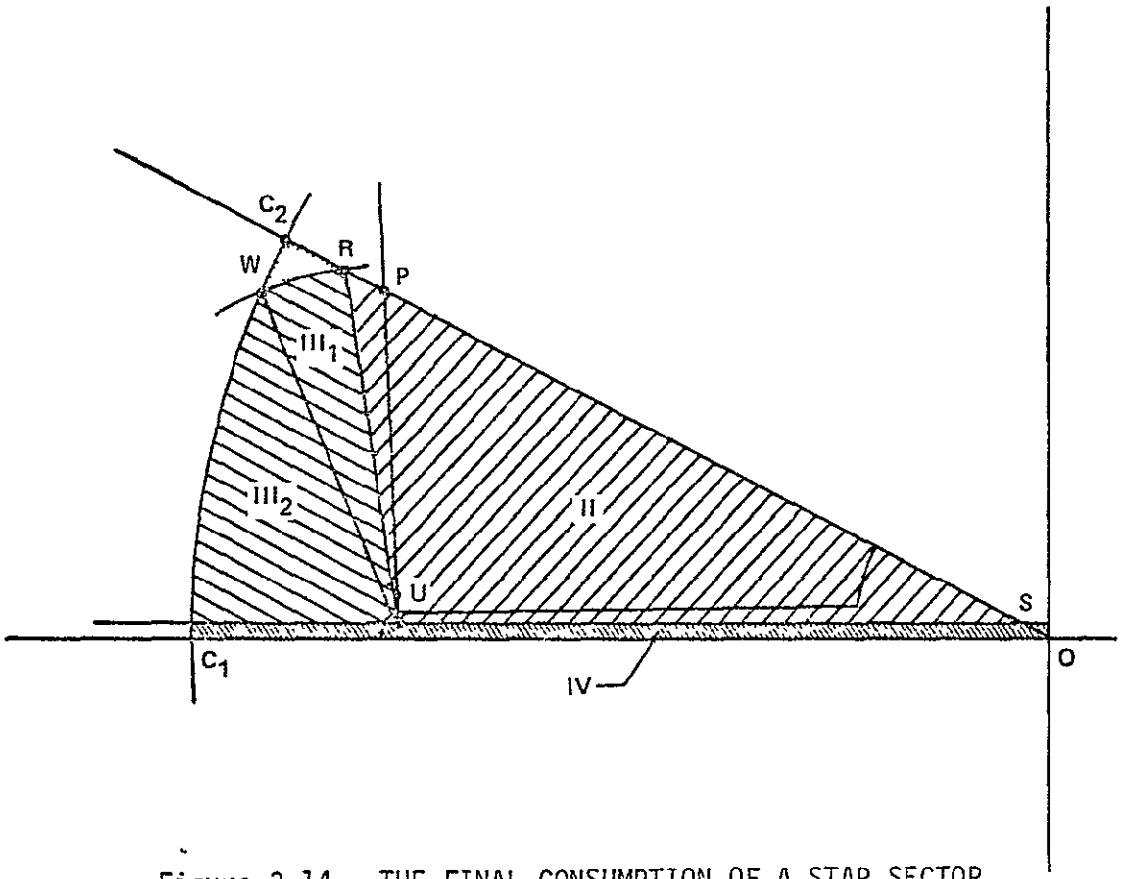

Figure 3-14. THE FINAL CONSUMPTION OF A STAR SECTOR

V is no longer of interest and is not calculated. Instead, the Bretschneider-Heron formula still works for sides $\overline{RS}$, $\overline{SU}$, and $\overline{UR}$ to find the port area contribution from region II. From angle ∢WUR, the port perimeter in III_1, the only fuel left is calculated. The area contribution from III_2 is updated.

These calculations are used to track the rest of the burn--burn-out occurring when R reaches C_2.

The above description is valid only in the region of the star and not in the star-CP transition region. The above procedure will be augmented when that region is assessed.

Port volume and burning surface area in mass addition regions are calculated using the frustum formula described above.

Section IV

PARTIALLY INHIBITED SLOTS

A partially inhibited slot exhibits irregular geometry during the burn. Not only is there a burning component in the radial direction, but also one in a longitudinal direction. The grain surface regresses according to Figure 4-1, where the inside corner at P produces the circular burning region pictured, due to normal regressions. This region appears after a distance equal to the length of the inhibitor buried in the grain has been burned.

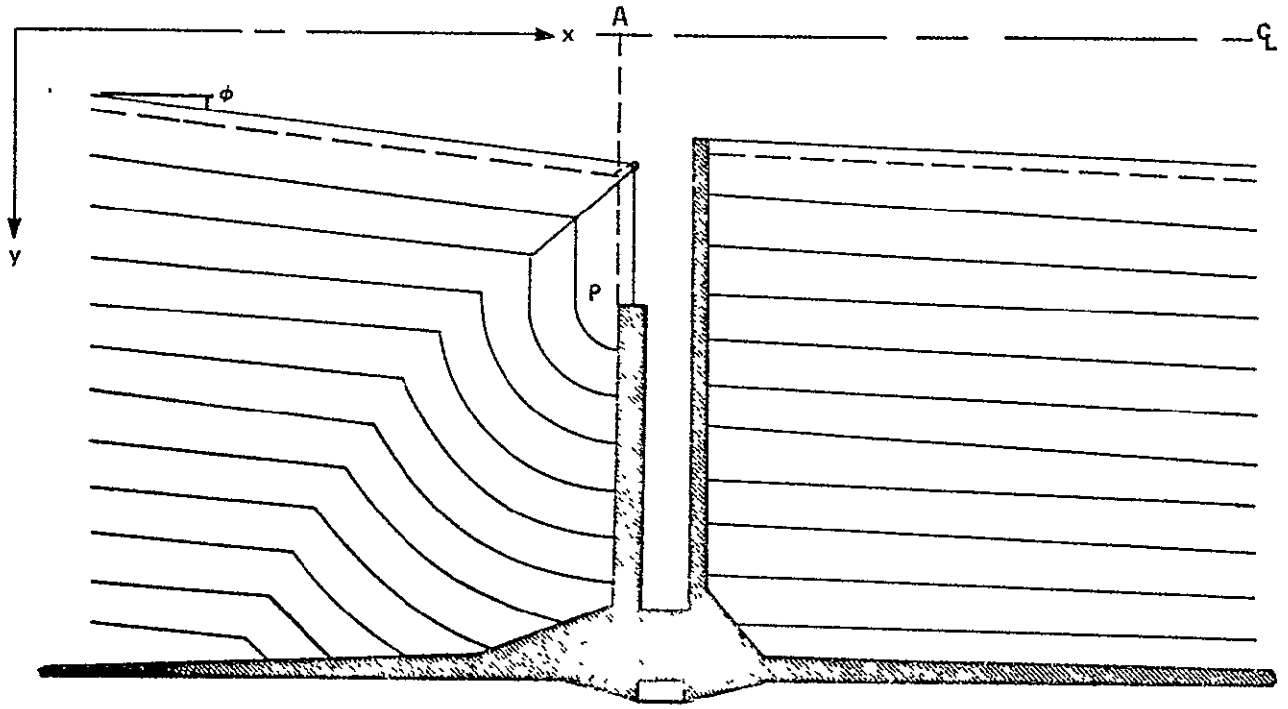

Figure 4-1. GRAIN REGRESSION IN A SLOT

The slope of the grain at the slot face (foreface of the slot aft face of the propellant) can be measured from the values input to the reference planes. The surface can then be placed in the linear form

$$y = x\tan\phi + r_1 - A\tan\phi + s_b/\cos\phi$$

where A is the longitudinal position, as indicated, along the motor axis; r_1 is the port radius at A; and s_b is the distance burned.

After burning has progressed so that the surface impinges directly on the circle, the following equations can be solved for the intersection point:

$$\text{circle:} \quad (x - A)^2 + (y - r_2)^2 = (s_b - T)^2$$

$$\text{line} \quad : \quad y = x\tan\phi + r_1 - A\tan\phi + s_b/\cos\phi$$

where r_2 is the distance from the centerline to P, at A, and T is the thickness of the inhibitor buried in the grain (Figure 4-2).

If the line equation is solved for s_b, the distance burned, then a form appears such as

$$s_b = \cos\phi(y - r_1 + A\tan\phi) - x\sin\phi$$

Taking the coefficients of x and y, and noticing that

$$\cos^2\phi + \sin^2\phi = 1$$

it can be stated that the intersection tracks out a parabola, again called a burn-back parabola.

Substituting the value of s_b, in terms of x and y into the circle equation, obtain a form such as

$$Ax^2 + Bxy + Cy^2 + Dx + Ey + F = 0 \qquad B^2 - 4AC = 0$$

where

$$A = \cos^2\phi \qquad D = -2(A - \sin\phi\cos\phi\ (r_1 - A\tan\phi + T/\cos\phi))$$

$$B = 2\sin\phi\cos\phi = \sin 2\phi \qquad E = -2(r_2 - \cos^2\phi\ (r_1 - A\tan\phi + T/\cos\phi))$$

$$C = \sin^2\phi \qquad F = A^2 + r_2^2 - \cos^2\phi(r_1 - A\tan\phi + T/\cos\phi)^2$$

where T is the thickness of the inhibitor imbedded in the grain. (Note that $B^2 - 4AC = 0$.)

Using the quadratic formula, the above second-degree equation for x is solved in terms of y. Knowing this, and knowing the case radius, the point of intersection of the burn-back parabola and the case can be computed. This

point then becomes an important position, because the region from this point to the slot interface will be considered one mass addition region. Notice that this length has a limiting value, that being the length $r_c - r_1$ where r_c is the case radius at A (Figure 4-2).

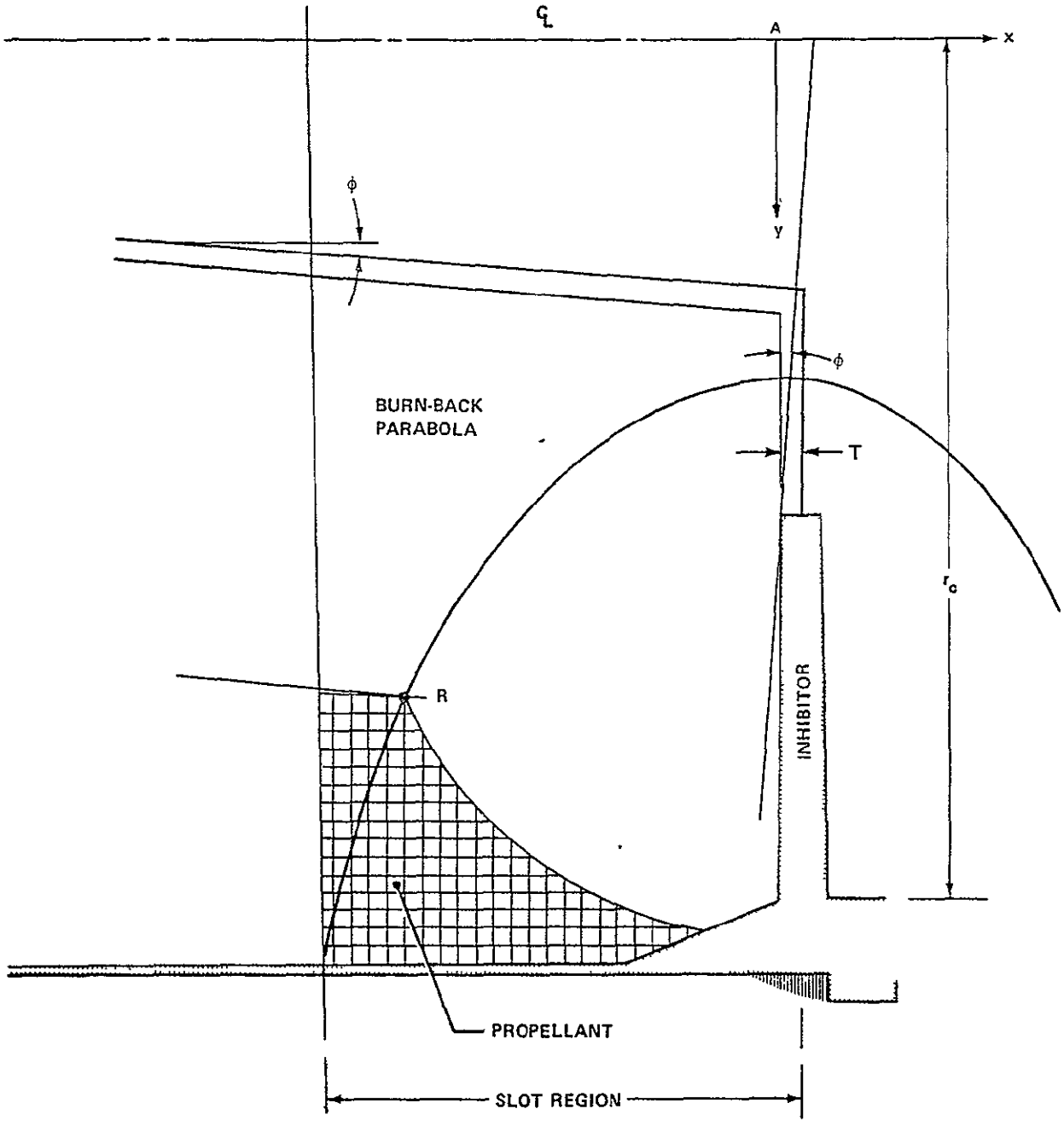

Figure 4-2. AN ANALYTICAL VIEW OF A SLOT REGION

Since the burn-back parabola has an equivalent form in terms of x and s_b instead of x and y, and since s_b is known at any time, the position point R can be calculated at any s_b. Port volume and burning surface area in this region are calculated as volumes and areas of revolution. The formulas for the "arced" region are developed in Appendix B, while the usual cone frustum formulas are used for the linear region. In order to keep equation consistency, it is assumed that the grain regression is constant in this particular mass addition region, that is, the burn rate at the slot face is the same as it is at the point of intersection of the burn-back parabola with the case. This is, however, a very small price paid for analyticity in this region.

At the beginning of the burn, the point R does not travel along a burn-back parabola, but along an angle bisector. In this region, special care has to be observed to include in the surface area calculations the annular region at the end of the grain (Figure 4-3). That is, when region 1 is revolved about the motor axis, the annulus created has a definite burning area. It is calculated as the difference in the areas of two circles, and added to the rest in that region.

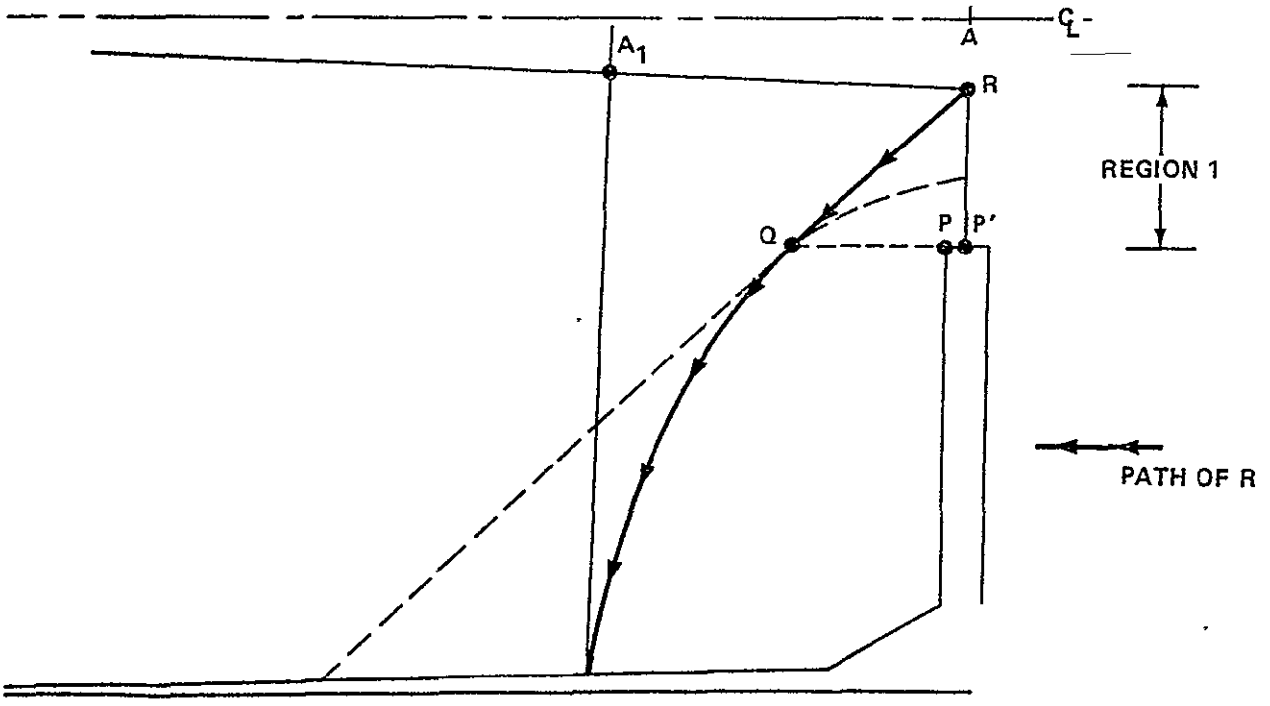

Figure 4-3. TRACKING THE PATH OF ABRUPT GEOMETRY CHANGE IN A SLOT REGION

The path that point R takes during the burn is also indicated in Figure 4-3. Because of normal regression, R moves along the angle bisector of $\sphericalangle A_1RP'$ until the burning surface has reached the level of point P. Point R then travels along the burn-back parabola to the case. There is a smooth transition from one curve to another, since the angle bisector is tangent to the burn-back parabola at Q. In effect, then, the path of R has a continuous derivative.

In Figure 4-4, the burning surface has regressed to a point where the circular region cuts the case insulation. Knowing the radius of the circle as $s_b - T$, and r_c at A, then the y-coordinate of point Q can be ascertained. Knowing, from input data, the slope of the grain at Q, the x-coordinate of Q is known. Since points P and S are known, angle $\sphericalangle QPS$ can be calculated, a further decrement of the circular sector established, and the true length of arc $\overline{RS}$ kept up with. Points Q and R then become the points (x_1, y_1) and (x_2, y_2) of Appendix B so that volume and burning surface area can be calculated.

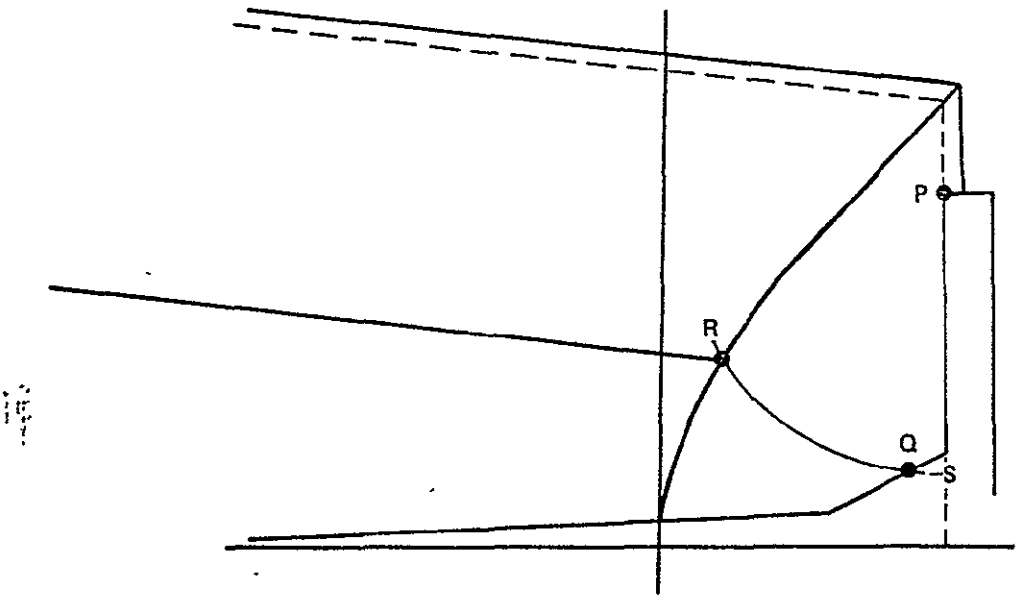

Figure 4-4. USE OF A BURN-BACK PARABOLA IN A SLOT

Section V

TRANSITION REGION

The region of transition between the star section and the CP section in the case where there is no inhibitor between them presents a realm of difficulties hitherto unencountered. What burning exists in the rest of the motor is one dimensional (radial) at best and easily two-dimensional at worst. Examples of one-dimensional burning exist in the CP section, and two-dimensional burning in the star and slot regions. The transition region, however, presents a third spatial dimension to the burning.

The region now under consideration, here called the transition region, is that region, pictured in Figure 5-1, where complex geometry appears during the burning because there is an uninhibited CP face presented in each star valley (Figure 5-2).

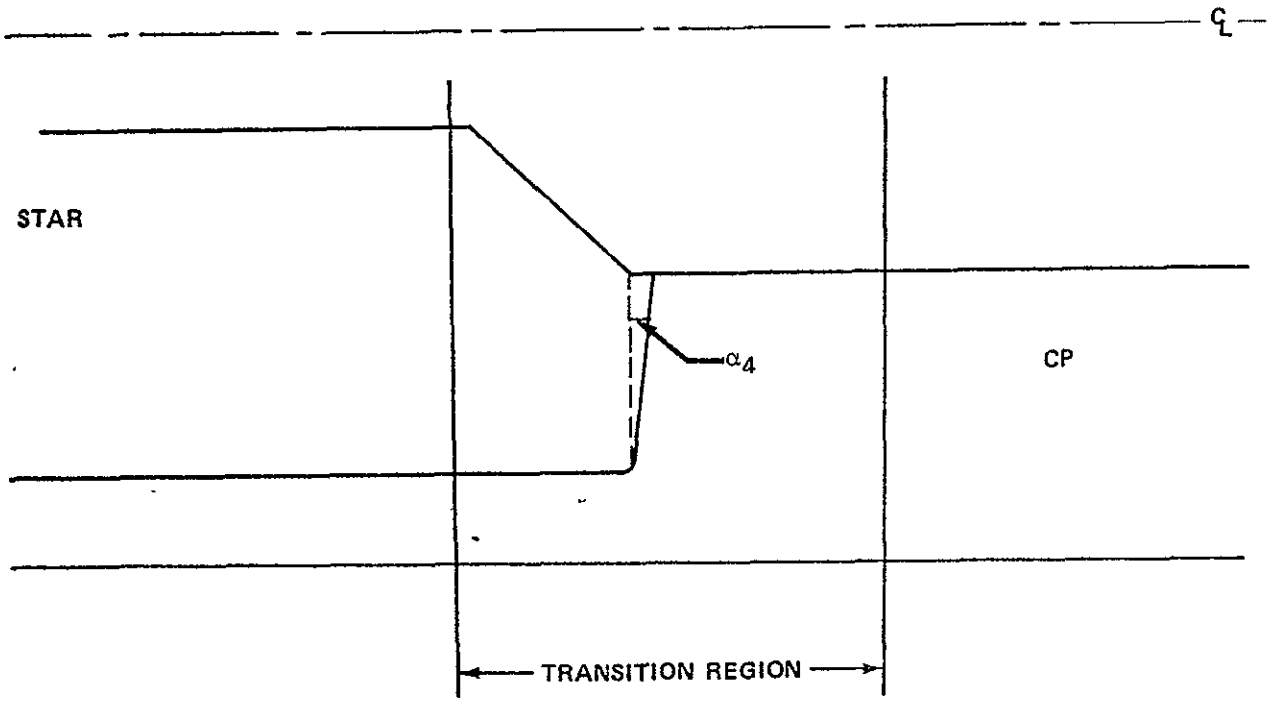

Figure 5-1. THE LIMITS OF A TRANSITION REGION

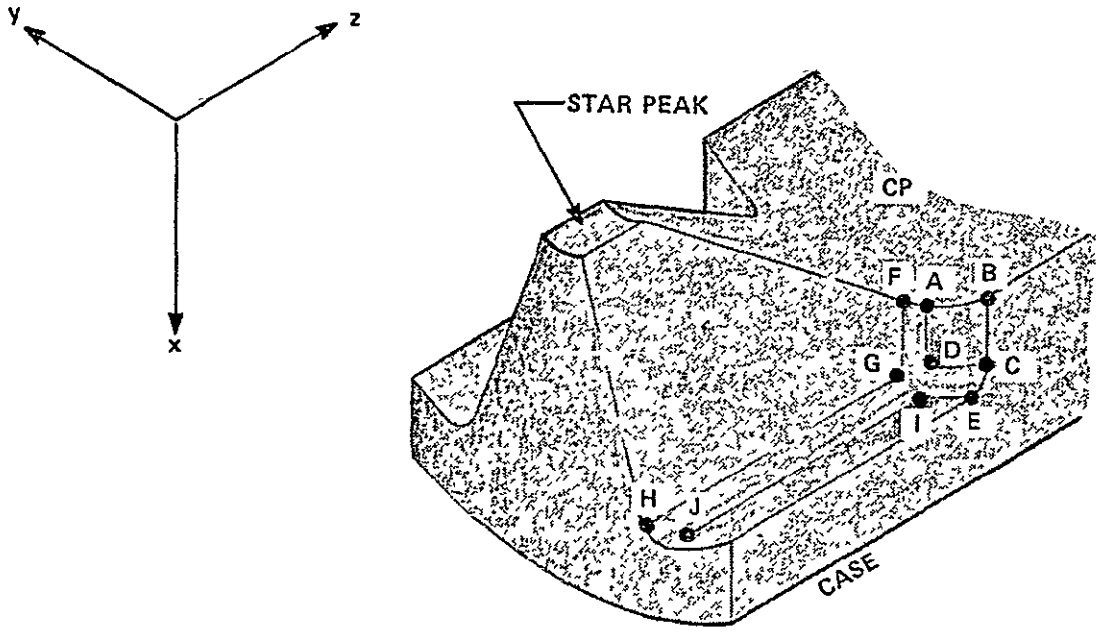

Figure 5-2. INITIAL RELATIONSHIPS AT A STAR-CP INTERFACE

The physical situation then exists where, during the burning, a newly created star region emerges from the CP region.

The angle α_4 of Figure 5-1 is generally not a zero angle in large motors. A tilt in the direction indicated will facilitate mandril withdrawal, and so α_4 will usually be a positive, but small, angle measure.

Figure 5-2 represents a view looking into a star valley in the transition region. Notice that it is the burning on face ABCD that produces the new star geometry. The radius of arc CE is generally not the fillet radius in the star trough. The object AFGHJIDA is due to the fillet radius and, produced longitudinally, closely represents a quarter of a cylinder. The region between D and I, however, since the cylinder is wrapped against the valley side on the one hand and the valley floor on the other, produces a toroid. Because of the slant produced by positive angle α_4 the region AFGD is again a cylinder, but now slanted off the perpendicular.

At ignition, the surfaces represented in Figure 5-2 all move in a direction perpendicular to the surface tangent at each point. As mentioned previously, area ABCD moves longitudinally, creating a new star-shaped region. The plane of the star valley wall moves in its usual direction. The toroidal channel grows in radius.

At a time further in the burn, a shape like that of Figure 5-3 emerges. Since the governing force that controls the star region (not the transition region) is the moving together of the two planes representing the valley sides, it can be seen that under the supposition of constant burn rate there will be a time after which the line joining the star peaks will be parallel to the motor axis. That supposition is not made; however, this line should vary from the parallel by only a small amount. After the line reaches parallelism (under the assumption, again, of constant burn rate), the whole star section is of homogeneous geometry; that is, the geometrical mensuration quantities at any plane perpendicular to the motor centerline are the same.

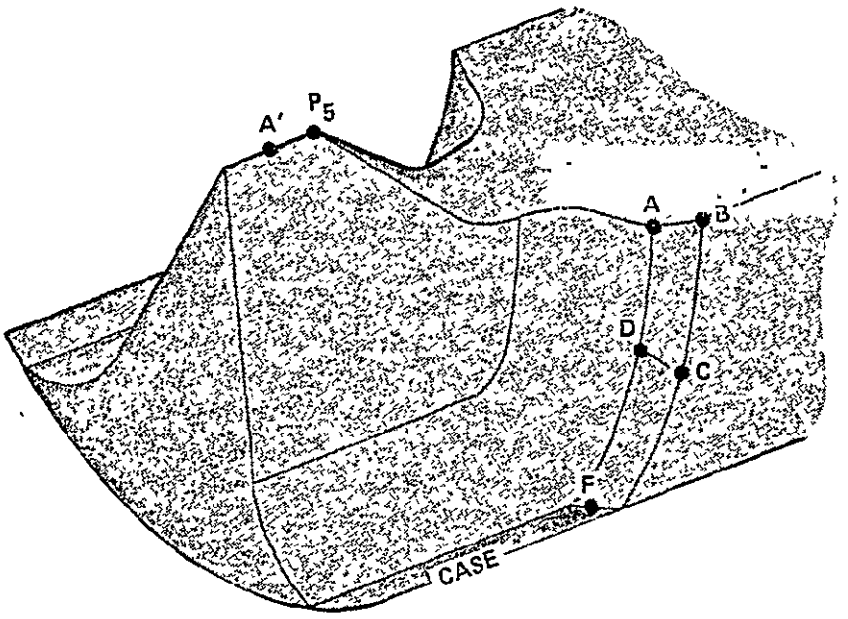

Figure 5-3. A STAR-CP INTERFACE DURING BURNING

While the general case is where the burn rate varies longitudinally along the motor axis, it is helpful and not too incorrect to assume constant burn rate. The computer code developed does not assume this, but the events themselves are intuitively easier to picture with that qualifier.

Notice in Figure 5-3 that a new star region is still being created as a result of the regression of plane ABCD. This continues throughout the burn, the only change being the subtle change occurring when ABCD burns out. The toroidal channel of Figure 5-2 has grown in dimensions; its center, however, remains in the same position. In Figure 5-3, web burn-through has occurred in the star valley, as seen from the presence of a bare case. It will be noted that the star peak region in which point A' is placed is receding at an accelerated rate, dependent only on the case sector angle and the angle of the valley side. Care must be taken in any analytical routine to include this fact.

Attention is now turned to Figure 5-4, which represents a time still further into the burning. Plane ABCD of Figure 5-2 is gone, as is most of the original star region. Notice that a star is still being created because of a longitudinal burning component at point B (Figure 5-4). That burning is, of course, governed by the radius of the arc connecting the star valley floor and the forward face of the CP section. This radius grows at the rate given by the burn-rate, and proceeds until no propellant is left. The growth of the toroidal channel produces the curved valley side. It is also the driver for telling where complete grain annihilation has occurred.

The modeling of the transition region is achieved by tracking seven important points, and then using a star geometry program based on the one described above, augmented to be more general. An increment-dividing plane is placed at each of these seven points; and as these points move, the IDP's associated with each point are allowed to move with them. Before going into specifics concerning the placement of these points and the philosophy associated therewith, time will be taken to describe the generalized star geometry model.

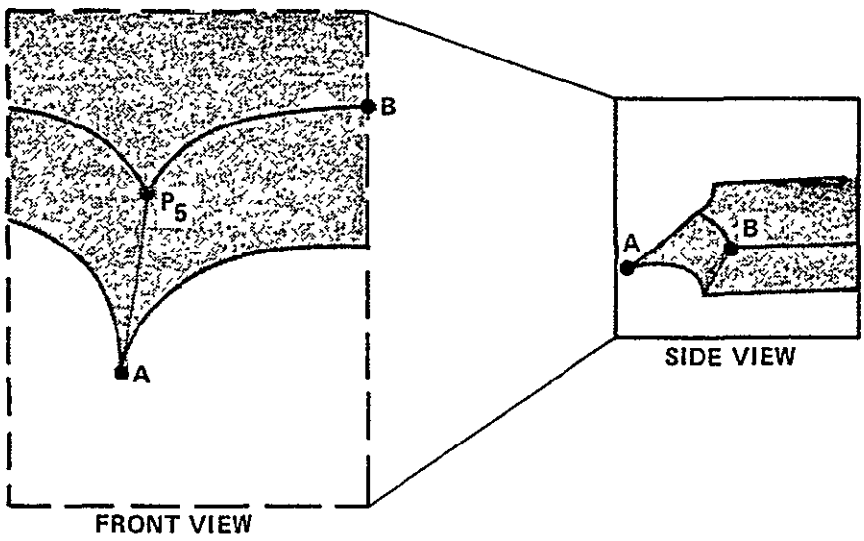

Figure 5-4. A STAR-CP INTERFACE LATE IN THE BURN

As just discussed, the star geometry routine needs the following pieces of information (Figure 5-5):

r_1	initial port radius
s_b	distance burned
r_2	distance from centerline to bottom of star valley - r_f
r_f	radius of the fillet in the star valley
r_{top}	width of the star valley at the top
r_{bot}	width of the star valley at the bottom
r_c	radius of the case (centerline to insulation)
N_{stars}	number of star points in a cross section

All other necessary constants can be calculated from this set. In terms of how the original star routine used this data, it was noticed that the set is redundant.

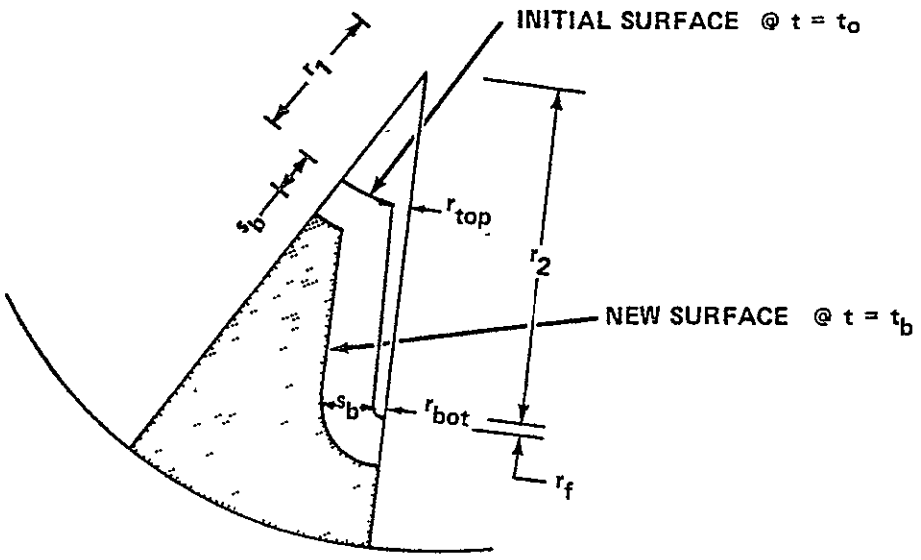

Figure 5-5. QUANTITY DEFINITIONS IN A STAR SECTOR

The terms involving r_1, s_b, and r_f can be replaced with the two new terms

$$\bar{r}_1 = r_1 + s_b$$
$$\bar{r}_f = r_f + s_b$$

that is, at any given time in the burn, the port radius is given by $\bar{r}_1$. But then, the values of r_1 and s_b need not be stored; and instead of obtaining values from r_1 and s_b, $\bar{r}_1$ can be used effectively with s_b set at zero. All information necessary to the routine can then be input as $\bar{r}_1$ or $r_1 + s_b$. Similar statements can be made concerning $\bar{r}_f$ and s_b.

To illustrate this point, consider Figure 5-6. Since the geometry routines, in effect, work with present port radius and present fillet radius (this is a simplified approach, but accurate), then it doesn't matter whether the routine is fed r_1 and s_b, or r_f and s_b and calculates $\bar{r}_1$ and $\bar{r}_f$, or whether $\bar{r}_1$ and $\bar{r}_f$ are fed directly as *initial* port radii and *initial* fillet radius and the burn distance is set equal to zero. The two approaches are the same, both logically and computationally.

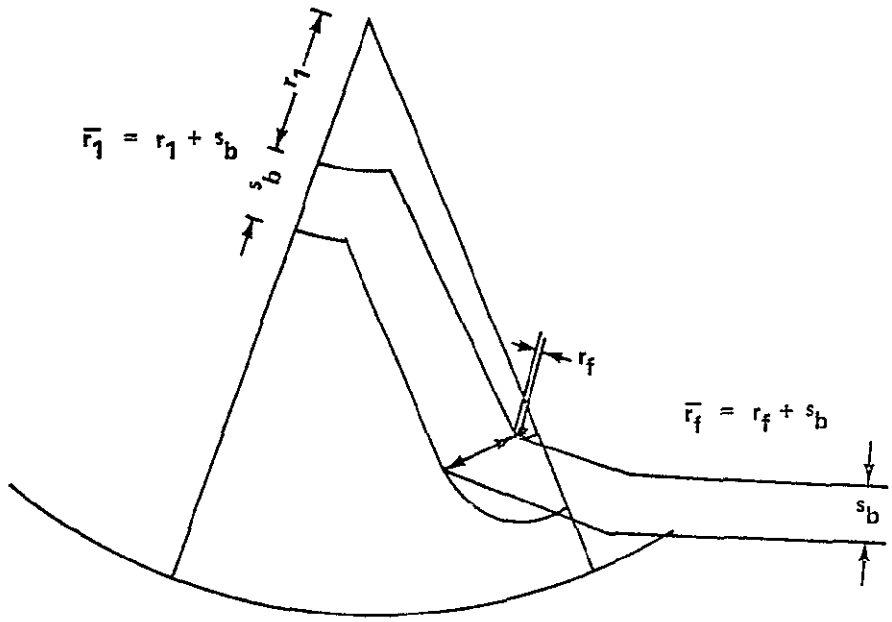

Figure 5-6. NOMENCLATURE FOR AN UPDATED STAR MODEL

Consider now the transition region just described. There are some semantics necessary before proceeding to the seven moving points. In the star geometry routine, the value r_1, either as input by itself or as input in the form $\bar{r}_1$, is the initial port radius. In the region under discussion, then, r_1 stands for that value of the port radius existing at a point the instant that the geometry at that point changed from CP configuration to a star configuration. Although this value is essentially *not* the initial port radius, it is the initial radius as concerns geometry calculations at that point as a star configuration. This sequence of events is shown in Figure 5-7. At ignition, the situation in (a) prevails, with an initial port radius, r_1. In (c), the moving plane has progressed to the point where the star is being burned into the cross sectional plane at A. The time that occurs is represented in (b). Notice that the advancing plane is directly at position A. At any time after this, the existing geometry at A is star shaped; at any time before, it is CP. That value of s_b which places the advancing plane right at A is called s_b^*, and the value $r_1 + s_b^*$ is then taken to be the initial port radius at A *(at that time when the geometry at A changed radically)*.

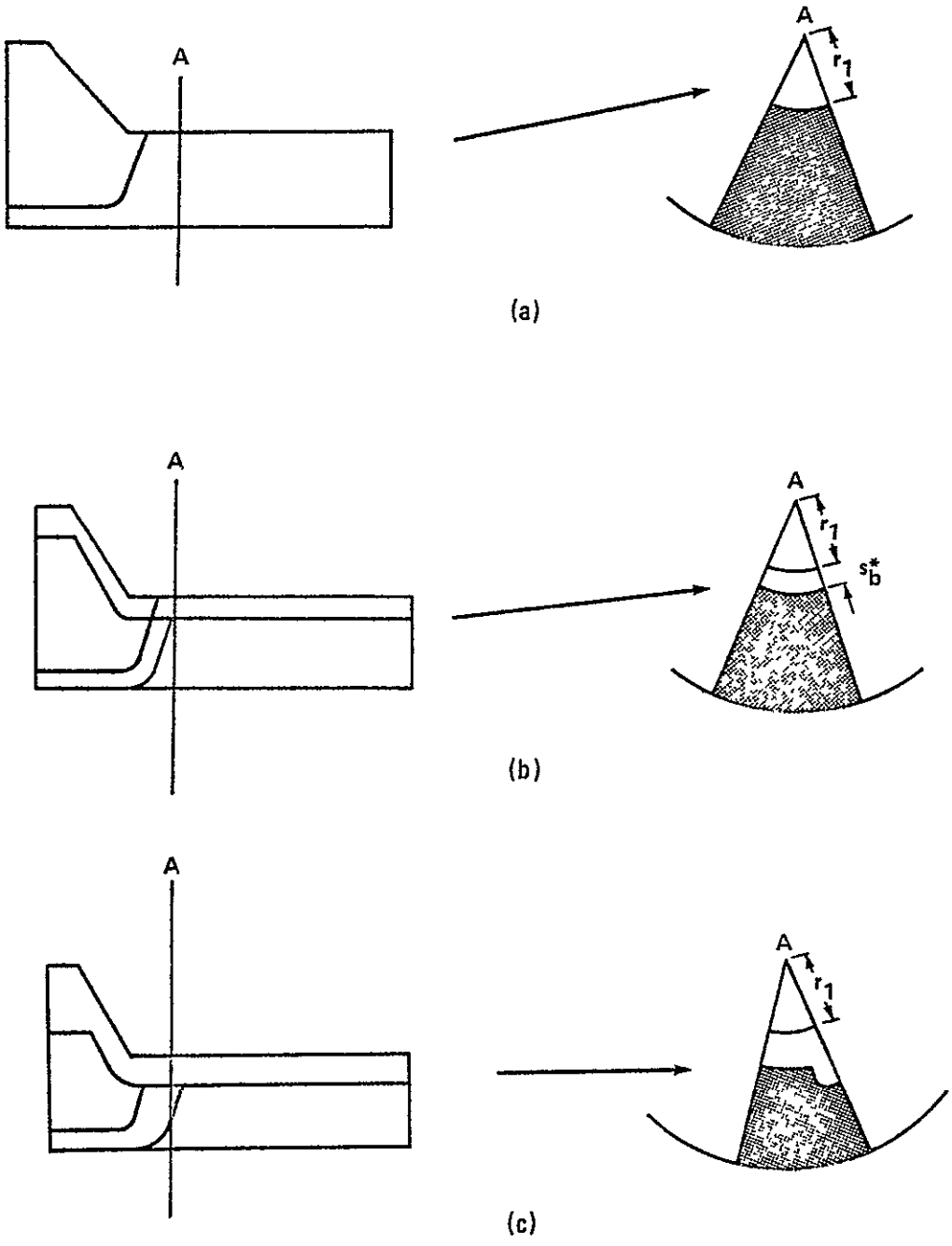

Figure 5-7. FORMATION OF A STAR VALLEY IN A PREVIOUSLY CP SECTION

For $s_b > s_b^*$,

$$r_1 + s_b = (r_1 + s_b^*) + (s_b - s_b^*),$$

which gives a general computational rule the likes of which have been discussed. The term $r_1 + s_b^*$ is the initial port radius at A; $s_b - s_b^*$ is the distance burned (after the geometry at A became star shaped).

The subtleties of those distinctions are necessary to properly supply the generalized star geometry routine with the necessary input parameters. The specific geometry in this region points out why it is necessary to have the CP routine working on a sector basis--in order to have the necessary continuity between star and CP. The calculations for r_1 can also be made for r_f.

5.1 TRACKING SEVEN POINTS

In order to adequately model the transition region, the region must be broken into at least six mass addition regions. At the beginning of the burn, some of these regions are degenerate, while at the end, other regions are degenerate. (A degenerate mass addition region is one between two IDP's occupying the same position.) The seven positions bounding these six mass addition regions will be the points tracked to determine the transition region geometry. The seven points have been chosen either to simplify volume and surface area calculations or to indicate abrupt changes in port geometry.

Figure 5-8 presents the initial position of the seven points, named P_1 to P_7, along with the path that each will take during the burn. The rest of subsection 5.1 deals with the definition of these points and the mathematical equations that govern their motions.

5.1.1 Tracking Point P_1

Point P_1 is established initially at the point just before the large taper which takes the star into the CP region. It marks this position until it reaches a point just before it moves down the arc indicated in Figure 5-8. When it reaches the arc, P_1 moves down a burn-back parabola. While on this arc, P_1 marks a position of radical geometry change.

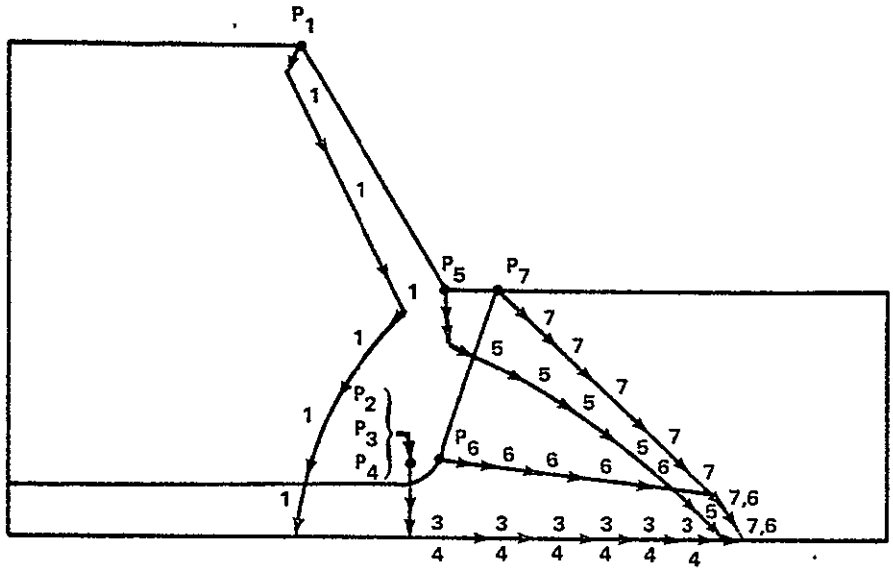

Figure 5-8. THE PATHS OF SEVEN IMPORTANT POINTS

The reason for P_1's strange descent before the arc is because that once the concave portion of a star peak is burned out, the star recedes at an increased rate. Figure 5-9 presents a more intimate view of the path of P_1. From surface AO_1 to surface BO_2 (AO_1 is the initial unburned surface) the point P_1 progresses down an angle bisector. Since the port radius is input at the initial position of P_1 through a reference plane there, and this same item is input for the two adjacent reference planes surrounding P_1, then the slope of the grain between A' and O_1, and between O_1 and A can be determined. Using the arc tangent function, angle α can be determined and so the angle O_2O_1A is known. P_1 proceeds along this angle bisector until the concave region of the star point at O_1 is burned out.

When point P_1 reaches O_2, the time begins where the grain regression is accelerated in region $B'O_2$. However, the acceleration is just a constant multiple of the burn-rate, as determined by the procedure described next.

Suppose the burn distance O_3O_3' is given to be 1. It is desired to obtain the grain regression constant, R, which will be the distance O_2O_2'. The only

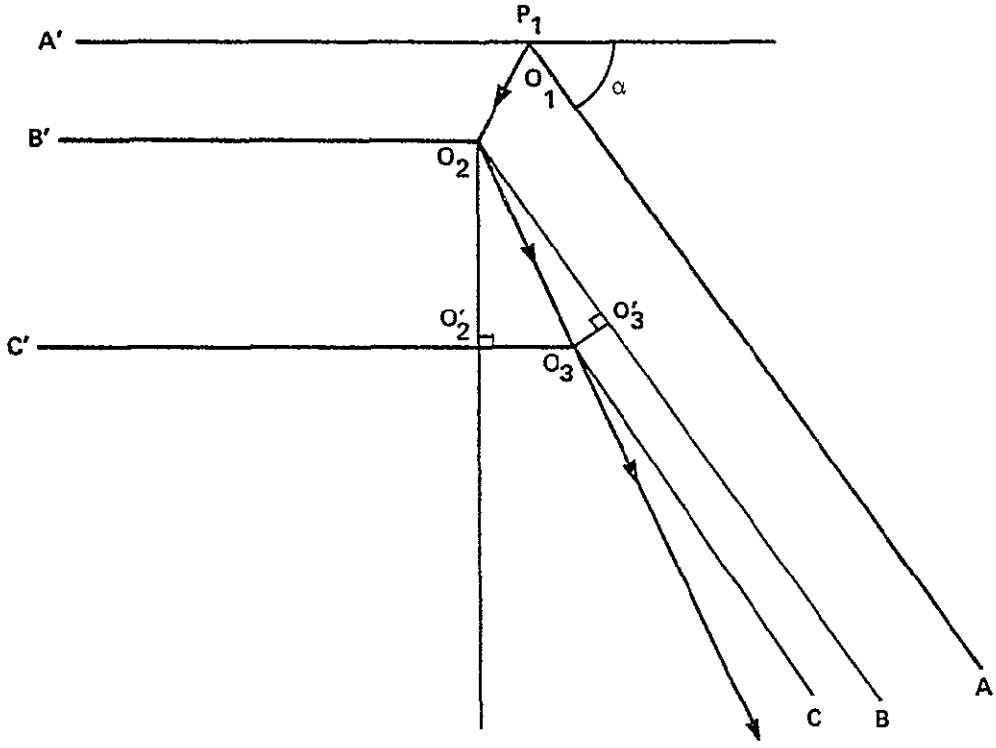

Figure 5-9. AN ANALYTICAL VIEW OF THE PATH OF P_1

things that will govern R are the angle of inclination of the star valley side (angle ϕ) and the sector angle ψ, that is, $\psi = \pi/n$ where n is the number of star points. By the choice of coordinate axes (Figure 5-2) the length R is a length on the star peak centerline.

The two line formulas are given by

$$y = x\tan\psi$$

$$y = -x\tan\phi + s_b/\cos\phi + C$$

where C is a constant

Substituting 0 and 1 for s_b (the points represented by 0_2 and $0_2'$ respectively) obtain

$$y_1 = -x_1\tan\phi + C$$

$$y_2 = -x_2\tan\phi + 1/\cos\phi + C,$$

so that $$y_2 - y_1 = -(x_2 - x_1)\tan\phi + \frac{1}{\cos\phi}$$

From the star peak centerline equation, obtain

$$y_2 - y_1 = (x_2 - x_1)\tan\psi$$

so that

$$(\tan\psi + \tan\phi)(x_2 - x_1) = 1/\cos\phi$$

or

$$x_2 - x_1 = \frac{1}{\cos\phi(\tan\psi + \tan\phi)}$$

Translating this distance to the star peak centerline there is

$$R = \overline{O_2O'_2} = \frac{x_2 - x_1}{\cos\psi} = \frac{1}{\cos\psi\cos\phi(\tan\psi + \tan\phi)}$$

As noted, R will be called the grain regression constant.

The path that point P_1 takes immediately after passing point O_2 can now be described. For an analytical view of the situation, consider Figure 5-10. Side AB is the initial grain surface, and CE is the burning surface after burning length $\overline{CB}$ from AB. $\overline{CB}$ is set to 1 in the above example. Since angle α is known; by congruence methods, angle $\measuredangle GBF$ also has angle measure α. Knowing that $\measuredangle GBH$ is right, then $\measuredangle FBH = \pi/2 - \alpha$. From this, and opposite angles, $\measuredangle ABI = \pi/2 - \alpha$. Likewise, $\measuredangle BCH = \frac{\pi}{2} - \alpha$. From the above discussion, it is known that length $\overline{AD} = R$, the grain regression constant, where $\overline{BC} = 1$, so $\overline{BH} = \cos\alpha$, $\overline{CH} = \sin\alpha$. But then, $\overline{IB} = R - \cos\alpha$ so that $\overline{AB} = (R - \cos\alpha)/\sin\alpha$

Hence, $$\tan\zeta = \frac{1}{\frac{R - \cos\alpha}{\sin\alpha}}$$

or $$\tan\zeta = \frac{\sin\alpha}{R - \cos\alpha}$$

But then,

$$\zeta = \arctan\left(\frac{\sin\alpha}{R - \cos\alpha}\right).$$

When R is exchanged for its value, ζ can be written as

$$\zeta = \arctan\left[\frac{\cos\phi\cos\psi\sin\alpha(\tan\phi + \tan\psi)}{1 - \cos\phi\cos\psi\cos\alpha(\tan\phi + \tan\psi)}\right].$$

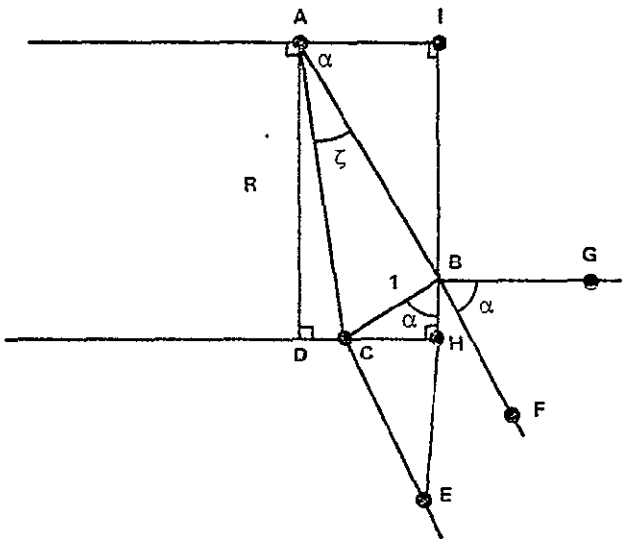

Figure 5-10. NOMENCLATURE TO DEFINE THE PATH OF P_1

Knowing ζ, then angle $\measuredangle DAC$ is known, and the path of P_1 after reaching O_2 (of Figure 5-9) is known. It is stressed that point P_1 cannot be truly extended down the angle bisector of $\measuredangle A'O_1A$ because of this accelerated nature of the regression of the surface $B'O_2$. In fact, the true path of P_1 is a radical divergence from the angle bisector, in general being in the opposite direction.

P_1 is now partially tracked. For the remaining portion of its path, consider the situation of Figure 5-11. The surface of the grain is given by curve DBCE, the arc $\overset{\frown}{BC}$ arising from the inside angle at A, and $\overline{AB} = \overline{AC}$. Point P_1 now is at B. Notice there is a sharp peak at B, indicating an abrupt change in geometry. This situation does not exist at C since line CE is tangent, to arc $\overset{\frown}{BC}$ at C. P_1 is then given the job of tracking the point B through time to be able to demarcate the change in geometry. At any time, arc $\overset{\frown}{BC}$ is given by a circle equation and line DB given by a trivial line equation. The intersection of the two, through time, gives rise to a burn-back parabola, along which P_1 will travel. The mathematics of the derivation

of the path of P_1 in this section of the burn is like that done above and is omitted.

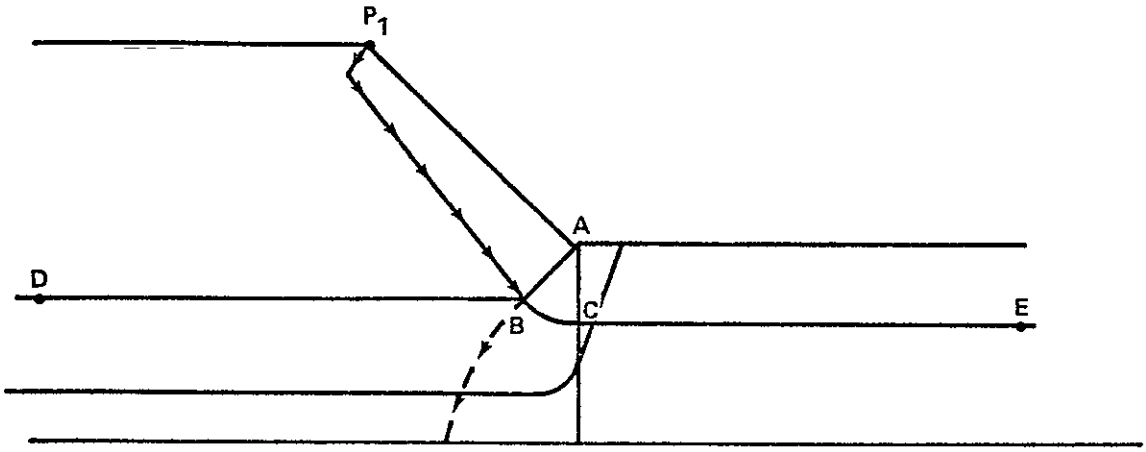

Figure 5-11. POINT P_1 TRAVELS ALONG A BURN-BACK PARABOLA

The mensuration quantities obtained for the mass addition region ending at P_1 are obtained in the same manner as those in the star region.

5.1.2 Point P_2 (Stationary)

Point P_2 is included as an increment dividing plane location only, and exists so that the mass addition region between P_1 and P_2 does not become too large. It is positioned at the center of the circle connecting the star valley floor with the CP face (Figure 5-12). It is not allowed to move, and the geometry there is always star geometry until burnout occurs.

The values of grain surface area and port volume between P_1 and P_2 belie the simplicity of the movement of P_2. Because of the circular trough appearing at A in Figure 5-11, the grain surface is not linear. For this reason, and for the reason that there does not exist a surface area formula as general as the prismatoid volume formula, it was deemed necessary to cut the interval between P_1 and P_2 into several subintervals, calculate initial grain constants at each cut point using the star geometry routine, and calculate the volume and surface area of the mass addition region as the sum of those quantities of each subinterval. The method used is to once again depend on the cone frustum formulas, which essentially means a linearization, or better, a piecewise linearization

of the grain between P_1 and P_2. The number of subintervals is given as a trade-off between accuracy and expediency.

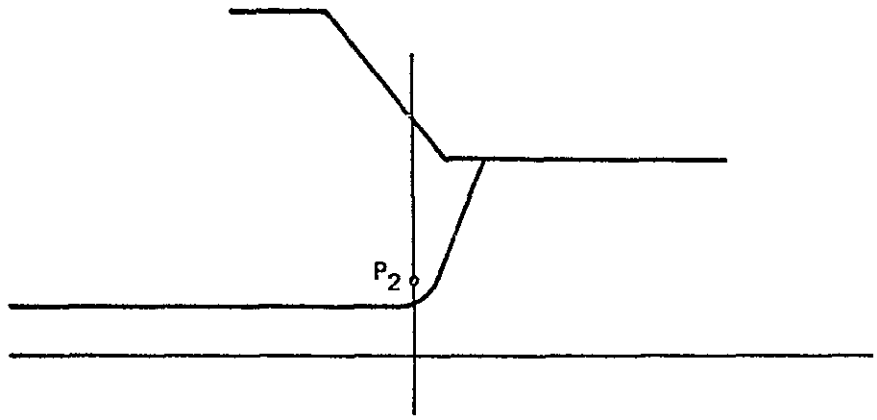

Figure 5-12. THE STATIONARY POSITION OF POINT P_2

5.1.3 Tracking Point P_3

P_3 is used to mark the position of point A in Figure 5-4--the point of grain annihilation. The point, of course, remains stationary until a given distance burned, and is then tracked in the aft direction.

The governing geometric figures which give rise to the analytic equations governing the motion of P_3 are the toroidal channel in the star valley and the plane which represents the centerline of a star peak produced longitudinally. As the toroid expands during the burning, it will intersect the mentioned plane. At the time of first intersection, the entire valley wall of the star has been eliminated. When the toroid gets large enough to reach the line given by the plane's intersection with the case wall, total annihilation of the grain at that point is assured. Once the toroid reaches this line, the point of intersection recedes toward the aft end. This point is P_3.

Using the Cartesian coordinate system described in Figure 5-2, the equation of the toroid (with respect to subsection 2.2) is given as

$$(x - \bar{r}_2)^2 + (z - P)^2 = \left(\sqrt{(r_f + s_b)^2 - (y - r_4)^2} + r_2 - \bar{r}_2\right)^2$$

where

r_f and s_b are described above, and

P = longitudinal position of plane P_2

$\bar{r}_2 = r_2 - r_3 + r_f$

r_3 = radius of the circle connecting the valley floor with the CP face

$r_4 = r_{bot} - r_f/\cos\phi$

ϕ = angle the star side makes with the x-axis.

The line given by the intersection of the centerline plane with the case wall is given in three space as

$$\begin{cases} x = r_c \cos\psi \\ y = r_c \sin\psi \\ z \end{cases}$$

Substituting this line into the toroid gives

$$z = P + \sqrt{\left(\sqrt{(r_f + s_b)^2 - (r_c \sin\psi - r_4)^2} + r_3 - r_f\right)^2 - (r_c \cos\psi - \bar{r}_2)^2}$$

where P is the position (longitudinal) of P_2 and $s_b \geq s_{b,m}$,where $s_{b,m}$ is the maximum burn distance at position P_2. Everything in this equation is known, and so P_3 can be determined directly; that is, the point of total grain annihilation can be calculated at any time during the burn.

The point is initially positioned at position P_2, and is stationary until $s_b \geq s_{b,m}$. It is then allowed to progress toward the aft end (determined by the choice of the plus sign in the above expression giving z). The geometric mensuration quantities existing at P_3 are simply made by the following instructions.

(1) If $s_b \leq s_{b,m}$ quantities at P_3 = quantities at P_2

(2) If $s_b \geq s_{b,m}$ port area is maximum at $\frac{1}{2} r_c^2 \psi$, port perimeter is 0.

When $s_b \geq s_{b,m}$,then there is a positive distance separating P_2 and P_3. Since no grain exists between these two planes, by the very definition of P_3, then no grain surface exists, and the port volume calculations are made using the frustum formula described above. To induce generality, notice that this same situation holds when $s_b \leq s_{b,m}$,since then the distance between P_2 and P_3 is zero, and so no surface area exists and the frustum formula for volume can be used, but will also yield zero.

5.1.4 Tracking Point P_4

P_4 marks, again, a position of abrupt geometry change. It is also placed at position P_2 at the beginning of the burn, and is used to mark the burnout of the star valley floor (see the region about point F in Figure 5-3). Its position is controlled by the growth of the circle (cylinder, actually), whose center is marked as P_2 in Figure 5-12. Point P_4 remains stationary at position P_2 until $s_b \geq s_{b,v}$ where $s_{b,v}$ gives the web thickness in the valley floor. Once this circle reaches the case wall, the growth of the circle then forces P_4 toward the end of the segment.

In the Cartesian coordinate system described in Figure 5-2 the circle and case plane are given by

$$\text{circle: } (x - \bar{r}_2)^2 + (z - P)^2 = (r_3 + s_b)^2$$

$$\text{plane: } x = r_c$$

where P represents the longitudinal position of plane P_2. Upon substitution, obtain

$$(r_c - \bar{r}_2)^2 + (z - P)^2 = (r_3 + s_b)^2$$

or

$$z = \sqrt{(r_3 + s_b)^2 - (r_c - \bar{r}_2)^2} + P \qquad s_b \geq s_{b,v}$$

where the plus sign denotes movement toward the aft end.

When $s_b \leq s_{b,v}$,the cross sectional port area and port fuel perimeter are assigned those at P_2. When $s_b \geq s_{b,v}$,those values are obtained through the use of the modified star geometry routine. The volume and grain surface area between P_3 and P_4 are obtained by cutting the distance between P_3 and P_4 into halves, using the cone frustum surface area formula in each half, and using the general prismatoid volume formula over the whole region.

5.1.5 Tracking Point P_5

The next point to be tracked is the point which specifies the position of burnout of the concave portion of the star peak. This is position P_5 on Figures 5-4 and 5-8. From Figure 5-2, it is clear that the quarter cylinder AFGD will control the position of P_5 for some of the burn, and the torus at the bottom of the valley will control it for the rest.

At the beginning, P_5 is placed at position A of Figure 5-11. It remains at that point until the concave portion of the star peak has burned out. In effect, P_5 is placed at A until the cylinder has grown large enough to intersect the star peak center plane. It is then allowed to travel in the positive z direction (Figure 5-2 for coordinate reference). When the burning surface at P_5 has reached a level close to $\bar{r}_2$, then the motion of P_5 is governed by the toroid mentioned above. This condition exists until P_5 reaches the case wall.

Notice from Figure 5-1 that the cylinder leans in the positive z direction by angle α_4. It also leans in the positive y direction by angle ϕ, the slant of the star valley side. In accordance with subsection 2.2, the cylinder has equation

$$\left[\frac{x - (\bar{r}_2 + z \sin(\frac{3\pi}{2} + \phi) \cot\alpha_4)}{(r_f + s_b)/\sin\alpha_4}\right]^2 + \left[\frac{y - (r_4 + z \cos(\frac{3\pi}{2} + \phi)\cot\alpha_4)}{r_f + s_b}\right]^2 = 1$$

If α_3 is the slope of the grain immediately after the initial position of P_5, then the port itself is a cone with equation

$$x^2 + y^2 - (\tan\alpha_3 z + r_1^*)^2 = 0$$

where r_1^* is the port radius at the initial position of P_5. At any particular time during the burn, the port surface, itself, has equation

$$x^2 + y^2 - (\tan\alpha_3 Z + r_1^* + s_b)^2 = 0$$

where s_b is understood again, to be the burn distance. The annihilation takes place at the star peak center plane which has equation

$$x = y/\tan\psi.$$

Substituting this into the cone equation, obtain

$$y = (\tan\alpha_3 z + r_1^* + s_b)\ \sin\psi$$

Hence,

$$x = (\tan\alpha_3 z + r_1^* + s_b)\ \cos\psi$$

Using these values and substituting back into the cylinder equation, there is

$$\left[\frac{(\tan\alpha_3 z + r_1^* + s_b)\ \cos\psi - (\bar{r}_2 + \sin(\frac{3\pi}{2} + \phi)\ \cot\alpha_4 z)}{(r_f + s_b)/\sin\alpha_4}\right]^2 +$$

$$\left[\frac{(\tan\alpha_3 z + r_1^* + s_b)\sin\psi - (r_4 + \cos\ (\frac{3\pi}{2} + \phi)\ \cot\alpha_4 z)}{r_f + s_b}\right]^2 = 1$$

which will reduce to a form such as

$$az^2 + bz + c = 0$$

where

$$a = (\tan\alpha_3\sin\psi - \sin\phi\cot\alpha_4)^2 + \sin^2\alpha_4(\tan\alpha_3\cos\psi + \cos\phi\cot\alpha_4)^2$$

$$b = 2\ [(\tan\alpha_3\sin\psi - \sin\phi\cot\alpha_4)\ (\sin\psi(r_1^* + s_b) - r_4) +$$

$$\sin^2\alpha_4(\tan\alpha_3\cos\psi + \cos\phi\cot\alpha_4)\ (\cos\psi(r_1^* + s_b) - \bar{r}_2)]$$

$$c = (\sin\psi(r_1^* + s_b) - r_4)^2 + \sin^2\alpha_4\ (\cos\psi(r_1^* + s_b) - \bar{r}_2)^2 - (s_b + r_f)^2$$

and so the position of P_5 can be deduced using the quadratic formula.

After the burning has taken the surface to about the level of $\bar{r}_2$, then the motion of P_5 is governed by the intersection of the torus with the star peak center plane.

As seen, the torus has equation

$$(x - \bar{r}_2)^2 + (z - P)^2 = (\sqrt{(r_f + s_b)^2 - (y - r_4)^2} + r_3 - r_f)^2$$

The plane has equation

$$x = (z\tan\alpha_3 + r_1^* + s_b)\ \cos\psi$$

$$y = (z\tan\alpha_3 + r_1^* + s_b)\ \sin\psi$$

Substituting these expressions for x and y above, yields

$$(z\tan\alpha_3\cos\psi + (r_1^* + s_b)\cos\psi - \bar{r}_2)^2 + z^2 =$$
$$(\sqrt{(r_f + s_b)^2 - (z\tan\alpha_3\sin\psi + (r_1^* + s_b)\sin\psi - r_4) + r_3 - r_f})^2$$

Notice that this is a fourth degree equation in z. Because of the complicated nature of this particular equation, a Newton-Raphson iteration process is utilized, with an initial guess of $z_0 = s_b$, the process converges rapidly. It is estimated that in this case only four iterations are necessary to bring the answer to within seven decimal place accuracy.

The mensuration quantities at P_5 are obtained by use of the modified star geometry routine. The surface area and port volume between P_4 and P_5 are calculated in the same way as those between P_3 and P_4.

5.1.6 Tracking Point P_6

The path of P_6 is probably the simplest, other than that of P_2. Notice that P_6 begins beneath point A (Figures 5-8 and 5-11) at the point of tangency of the CP face with the circle in the star valley. It progresses in a linear fashion until it overtakes point P_7, at which time the two are considered the same.

The governing equation is

$$z = s_b\cos\alpha_4$$

$$x = \bar{r}_2 + r_3\sin\alpha_4 + s_b\sin\alpha_4.$$

The mensuration quantities here are obtained from the modified star geometry routine, and the port volume and surface area are obtained in the same manner as that between P_3 and P_4.

5.1.7 Tracking Point P_7

The final point to be tracked is point P_7. At any time, points P_7 and P_1 mark the boundary of the defined transition region. Point P_7 is initially placed at the intersection of the CP region with the star at the aft position of the taper of a CP face (Figure 5-8). At the beginning, P_7 is tracked along

the angle bisector as shown in Figure 5-8. The angles are all known, so the angle bisector is known. The governing equations are

$$\begin{cases} z = z^* + s_b \dfrac{\sin\left(\frac{\pi}{4} - \frac{\alpha_4 + \alpha_3}{2}\right)}{\sin\left(\frac{\pi}{4} - \frac{\alpha_3 - \alpha_4}{2}\right)} \\ x = (z - z^*)\ \tan\alpha_3 + s_b/\cos\alpha_3 + x^* \end{cases}$$

where z^* is the initial position of P_7 and x^* is the port radius, there.

When Point P_6 catches P_7, as it must since they travel at the same rate but move in different angles, then point P_7 must travel down the burn-back parabola evolving from the grain surface and the intersection of the circle growing from position P_2, that is, the burn-back parabola generated from the equation set

$$\begin{cases} \text{circle:} & (x - \bar{r}_2)^2 + (z - P)^2 = (s_b + r_3)^2 \\ \text{line:} & x = (z - z^*)\tan\alpha_3 + s_b/\cos\alpha_3 + x^* \end{cases}$$

where P is the longitudinal position of point P_2.

The mensuration quantities are calculated by the CP routine, and the port volume and surface area of the region between P_6 and P_7 (when they are not zero) are calculated in the same manner as that between P_3 and P_4.

5.2 SUMMARY OF TRANSITION REGION

In Section V, the quantities of port volume and port fuel surface area were calculated as corollaries of the positions of seven points. These formulas ultimately depend only upon burn distance, and the particular dependent variable is calculated anew at each new value of burn-distance. In this manner, any computational errors are not accumulative, but should remain at the same level.

The difficulty of the region arises from the appearance of nonlinear star sides. This forces linear approximations to be made because of the absence in the literature of generalized surface area formulas to handle nonlinearity.

Section VI

GENERAL SUMMARY

This document was designed to present an analysis of the geometrical changes occurring in a burning solid rocket motor. From very simple assumptions about the grain regression, a unified functional approach was built to look at the regression problem as one of being functional in nature, depending only on the burn distance.

The burning in each particular geometrical region contributes to the overall result. The solution at any particular burn distance is initiated by specifying a burn rate and a delta time at each increment dividing plane. No assumptions were made as to the behavior of the burn rate, and it is allowed to vary in any fashion.

Once the burn rate and delta time are established at each IDP, the code progresses from plane to plane, calculating port perimeter and port area. From these quantities, the numerical values of port surface area and port volume are calculated for the mass addition region between the two planes. In a slot, only port volume is needed since no fuel surface area exists. This procedure is continued until the aft tangent plane is reached, at which time the code is ready for the next case.

Information from the reference plane input is used by the code to determine where the geometry delineations occur.

The results of this task are twofold: firstly, the incorporation of this geometry model into the SRB prediction program. No difficulties in this respect are foreseen; however, this incorporation is a large task in itself because of the tediousness and sensitivities involved. So that the reader can have a better understanding of what this code actually produces as useable quantities, Appendix C presents a sample case. Secondly, through equations like those presented here, and others depending on this geometry model, it is now felt that the theory exists to construct a computer program to calculate moments of inertia and centers of gravity of a burning SRM in a selfsufficient manner.

Section VII

REFERENCES

1. Smith, William K., *Calculus With Analytic Geometry*, The MacMillan Company, Toronto, Ontario, 1969.

2. *CRC Standard Mathematical Tables*, 21st Edition, Samuel M. Selby, ed., 1973, The Chemical Rubber Co., Cleveland, Ohio.

3. *Solid Rocket Booster Performance Evaluation Model*, Vol. 1, September 1974. Prepared for NASA by the Boeing Aerospace Co., Huntsville, Alabama, Reference No. DCN 1-2-50-23786.

APPENDIX A

SUPPLEMENTARY GEOMETRY

THE BRETSCHNEIDER–HERON FORMULA*

Consider the object in Figure A-1.

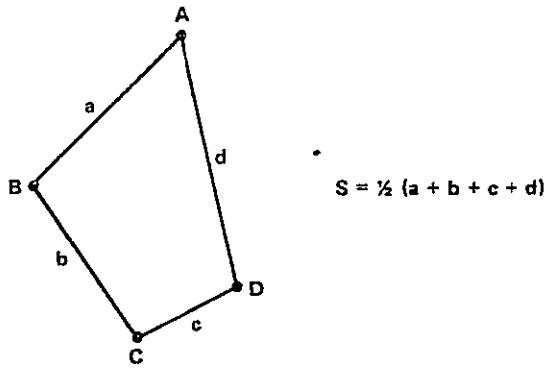

Figure A-1. A GENERAL QUADRILATERAL

The Bretschneider formula for the area, K, of quadrilateral ABCD is given by

$$K = \sqrt{(s-a)\ (s-b)\ (s-c)\ (s-d) - abcd\ \cos^2\zeta}$$

where ζ is either $\frac{A + C}{2}$ or $\frac{B + D}{2}$ and $s = \frac{1}{2}(a + b + c + d)$, where it is assumed that the quadrilateral is convex (that is, no corners greater than 180 degrees, and not a skew projection from 3-space).

In order to substantiate the formula, consider the augmented form given in Figure A-2, where line segment $\overline{BD}$ has been drawn in and labelled e.

Now, e itself is known by the law of cosines in two different manners:

$$e^2 = a^2 + d^2 - 2ad\ \cos A$$

This appendix has been provided to correct an error given in the definition of the Bretschneider Formula in the 21st Edition of the CRC Mathematical Handbook. This appendix provides the corrected equation and shows the theoretical development.

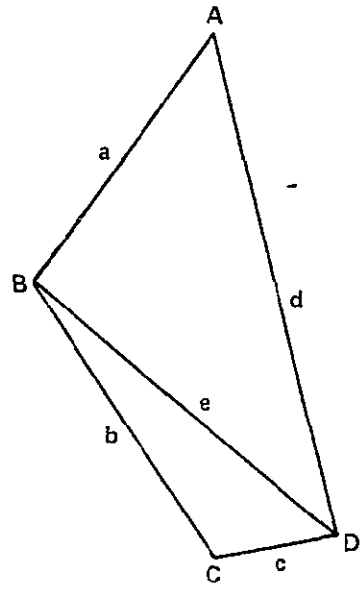

Figure A-2. A TRIANGULARIZATION OF A GENERAL QUADRILATERAL

and

$$e^2 = b^2 + c^2 - 2bc \cos C.$$

The angles A, B, C, D and sides a, b, c, d are, of course, considered to be known quantities.

In Figure A-2, the quadrilateral, denoted $\square ABCD$, is triangularized into two subtriangles, ΔABD and ΔBCD. The area K of $\square ABCD$, denoted $K_{\square ABCD}$, is the sum of the two triangular areas $K_{\Delta ABD}$ and $K_{\Delta BCD}$.

From elementary trigonometry,

$$K_{\Delta ABD} = \frac{1}{2} ad \sin A$$

and

$$K_{\Delta BCD} = \frac{1}{2} bc \sin C$$

Hence,

$$K^2_{\square ABCD} = K^2_{\Delta ABD} + 2K_{\Delta ABD}K_{\Delta BCD} + K^2_{\Delta BCD}$$

$$= \frac{1}{4}\,[a^2d^2\sin^2A + b^2c^2\sin^2C] + \frac{1}{2}\,abcd\,\sin A\,\sin C.$$

Using the cosine half angle formula (remembering that no angle in the quadrilateral is greater than 180 degrees), and the formula for the cosine of the sum of two angles, obtain

$$\sin A\sin C = 1 + \cos A\cos C - 2\cos^2\left(\frac{A+C}{2}\right).$$

Then

$$K^2_{\square ABCD} = \frac{1}{4}\,[a^2d^2\sin^2A + b^2c^2\sin^2C] + \frac{1}{2}\,abcd\,\left[1 + \cos A\cos C - 2\cos^2\left(\frac{A+C}{2}\right)\right.$$

$$= \frac{1}{4}\,[a^2d^2(1 - \cos^2A) + b^2c^2(1 - \cos^2C) + 2abcd + 2abcd\,\cos A\cos C]$$

$$- abcd\,\cos^2\left(\frac{A+C}{2}\right)$$

using $\sin^2\alpha + \cos^2\alpha = 1$.

Factoring, obtain

$$K^2_{\square ABCD} = \frac{1}{4}\,((ad + bc)^2 - (ad\,\cos A - bc\,\cos C)^2) - abcd\,\cos^2\left(\frac{A+C}{2}\right)$$

Using the expressions for e above,

$$ad\,\cos A = \frac{1}{2}\,(a^2 + d^2 - e^2)$$

$$bc\,\cos C = \frac{1}{2}\,(b^2 + c^2 - e^2)$$

so that

$$ad\,\cos A - bc\,\cos C = \frac{1}{2}\,(a^2 + d^2 - b^2 - c^2).$$

Then, using this identity, it is easy to show that

$$\frac{1}{4}\left((ad + bc)^2 - (ad\ \cos A - bc\ \cos C)^2\right) = (s-a)\ (s-b)\ (s-c)\ (s-d).$$

From this, the Bretschneider formula is obtained as

$$K^2_{\square ABCD} = (s-a)\ (s-b)\ (s-c)\ (s-d) - abcd\ \cos^2\left(\frac{A + C}{2}\right)$$

But

$\cos^2\left(\frac{A + C}{2}\right) = \cos^2\left(\frac{B + D}{2}\right)$, so the formula is stated

$$K_{\square ABCD} = \sqrt{(s-a)\ (s-b)\ (s-c)\ (s-d) - abcd\ \cos^2\zeta}$$

When one side of the quadrilateral is degenerate, that is, has zero length so that two vertices coincide, then another familiar formula arises. To see this, suppose that d = 0, that is, side $\overline{AD}$ is degenerate.

Then using the Bretschneider formula

$$K_{\square ABCD} = \sqrt{(s-a)\ (s-b)\ (s-c)\ (s-0) - abc(0)\ \cos^2\zeta}$$

or

$$K_{\square ABCD} = \sqrt{s(s-a)\ (s-b)\ (s-c)}$$

which is Heron's formula for the area of the general triangle with $s = \frac{1}{2}(a + b + c + d) = \frac{1}{2}(a + b + c)$.

Notice, however, that only Bretschneider's formula need be referenced, for with a degenerate side, Heron's formula is obtained. Referencing the star burning section, this property is used heavily, and the Bretschneider formula occurs with the name Bretschneider-Heron formula to denote the case when the formula is used to calculate the area of a triangle or a quadrilateral, or both. The two cases are shown simultaneously in Figure A-3.

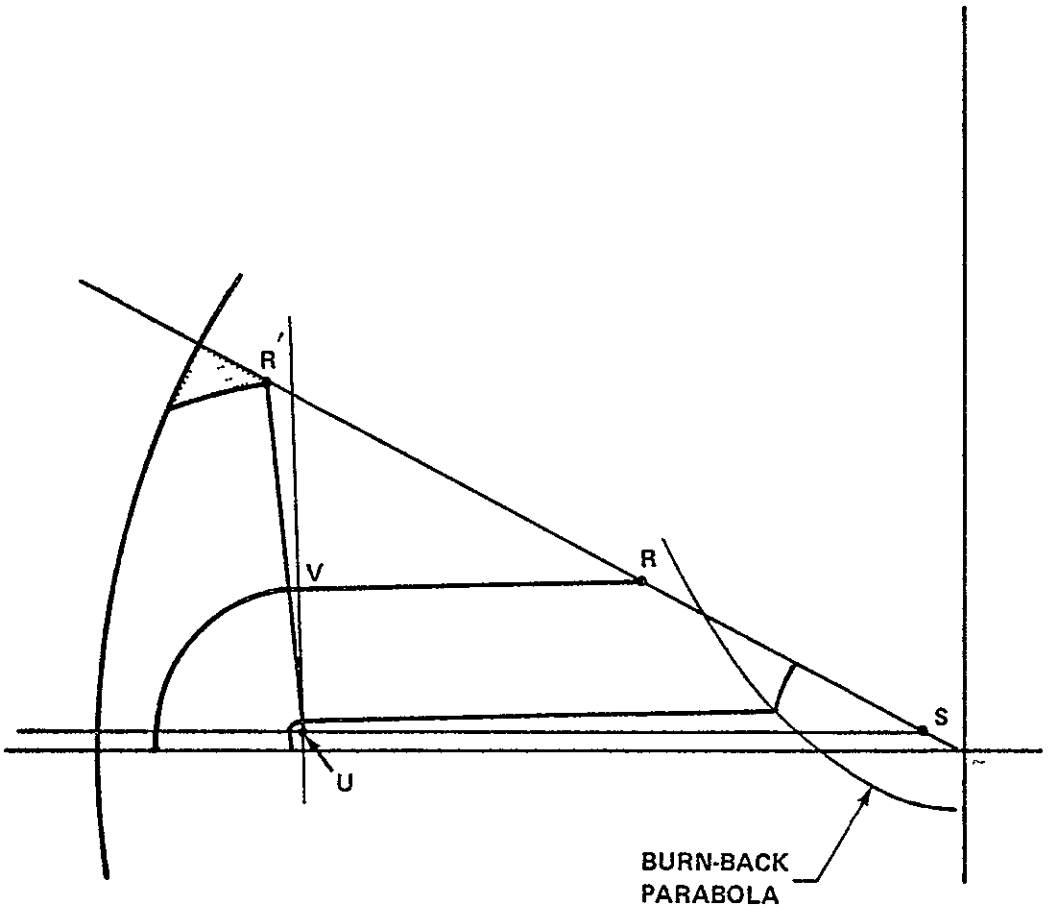

Figure A-3. THE USE OF THE BRETSCHNEIDER-HERON FORMULA

Knowing angles R, S, U, V, and sides $\overline{RS}$, $\overline{SU}$, $\overline{UV}$, and $\overline{VR}$, the Bretschneider-Heron formula can be used to calculate port area in quadrilateral RSUV. Further in the burn, R progresses to R' and sides $\overline{R'S}$, $\overline{SU}$, $\overline{UR'}$ are known; and the Bretschneider-Heron formula is used to calculate port area contributed by triangle R'SU, not mattering what the angles $\measuredangle UR'S$, $\measuredangle R'SU$, and $\measuredangle SUR'$ are.

Attention now is turned to another star-burning anomaly, that being to calculate the area of an angular segment of a sector of a circle. Consider the situation described in Figure A-4.

The objective is to calculate the area ABC. Angle α is known and $\beta = \pi - \alpha$, so $\sin\beta = \sin(\pi-\alpha) = \sin\alpha$.

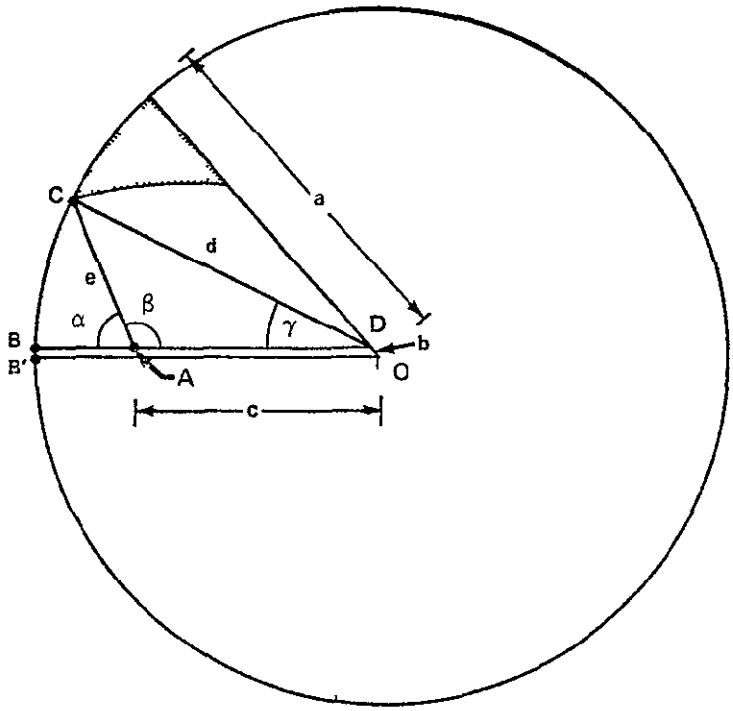

Figure A-4. THE DETERMINATION OF A PARTIAL SECTOR AREA OF A CIRCLE

Using the law of cosines

$$\gamma = \sin^{-1} (e\sin\beta/a).$$

The area of the circular sector ΔCOB^1 is given by $A_{sec} = \frac{1}{2} (a + b)^2\gamma$. Considering $\square BDOB'$, and subtracting the area of this quadrilateral using Bretschneider's formula, there is

$$A_{\Delta CDB} = \frac{1}{2} (a + b)^2\gamma - A_{\square BDOB'} .$$

The area of triangle ΔACD is given by

$$A_{\Delta ACD} = \frac{1}{2} ec \sin\beta$$

$$= \frac{1}{2} ec \sin\alpha$$

Hence, the area of the pie-shaped piece ABC is given by

$$A_{\Delta ABC} = \frac{1}{2}(a + b)^2\gamma - A_{\square BDOB'} - \frac{1}{2} ec \sin\alpha$$

$$= \frac{1}{2}(a + b)^2 \sin^{-1}(es\ina/a) - A_{\square BDOB'} - \frac{1}{2} ec \sin\alpha.$$

This particular expression is a close approximation to the real case, since the term $A_{\square BDOB'}$ is an approximation to the true area of BDOB', which is not a true quadrilateral.

APPENDIX B

SURFACE AREA AND VOLUME OF A TOROIDAL CHANNEL

MENSURATION QUANTITIES IN A TOROIDAL CHANNEL

Consider the situation of Figure B-1 where two circular arc lengths are established in the x-y Cartesian coordinate system, governed from the circle formula

$$(x-a)^2 + (y-b)^2 = r^2. \tag{B-1}$$

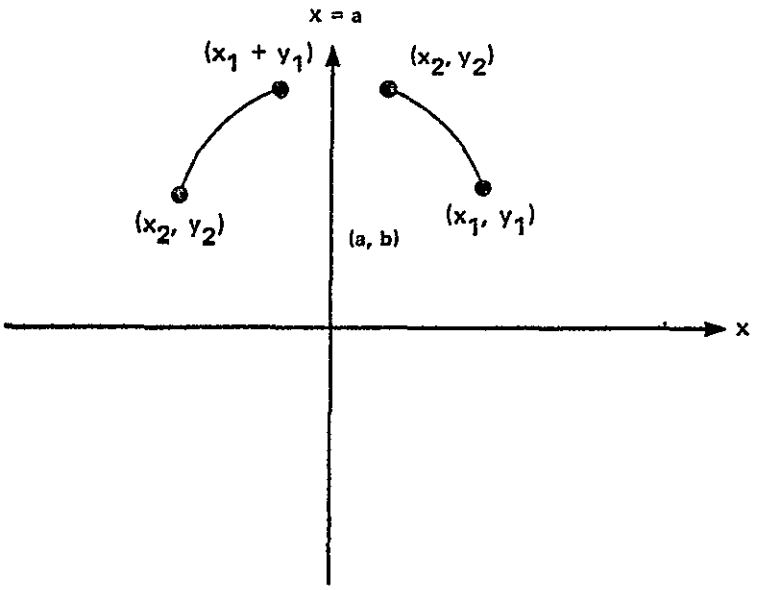

Figure B-1. ARCS USED TO GENERATE A TOROIDAL SURFACE

This formula can be replaced by an equivalent form by solving for y in terms of x as

$$y = b \pm \sqrt{r^2 - (x-a)^2} \tag{B-2a}$$

which, of course, is not a functional relationship. Interest here is in the upper semicircular region, and a true functional relation appears as

$$y = b + \sqrt{r^2 - (x-a)^2} \tag{B-2b}$$

From (B-1), the derivative of y can be obtained implicitly as

$$\frac{dy}{dx} = -\frac{x-a}{y-b} \tag{B-3}$$

so that

$$1 + \left(\frac{dy}{dx}\right)^2 = 1 + \frac{(x-a)^2}{(y-b)^2} = \frac{(x-a)^2 + (y-b)^2}{(y-b)^2}$$

$$= \frac{r^2}{(y-b^2)}$$

$$= \frac{r^2}{r^2 - (x-a)^2} \tag{B-4}$$

The length of arc can now be calculated for the arc between x_2 and x_1 (on either side of the line $x = a$) as

$$s = \int_{x_2}^{x_1} \sqrt{\frac{r^2}{r^2 - (x-a)^2}}\, dx$$

$$= r \int_{x_2}^{x_1} \frac{dx}{\sqrt{r^2 - (x-a)^2}}$$

$$= r \left[\arcsin \frac{x-a}{r}\right] \Bigg|_{x_2}^{x_1}$$

$$= r \left[\arcsin \frac{x_1 - a}{r} - \arcsin \frac{x_2 - a}{r}\right]$$

If the arc from x_2 to x_1 (in either case) is revolved about the x-axis, a toroidal channel emerges. The surface area and volume of the channel will now be calculated (Figure B-2).

The general formula for the area of revolution is, or course,

$$K = 2\pi \int_{\zeta_1}^{\zeta_2} y \sqrt{1 + \left(\frac{dy}{dx}\right)^2}\, dx,$$

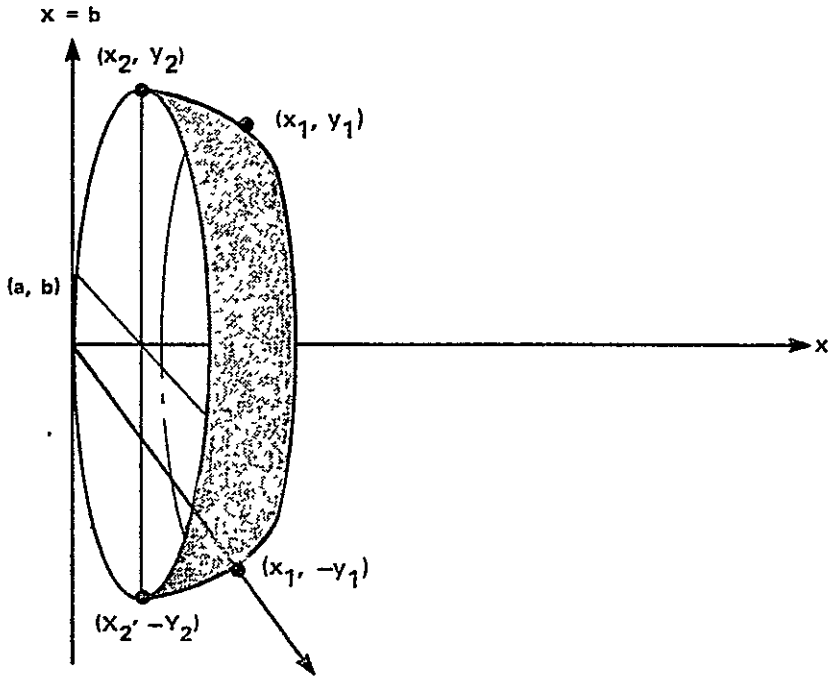

Figure B-2. A TOROIDAL SURFACE OF REVOLUTION

which interprets, in this case, as

$$K = 2\pi r \int_{x_2}^{x_1} \left(b + \sqrt{r^2 - (x-a)^2} \right) \Big/ \sqrt{r^2 - (x-a)^2} \; dx$$

using (B-2b) and (B-4).

But then,

$$K = 2\pi r \int_{x_2}^{x_1} \left(\frac{b}{\sqrt{r^2 - (x-a)^2}} + 1 \right) dx$$

$$= 2\pi br \int_{x_2}^{x_1} \frac{dx}{\sqrt{r^2 - (x-a)^2}} + 2\pi r \int_{x_2}^{x_1} dx$$

$$= 2\pi r\,(x_1 - x_2) + 2\pi b\left[\arcsin\frac{x_1 - a}{r} - \arcsin\frac{x_2 - a}{r}\right]$$

$$\underbrace{\qquad\qquad\qquad\qquad\qquad\qquad}_{\text{arc length}}$$

$$= 2\pi(r(x_1 - x_2) + b\ (\text{arc length})).$$

The general formula for finding the volume inside a surface formed by revolving a planar arc length about the x-axis is given by

$$V = \pi \int_{\zeta_1}^{\zeta_2} \pi y^2\, dx.$$

Adapting this general formula to the particular case at hand yields

$$V = \pi \int_{x_2}^{x_1} \left[b + \sqrt{r^2 - (x-a)^2}\right]^2 dx$$

$$= \pi \int_{x_2}^{x_1} \left(b^2 + 2b\sqrt{r^2 - (x-a)^2} + r^2 - (x-a)^2\right) dx$$

$$= \pi \left[b^2\,(x_1 - x_2) + 2b \int_{x_2}^{x_1} \sqrt{r^2 - (x-a)^2}\, dx + r^2\,(x_1 - x_2) - \int_{x_2}^{x_1} (x_1 - a)^2 dx\right]$$

$$= \pi \left[b^2\,(x_1 - x_2) + r^2\,(x_1 - x_2) + b\left[(x_1 - a)\sqrt{r^2 - (x_1 - a)^2} + r^2 \arcsin\frac{x_1 - a}{r} - (x_2 - a)\sqrt{r^2 - (x_2 - a)^2} - r^2 \arcsin\frac{x_2 - a}{r}\right] - \frac{(x_1 - a)^3}{3} + \frac{(x_2 - a)^3}{3}\right]$$

$$V = \frac{1}{2} r K + \pi \left[b^2 (x_1 - x_2) + b \left[(x_1 - a) \sqrt{r^2 - (x_1 - a)^2} \right. \right.$$

$$\left. \left. - (x_2 - a) \sqrt{r^2 - (x_2 - a)} \right] - \frac{(x_1 - a)^3}{3} + \frac{(x_2 - a)^3}{3} \right]$$

APPENDIX C
SAMPLE RESULTS

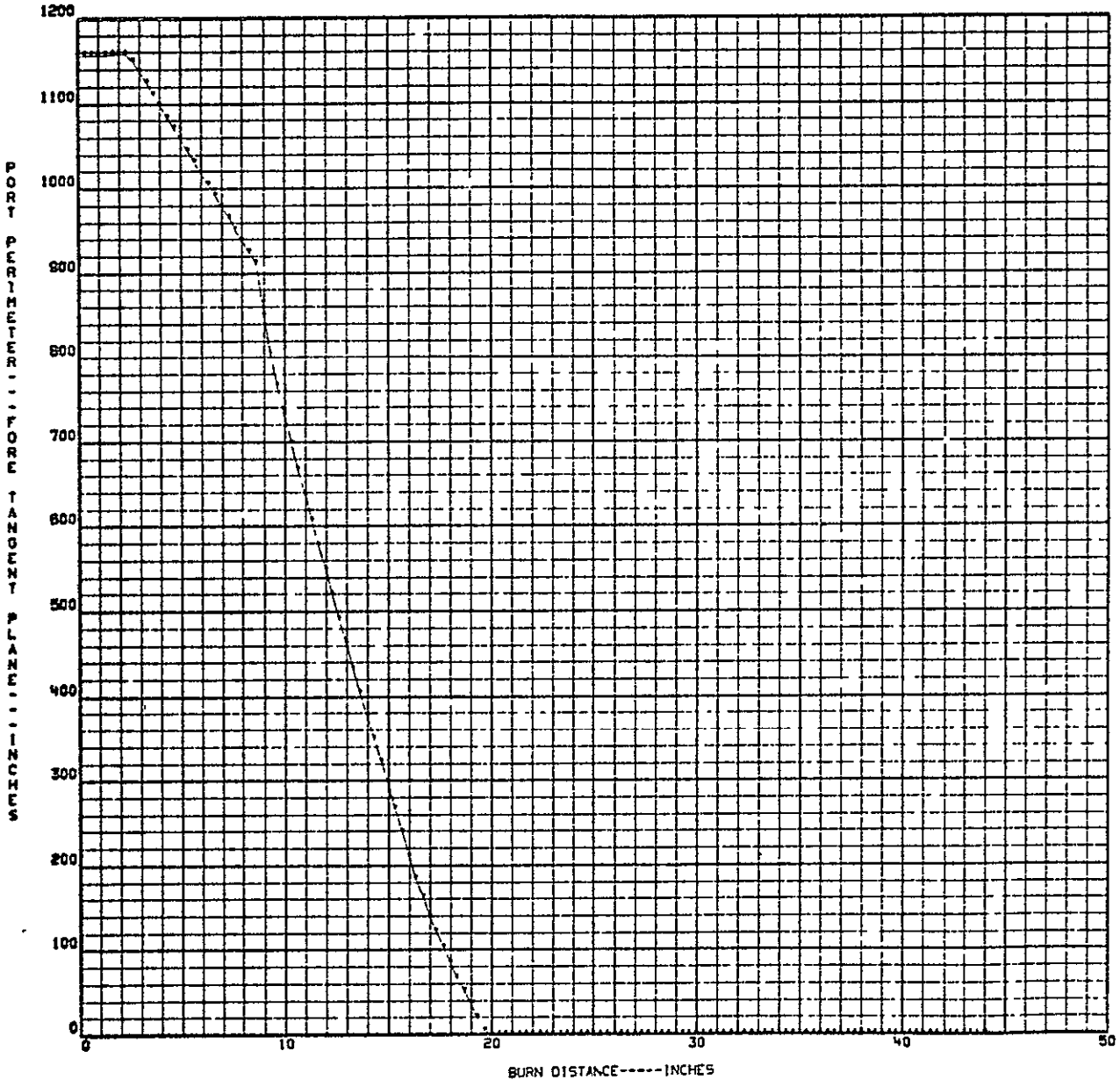

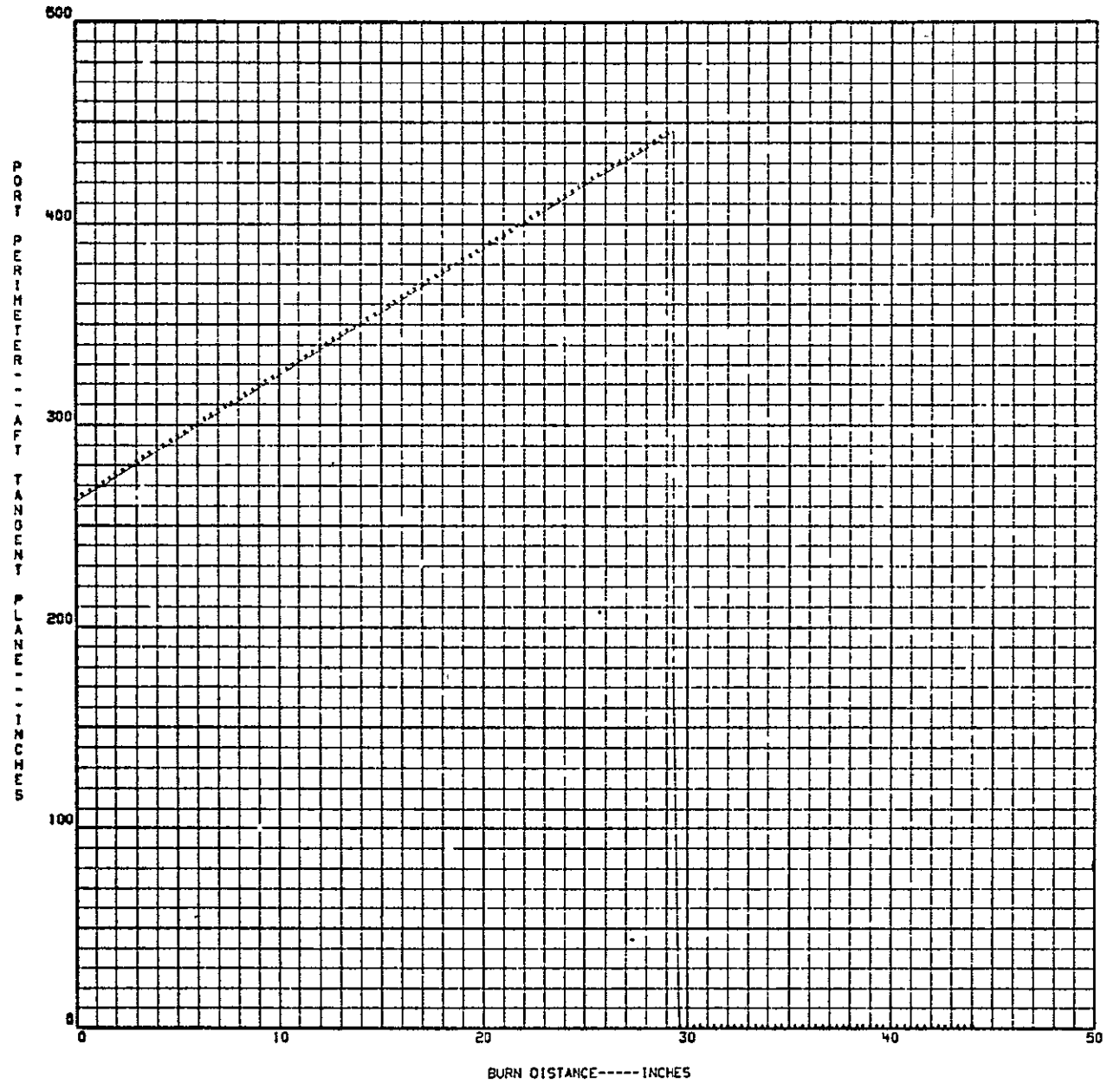
PORT PERIMETER--AFT TANGENT PLANE--INCHES
500
400
300
200
100
0
0
10
20
30
40
50
BURN DISTANCE-----INCHES

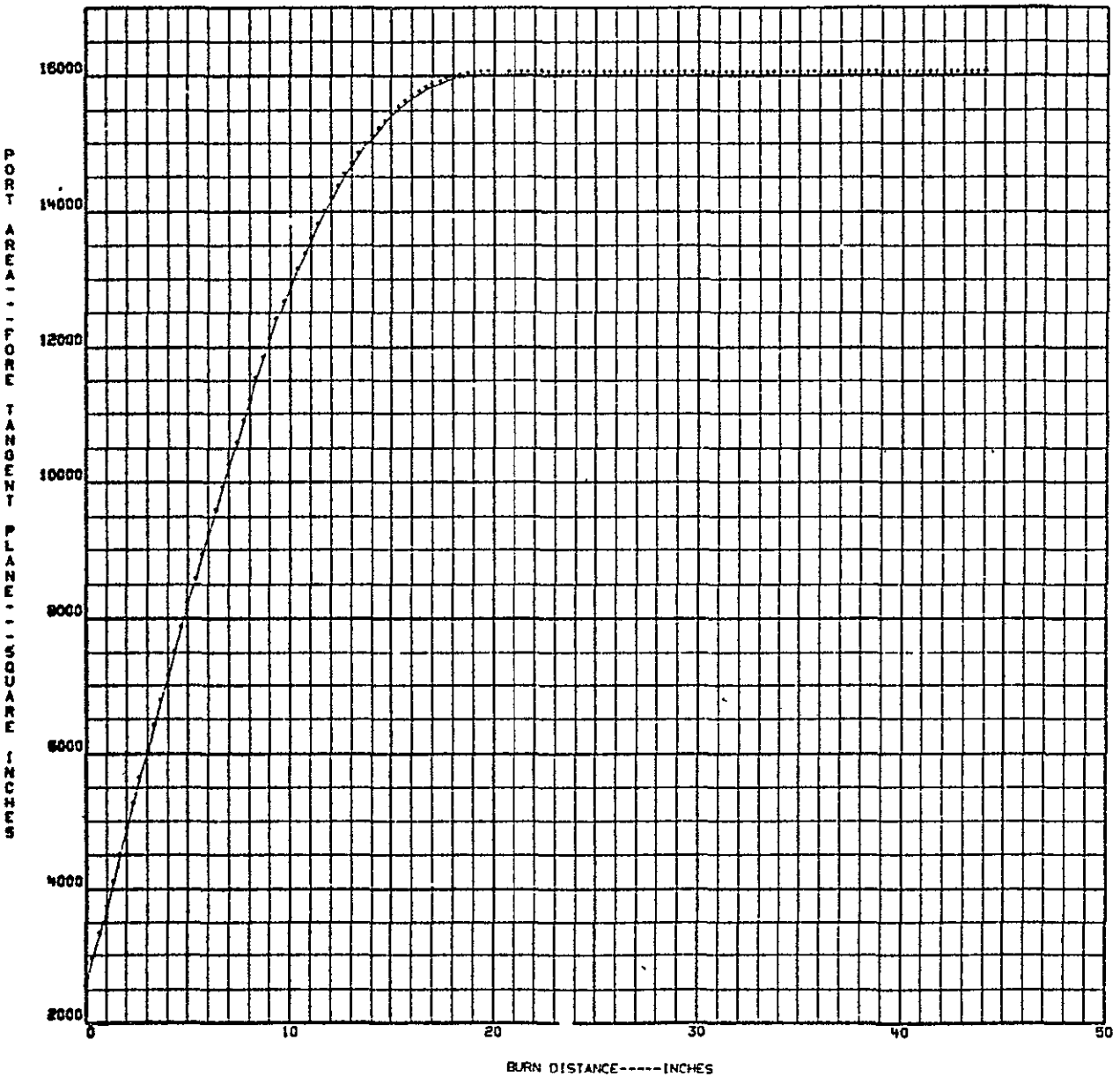

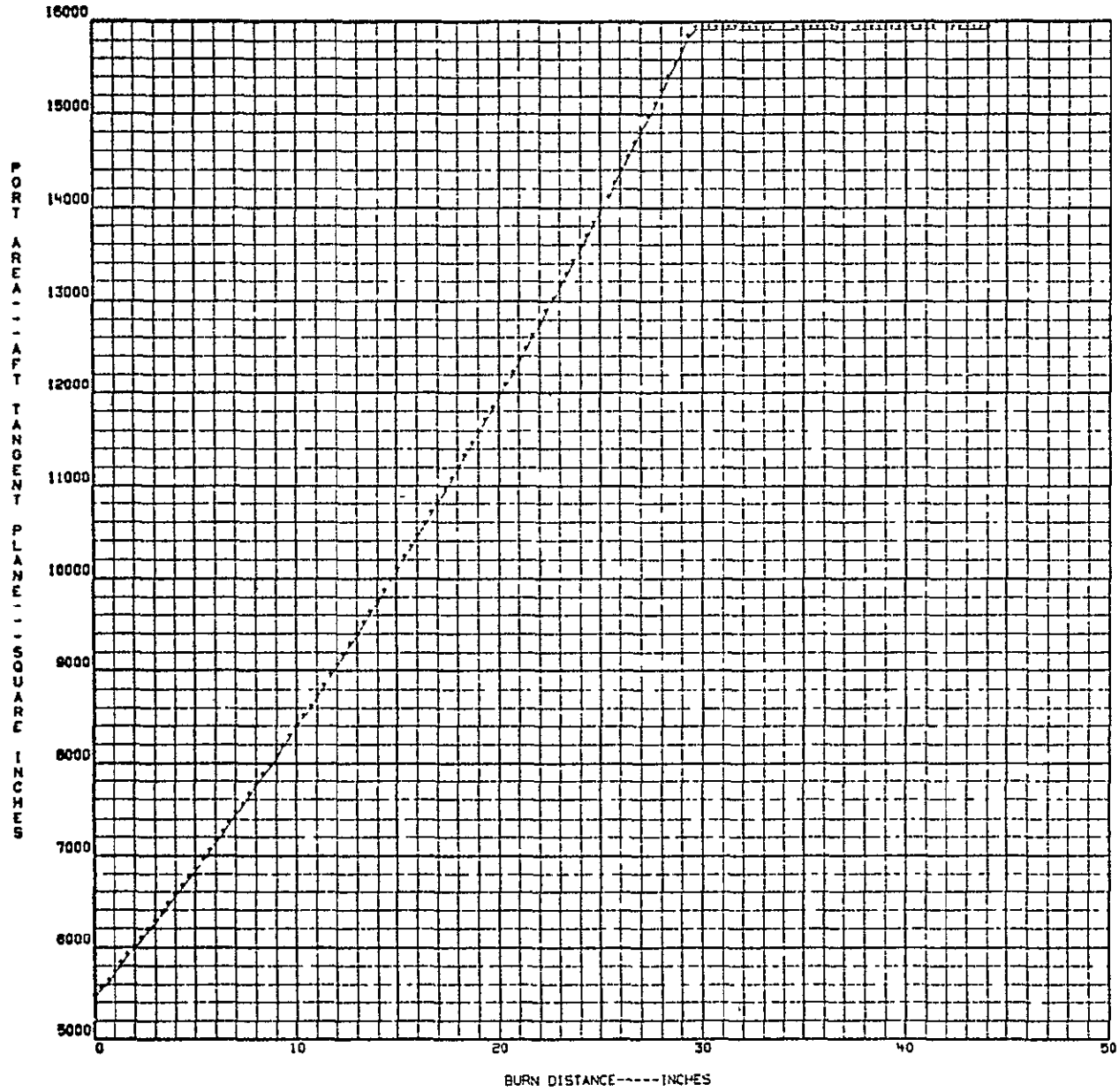
PORT AREA--AFT TANGENT PLANE--SQUARE INCHES
16000
15000
14000
13000
12000
11000
10000
9000
8000
7000
6000
5000
0
10
20
30
40
50
BURN DISTANCE-----INCHES

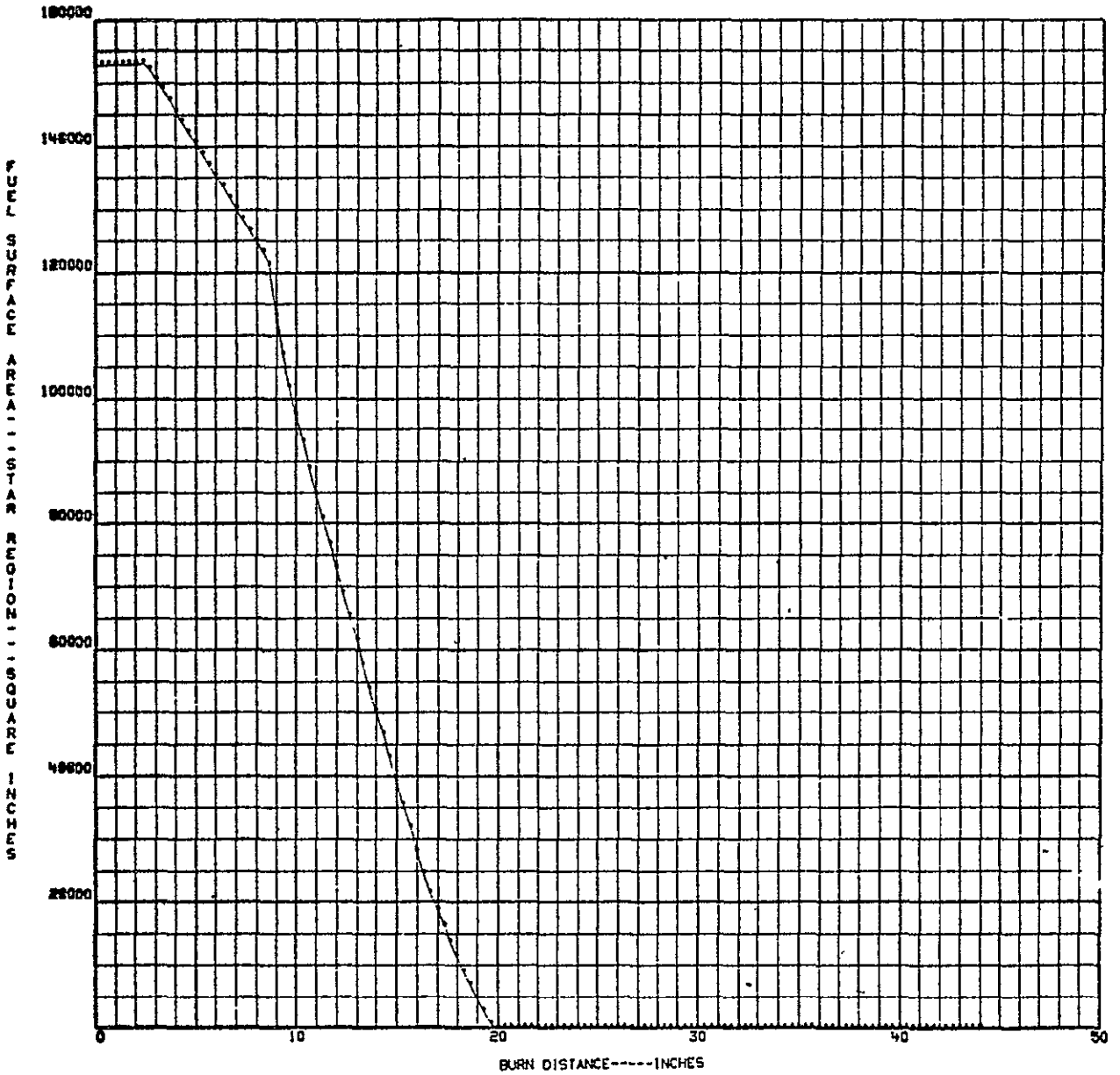
160000
140000
120000
100000
80000
60000
40000
20000
0
10
20
30
40
50
FUEL SURFACE AREA--STAR REGION--SQUARE INCHES
BURN DISTANCE-----INCHES

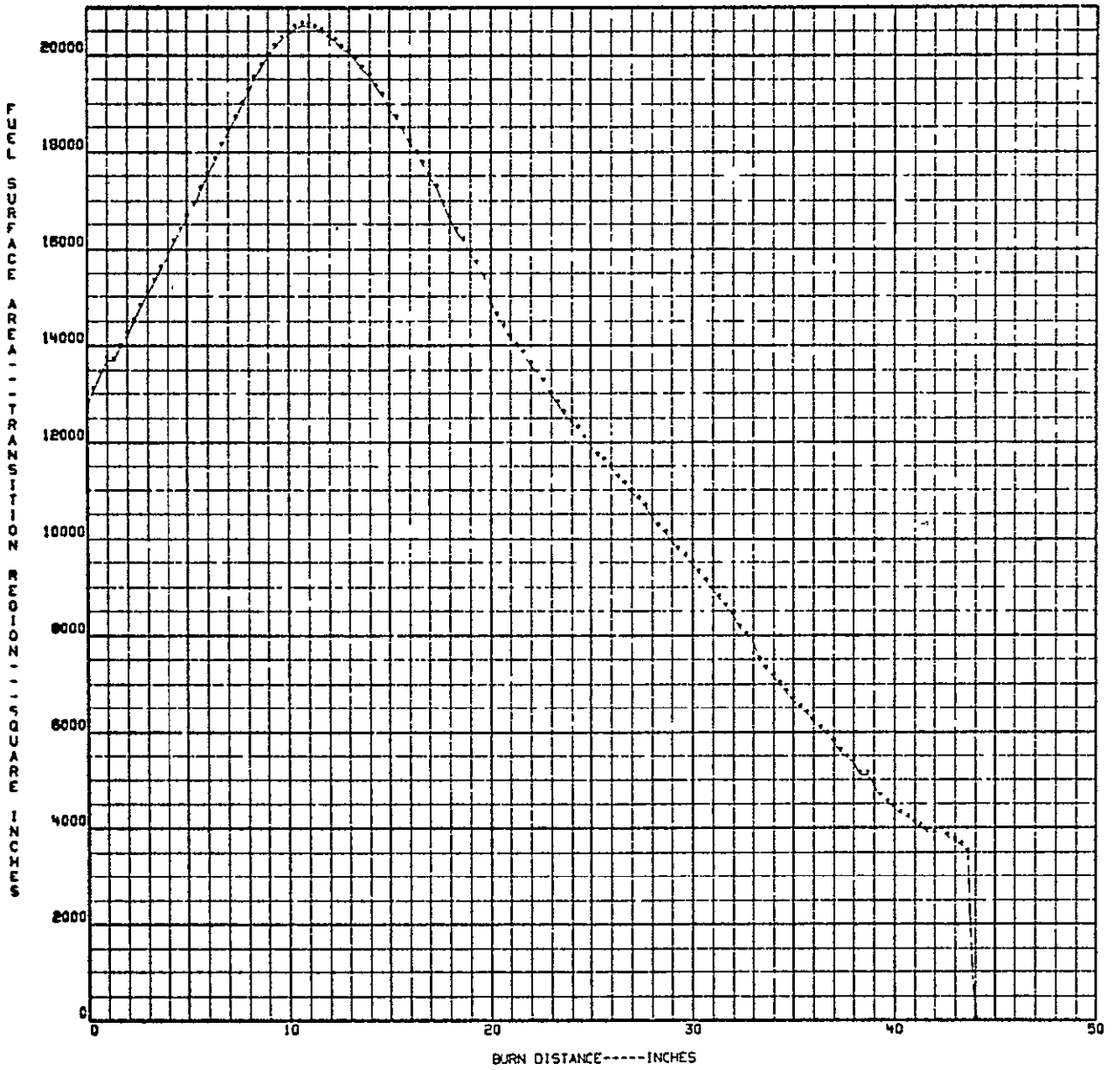
FUEL SURFACE AREA--TRANSITION REGION--SQUARE INCHES
20000
18000
16000
14000
12000
10000
8000
6000
4000
2000
0
0
10
20
30
40
50
BURN DISTANCE-----INCHES

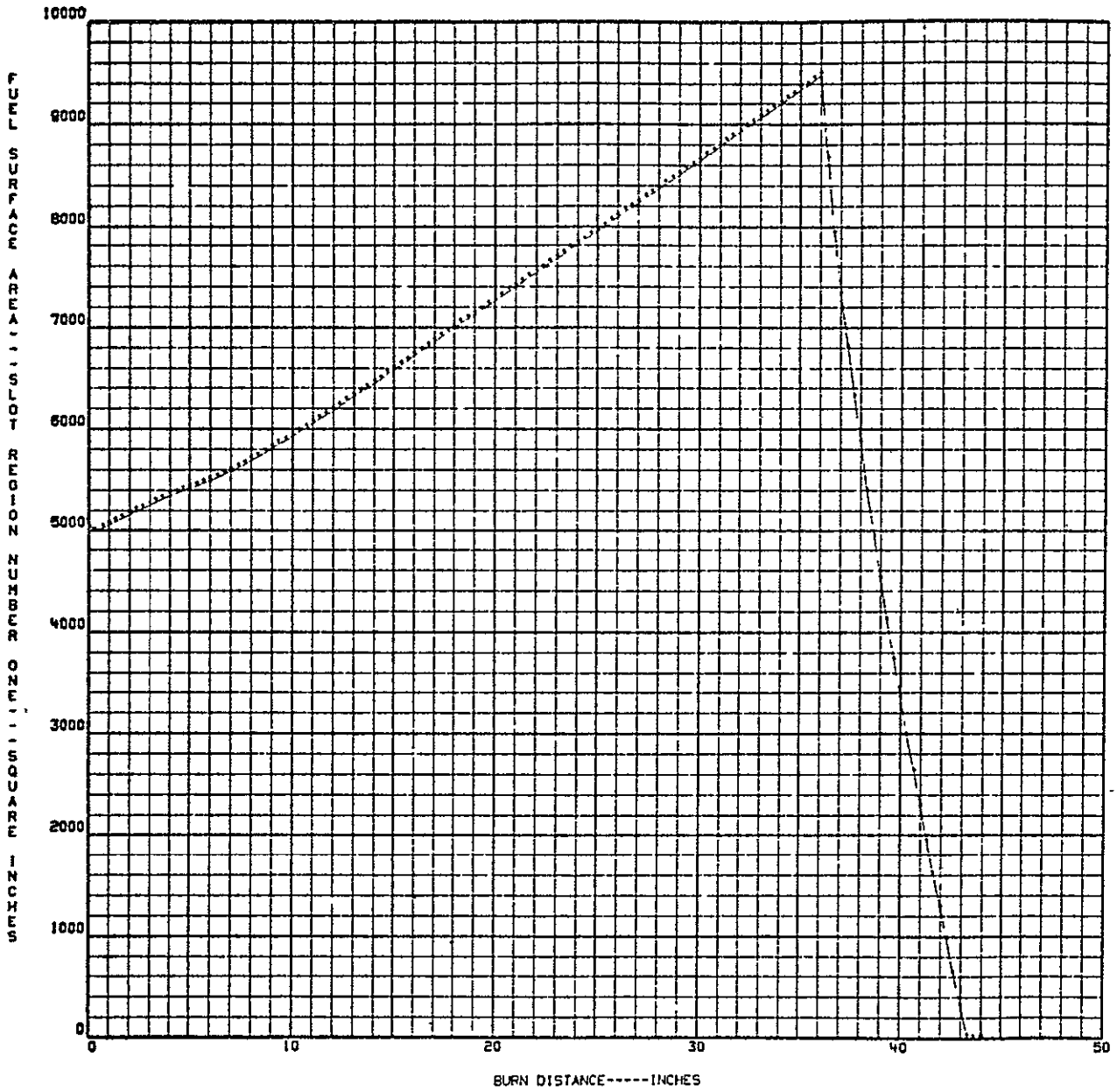

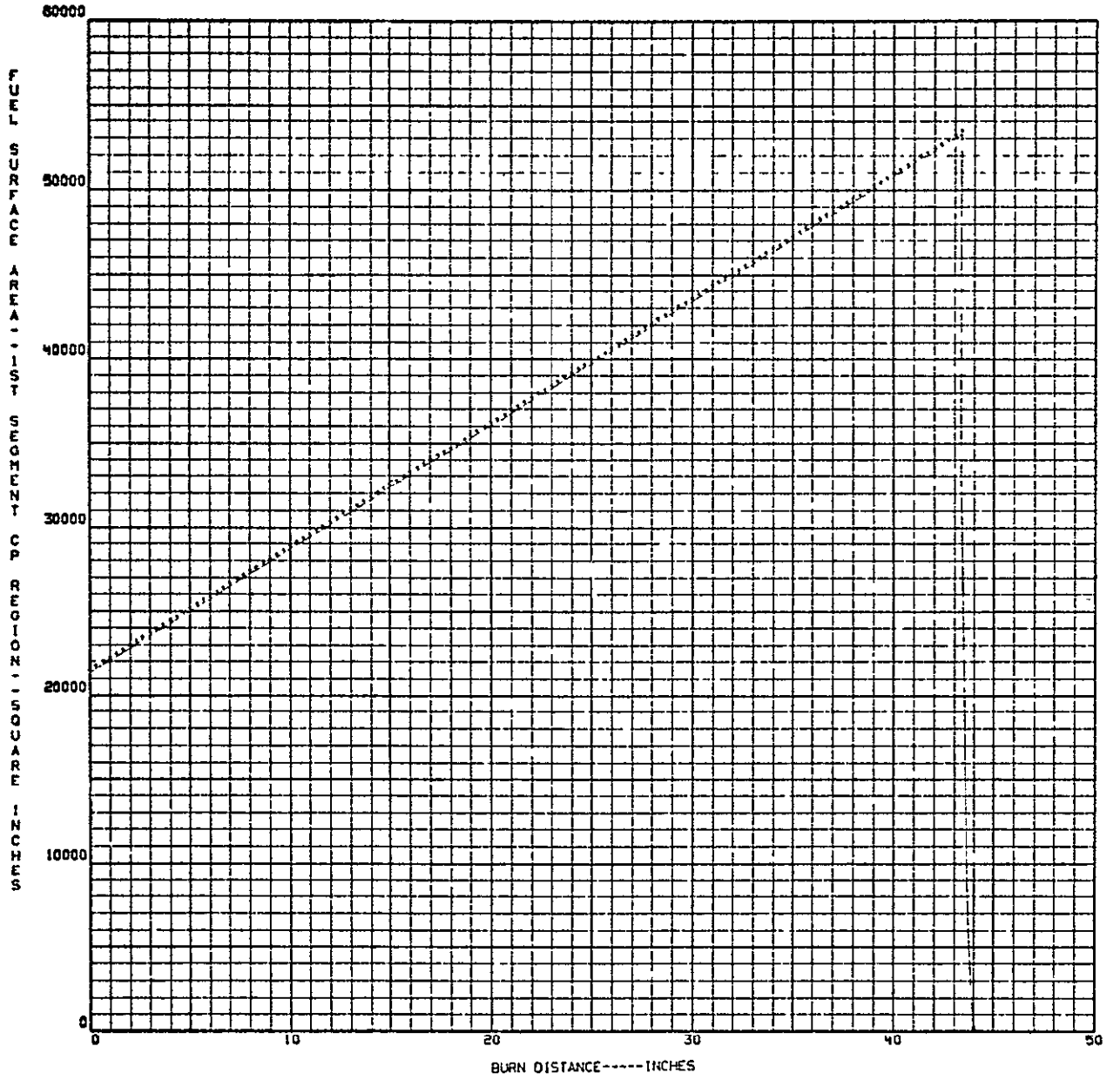
FUEL SURFACE AREA - 1ST SEGMENT CP REGION - SQUARE INCHES
60000
50000
40000
30000
20000
10000
0
0
10
20
30
40
50
BURN DISTANCE-----INCHES

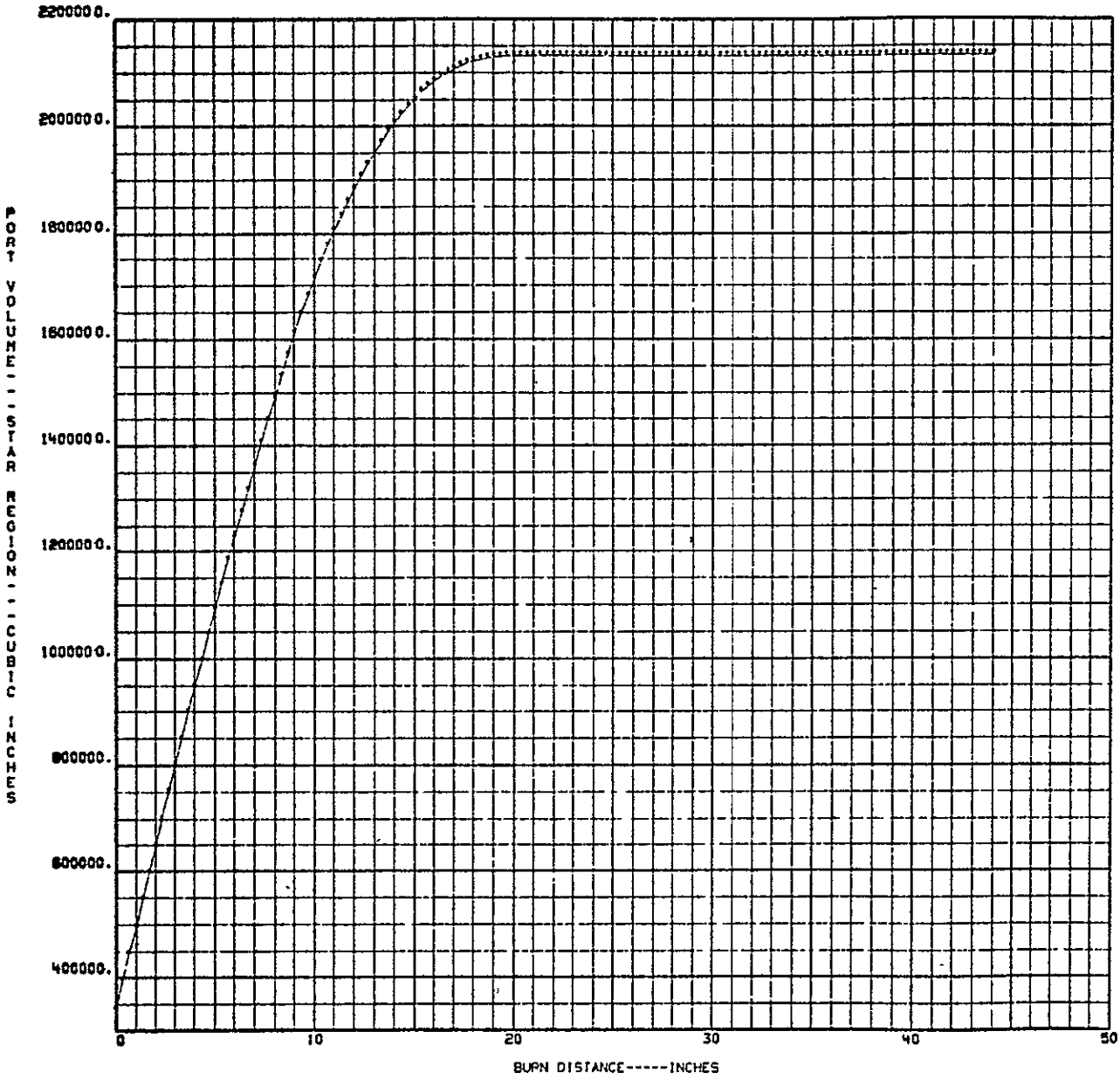
2200000.
2000000.
1800000.
1600000.
1400000.
1200000.
1000000.
800000.
600000.
400000.
PORT VOLUME--STAR REGION--CUBIC INCHES
0
10
20
30
40
50
BURN DISTANCE-----INCHES

C-2

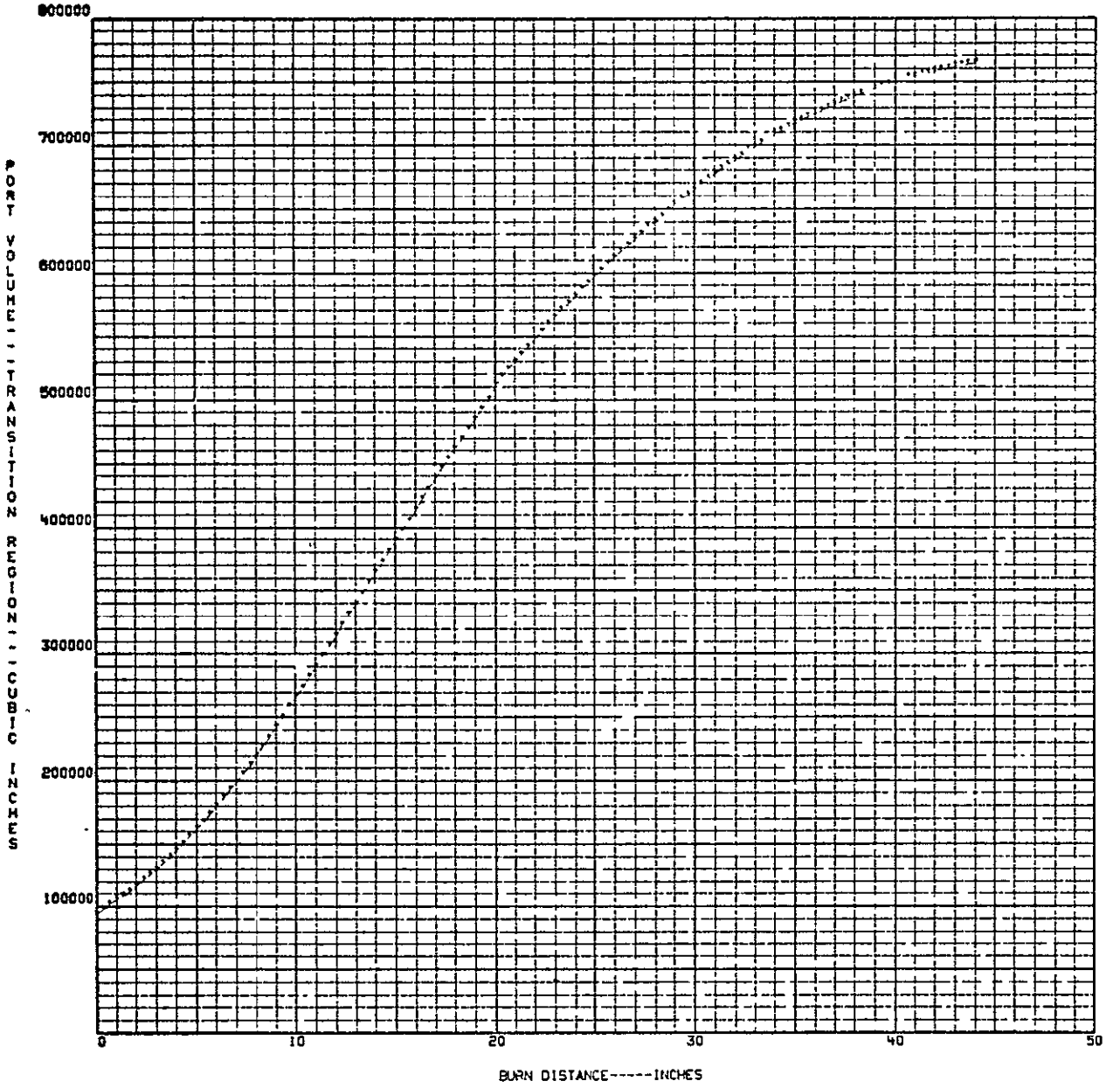
800000
700000
600000
500000
400000
300000
200000
100000
PORT VOLUME--TRANSITION REGION--CUBIC INCHES
0
10
20
30
40
50
BURN DISTANCE-----INCHES

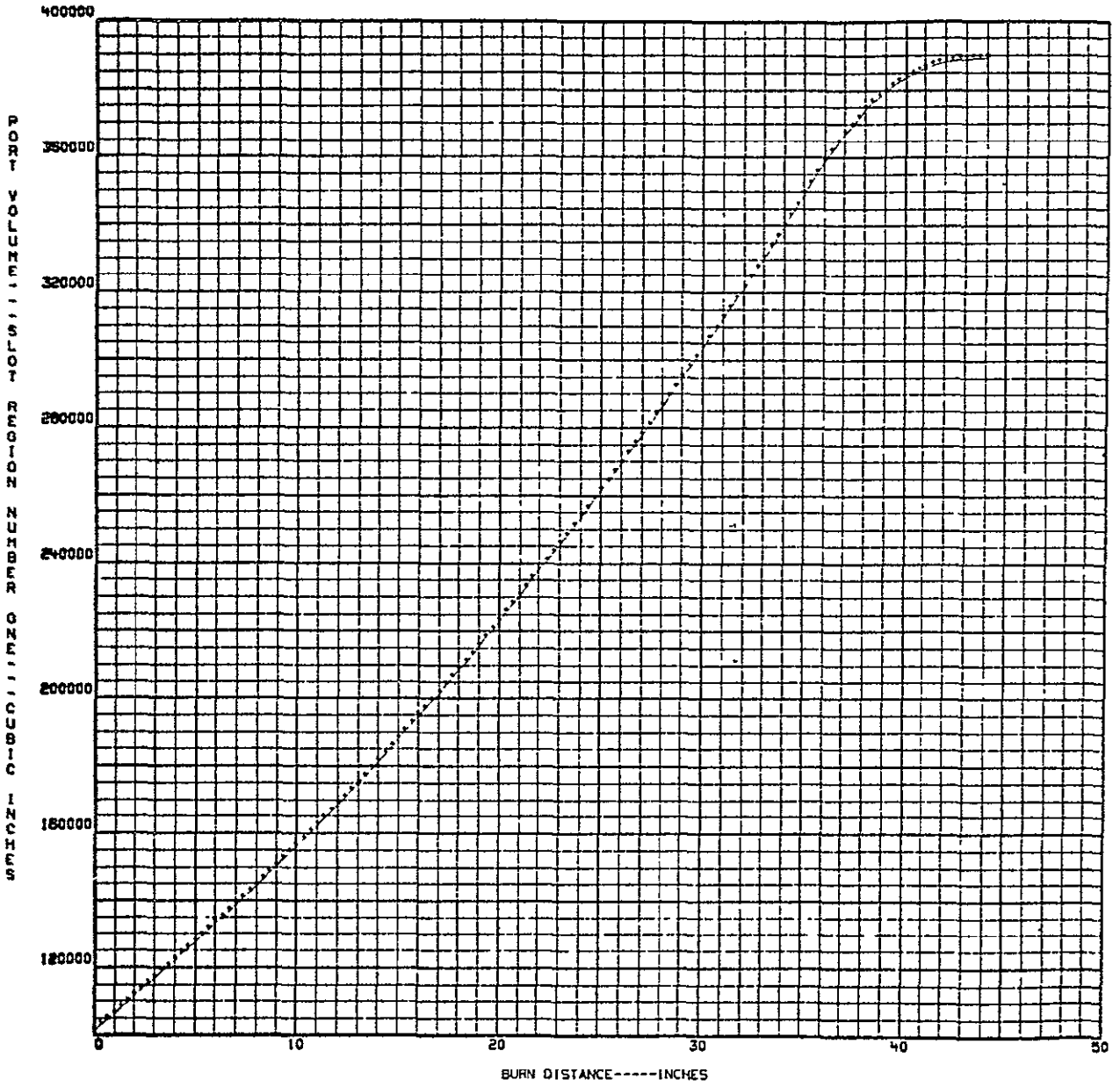

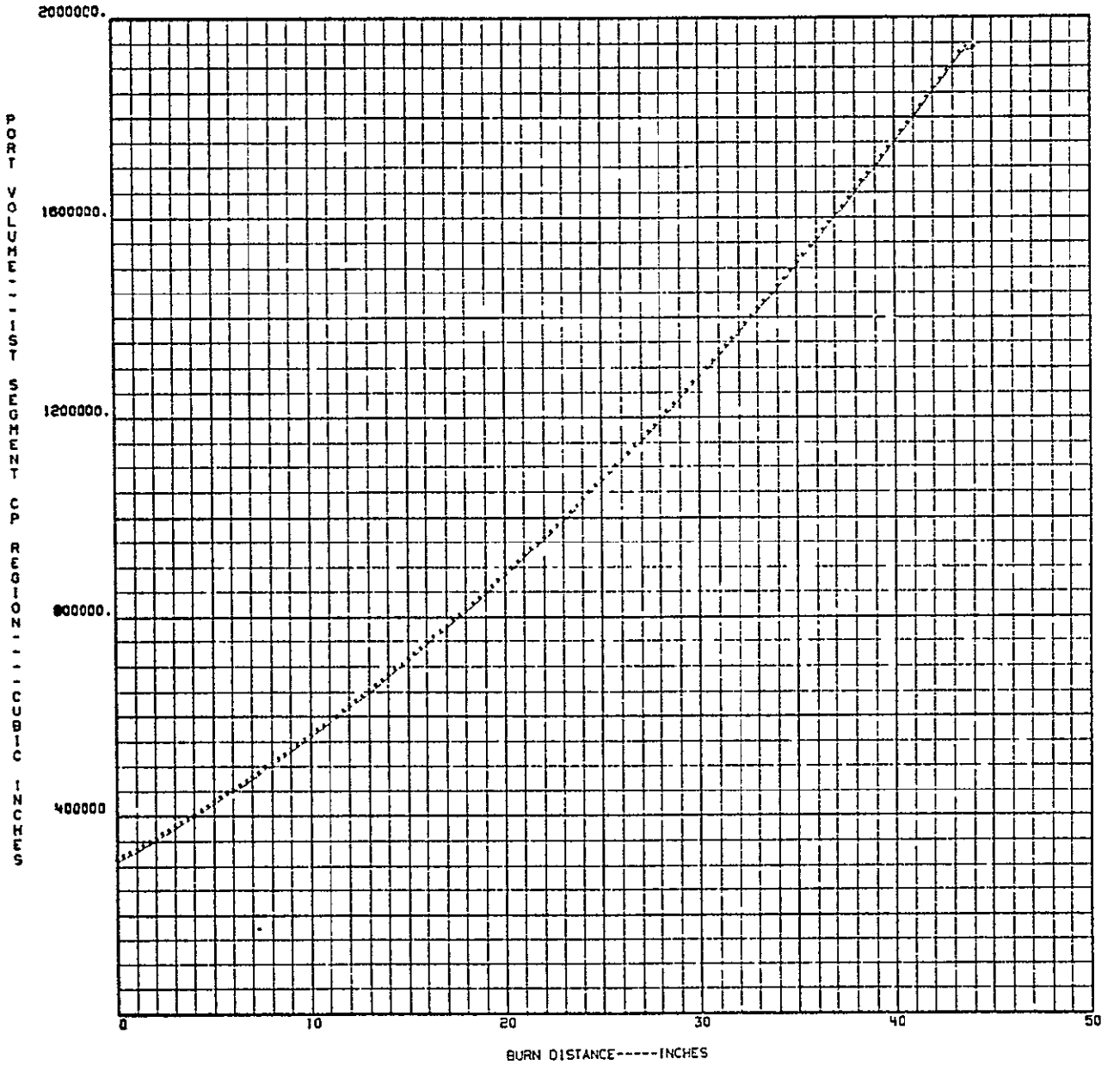
2000000.
1600000.
1200000.
800000.
400000
PORT VOLUME--1ST SEGMENT CP REGION--CUBIC INCHES
0
10
20
30
40
50
BURN DISTANCE-----INCHES

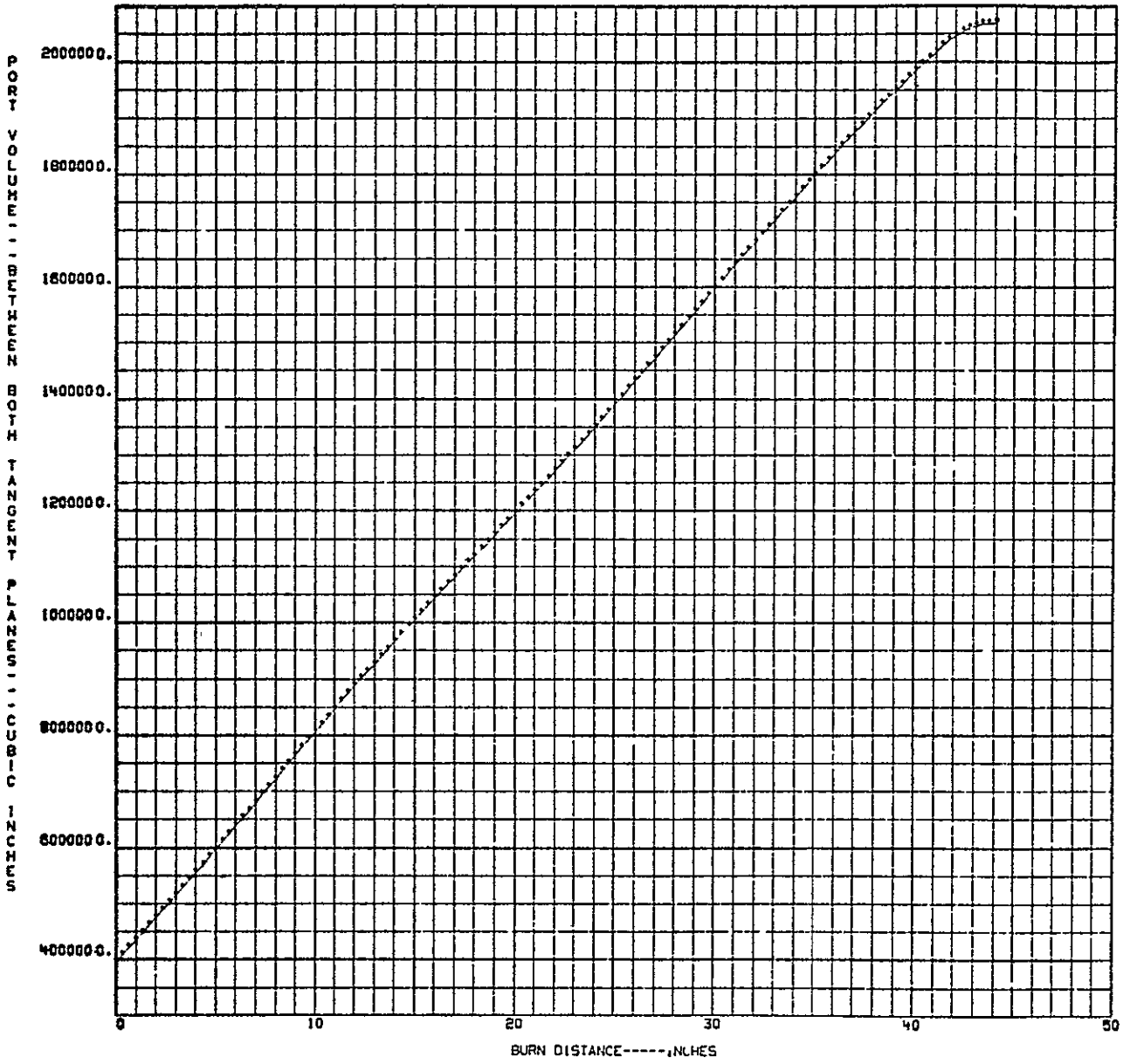
PORT VOLUME--BETWEEN BOTH TANGENT PLANES--CUBIC INCHES
2000000.
1800000.
1600000.
1400000.
1200000.
1000000.
800000.
600000.
400000.
0
10
20
30
40
50
BURN DISTANCE-----INCHES

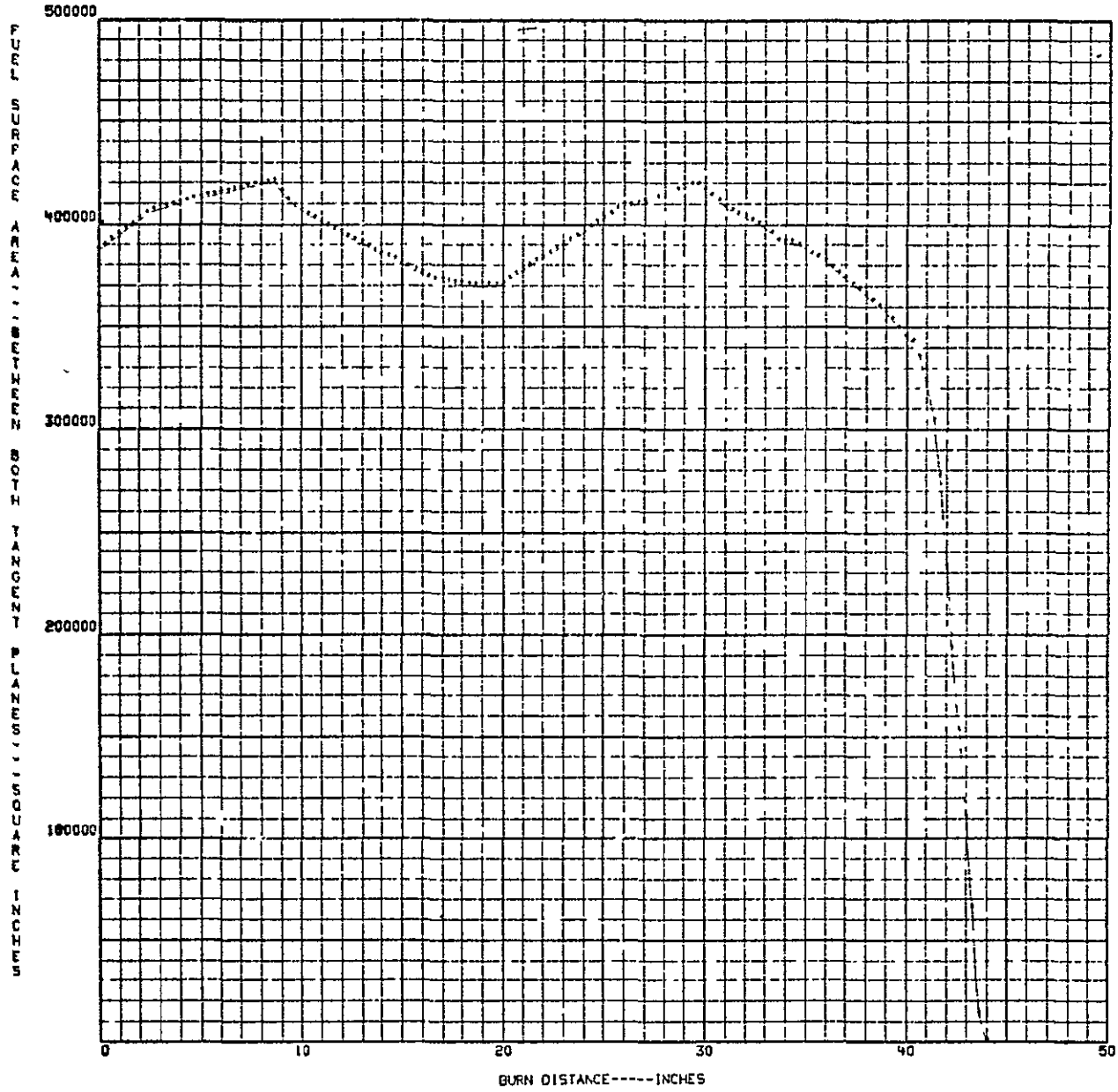
FUEL SURFACE AREA - BETWEEN BOTH TANGENT PLANES - SQUARE INCHES
500000
400000
300000
200000
100000
0
10
20
30
40
50
BURN DISTANCE-----INCHES

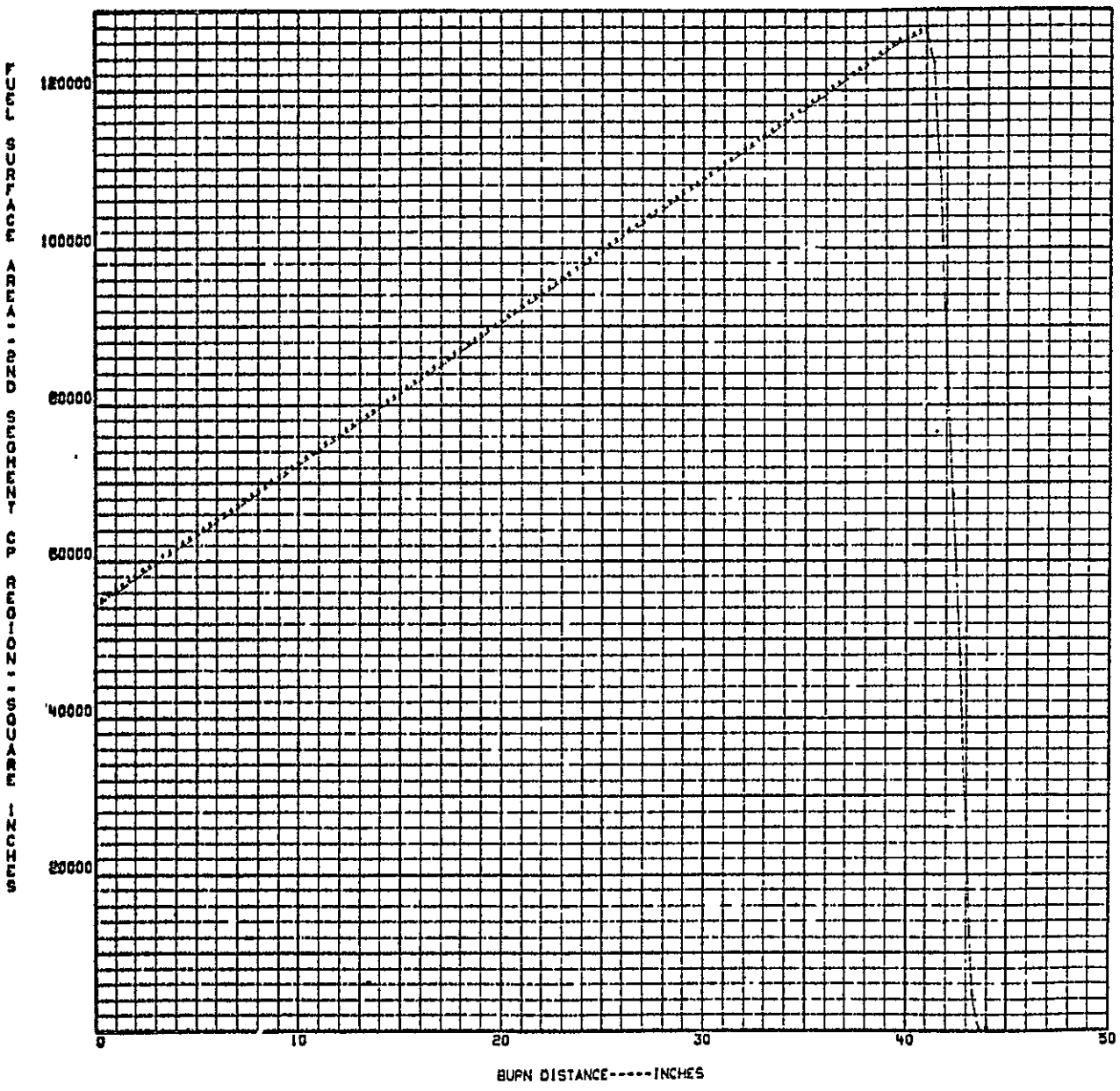

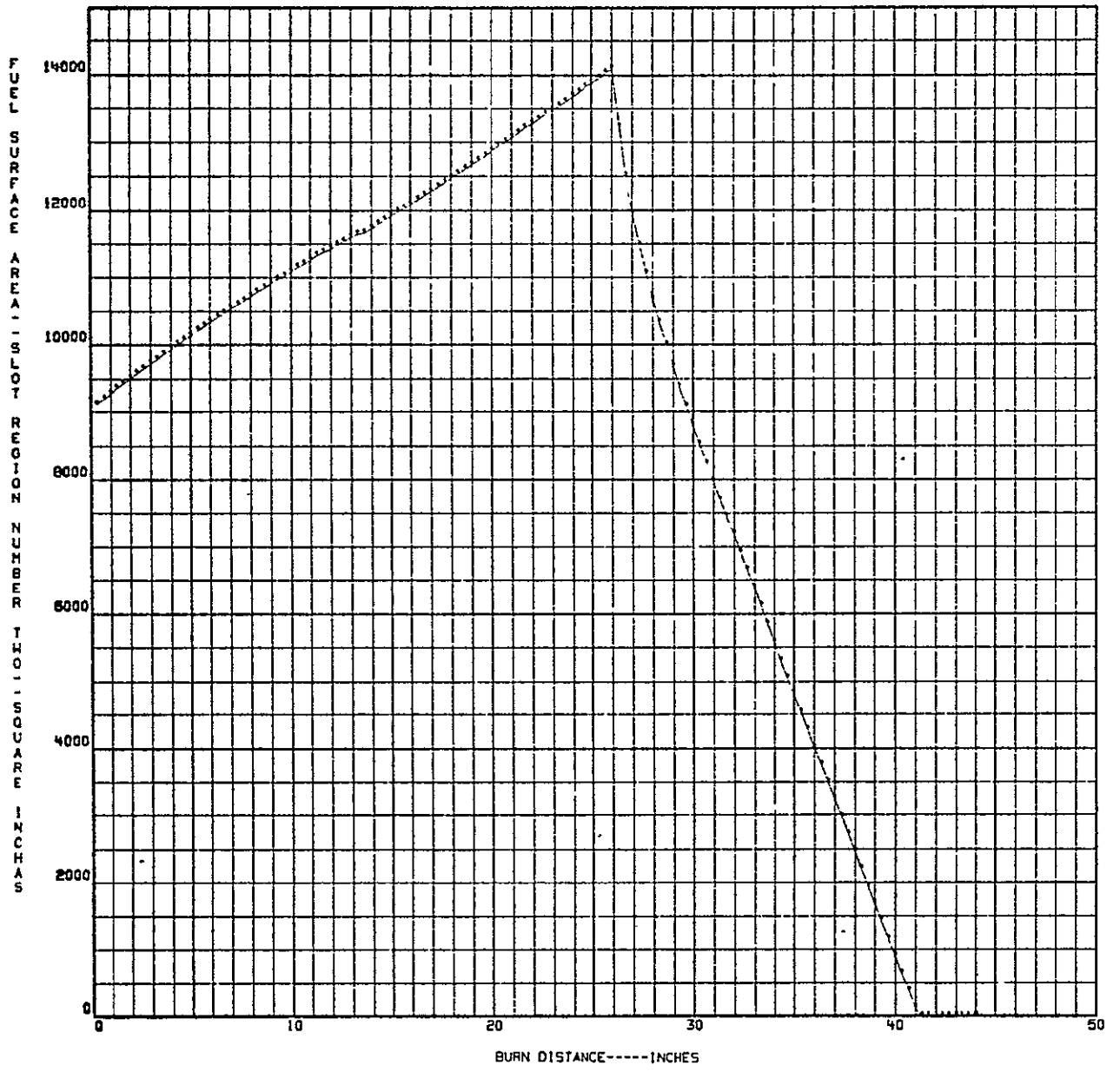
FUEL SURFACE AREA - SLOT REGION NUMBER TWO - SQUARE INCHES
14000
12000
10000
8000
6000
4000
2000
0
0
10
20
30
40
50
BURN DISTANCE-----INCHES

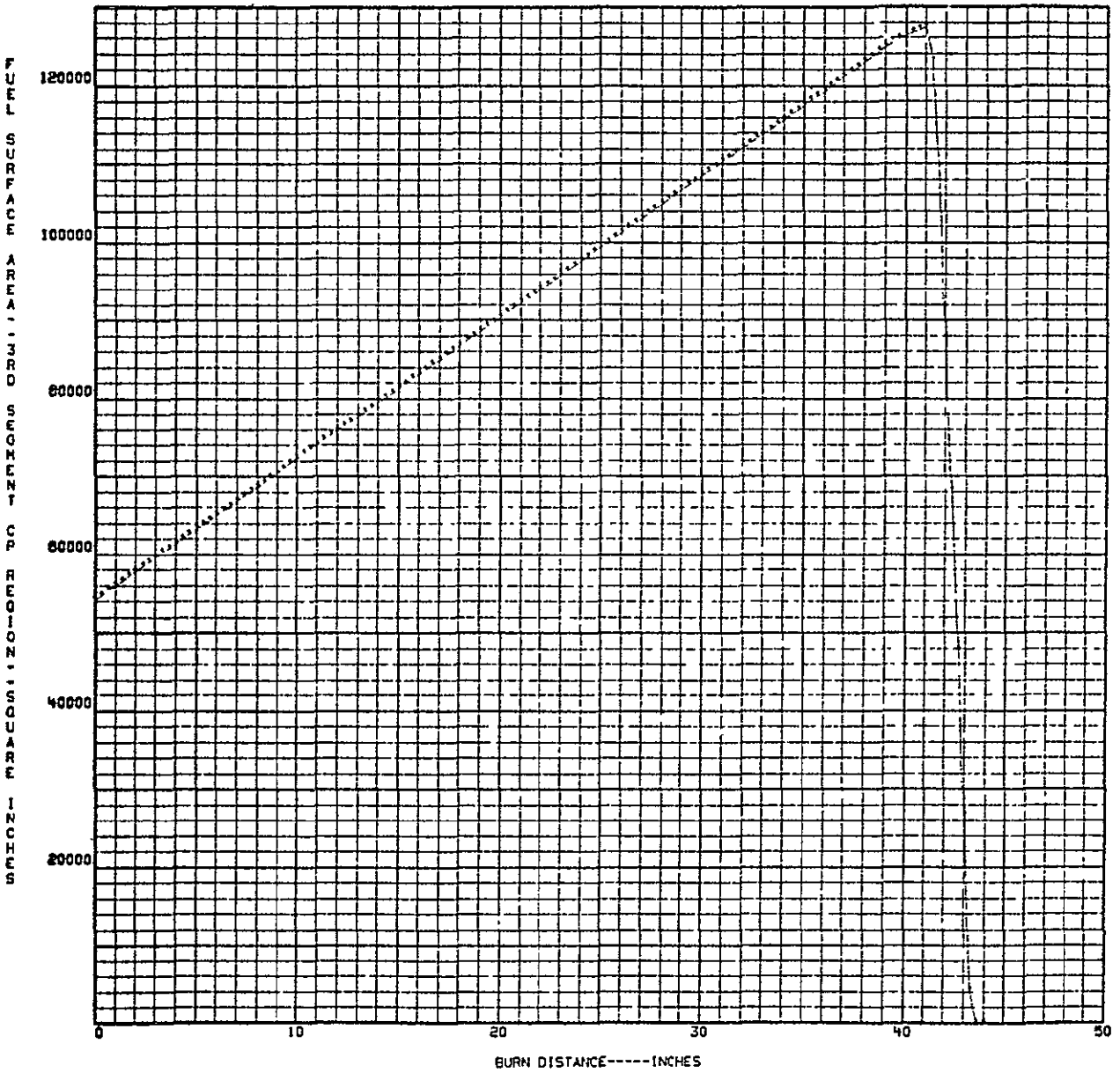
FUEL SURFACE AREA - 3RD SEGMENT CP REGION - SQUARE INCHES
120000
100000
80000
60000
40000
20000
0
10
20
30
40
50
BURN DISTANCE-----INCHES

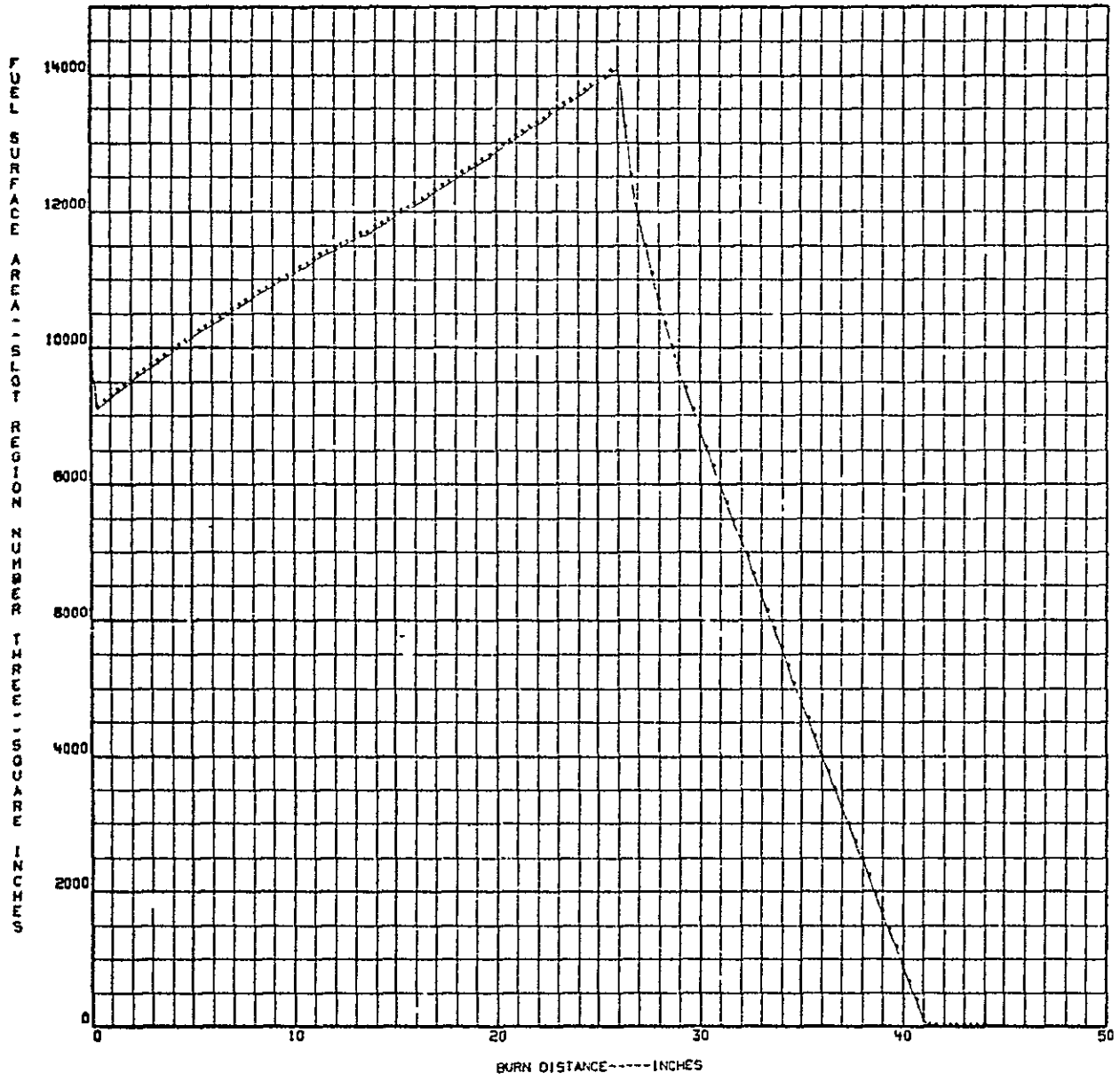
FUEL SURFACE AREA - SLOT REGION NUMBER THREE - SQUARE INCHES
14000
12000
10000
8000
6000
4000
2000
0
0
10
20
30
40
50
BURN DISTANCE-----INCHES

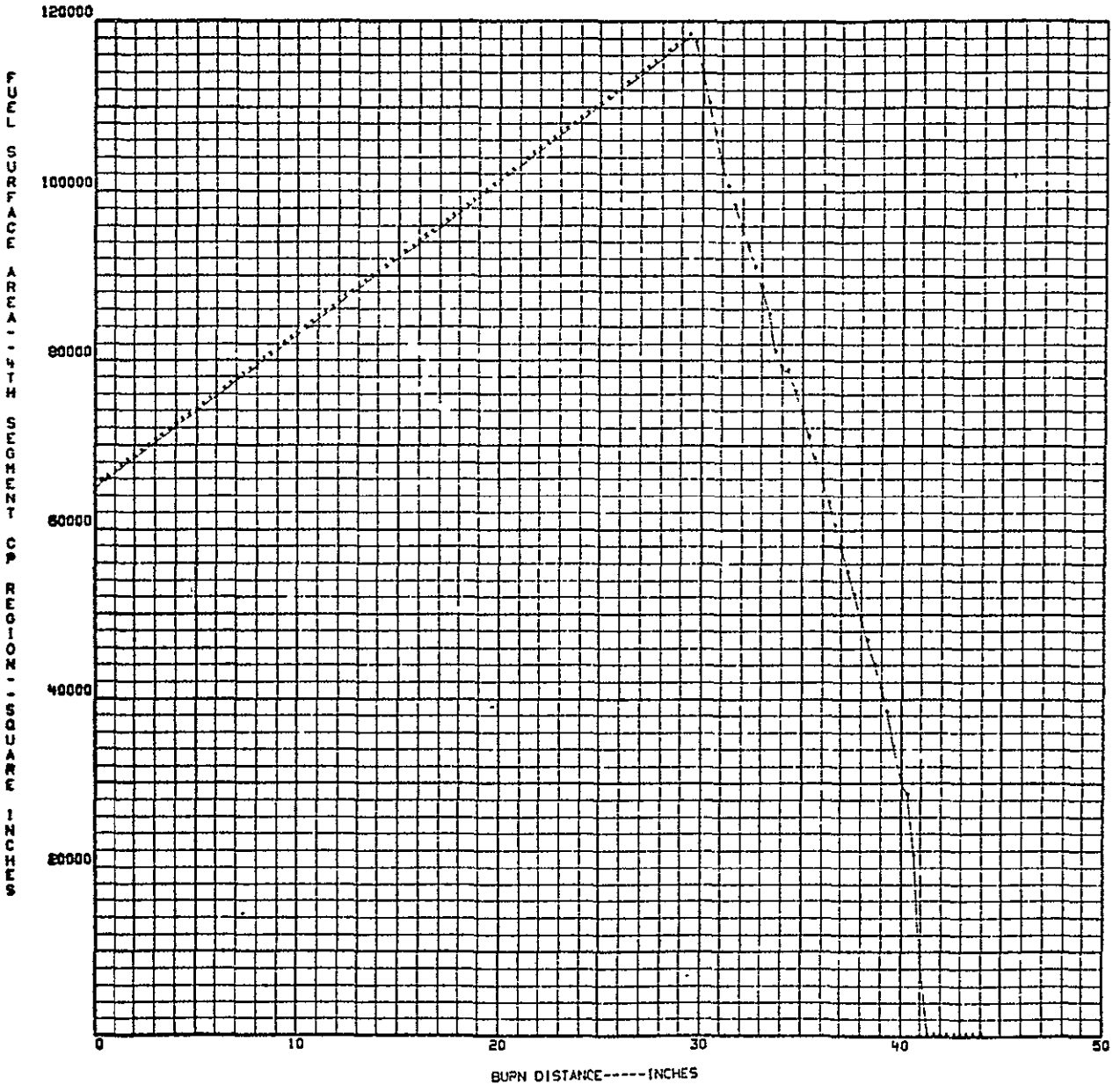

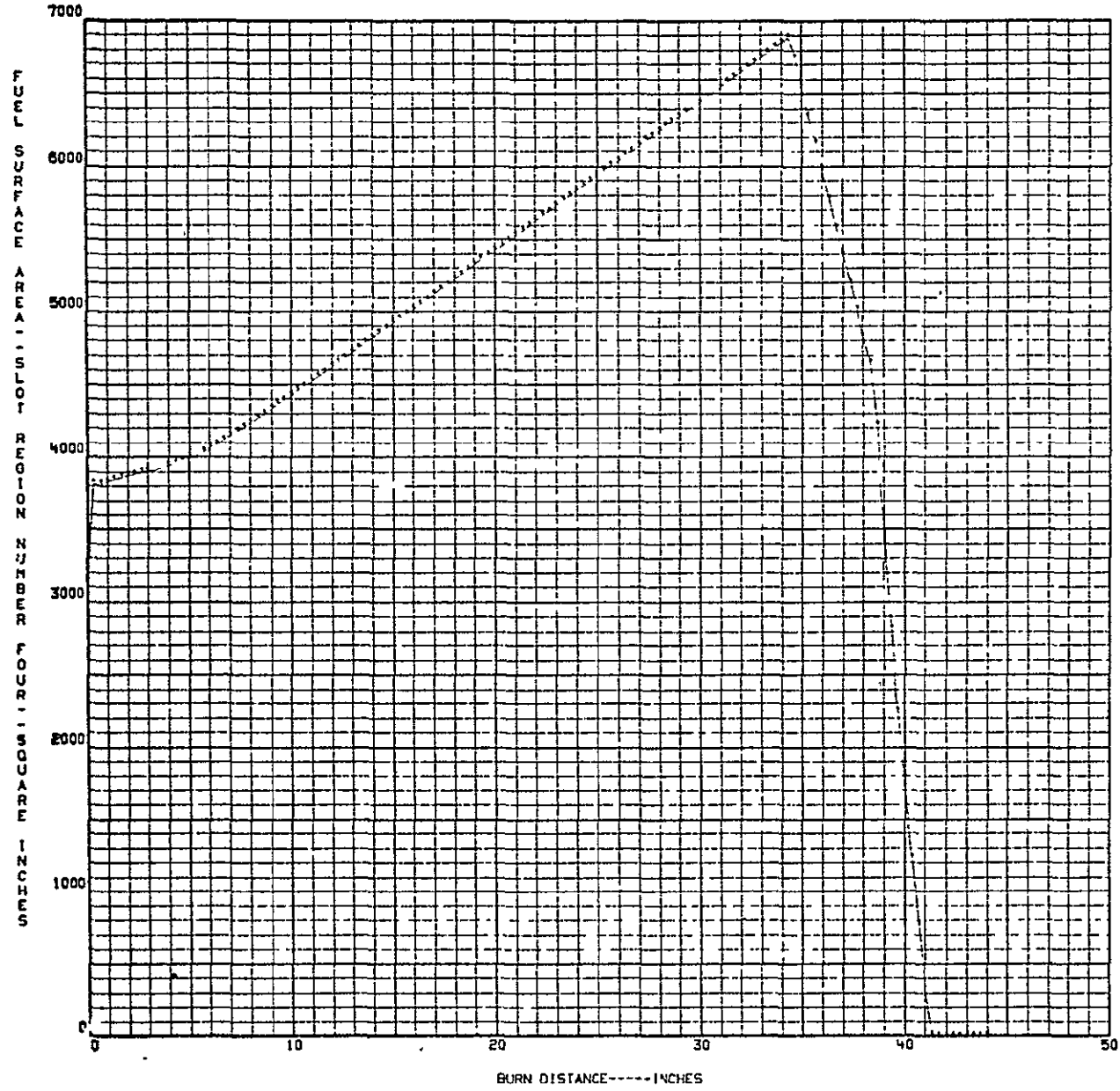
FUEL SURFACE AREA - SLOT REGION NUMBER FOUR - SQUARE INCHES
7000
6000
5000
4000
3000
2000
1000
0
0
10
20
30
40
50
BURN DISTANCE-----INCHES

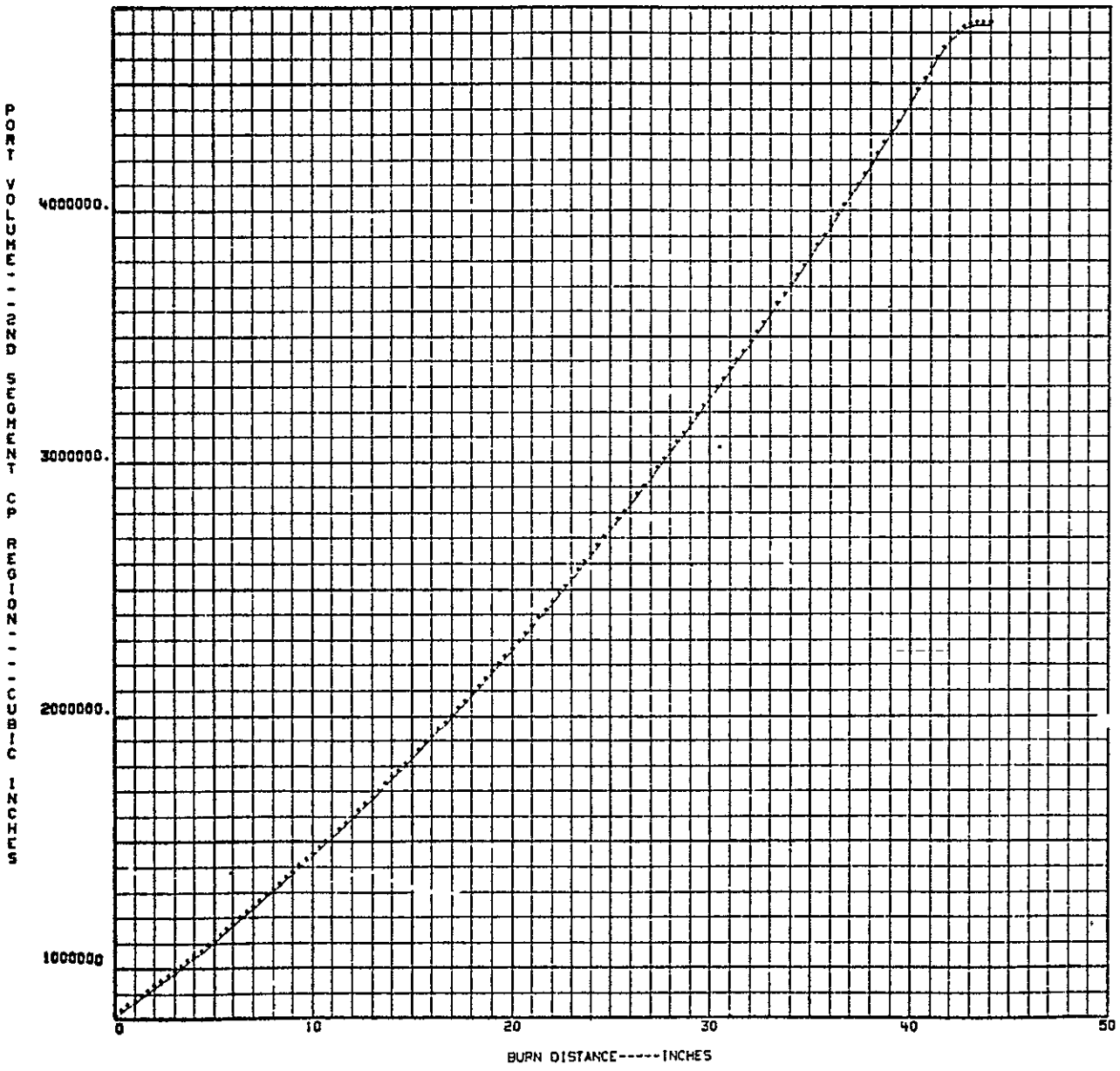
PORT VOLUME--2ND SEGMENT CP REGION--CUBIC INCHES
4000000.
3000000.
2000000.
1000000
0
10
20
30
40
50
BURN DISTANCE-----INCHES

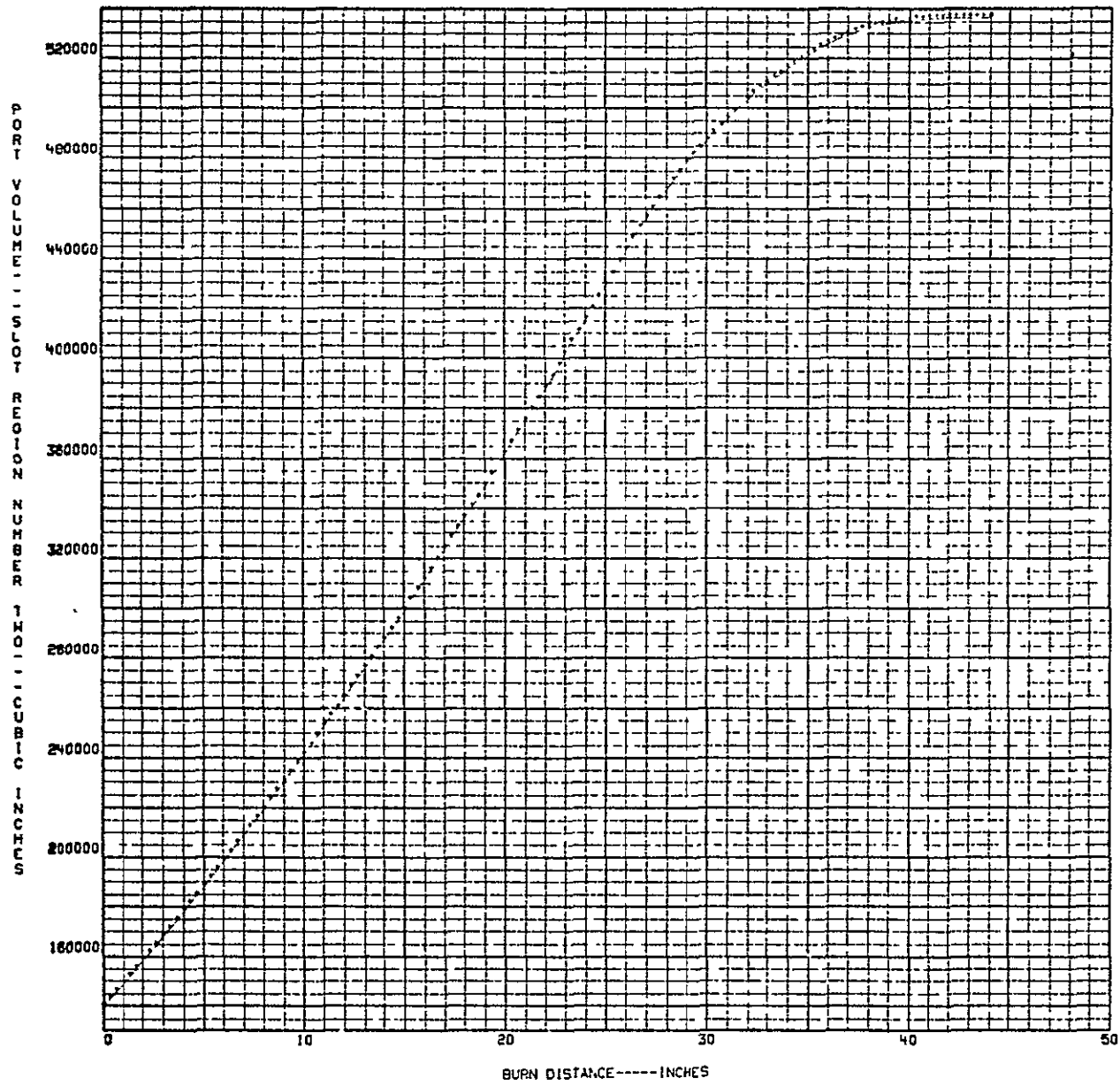
PORT VOLUME--SLOT REGION NUMBER TWO--CUBIC INCHES
520000
480000
440000
400000
360000
320000
280000
240000
200000
160000
0
10
20
30
40
50
BURN DISTANCE-----INCHES

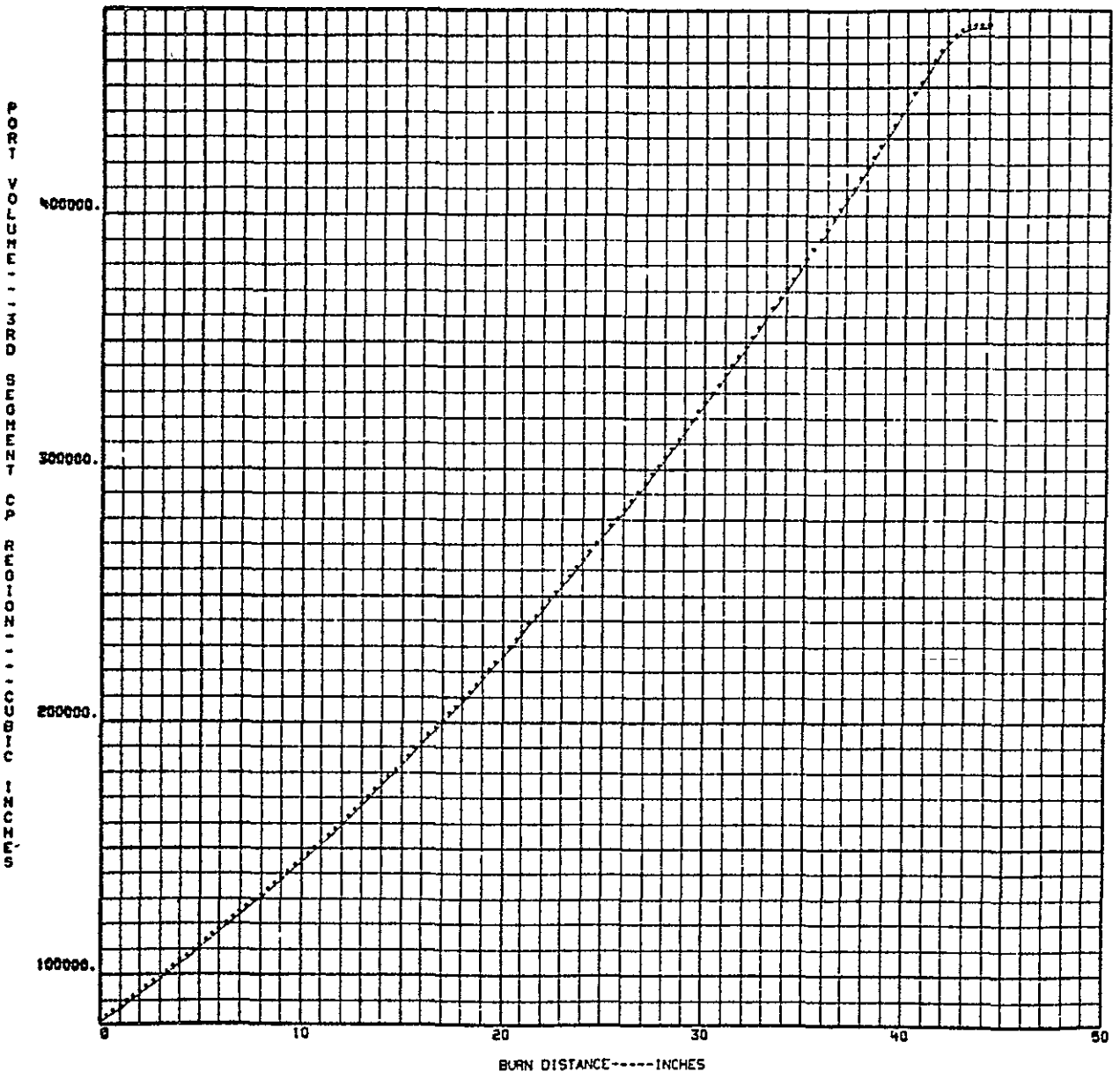

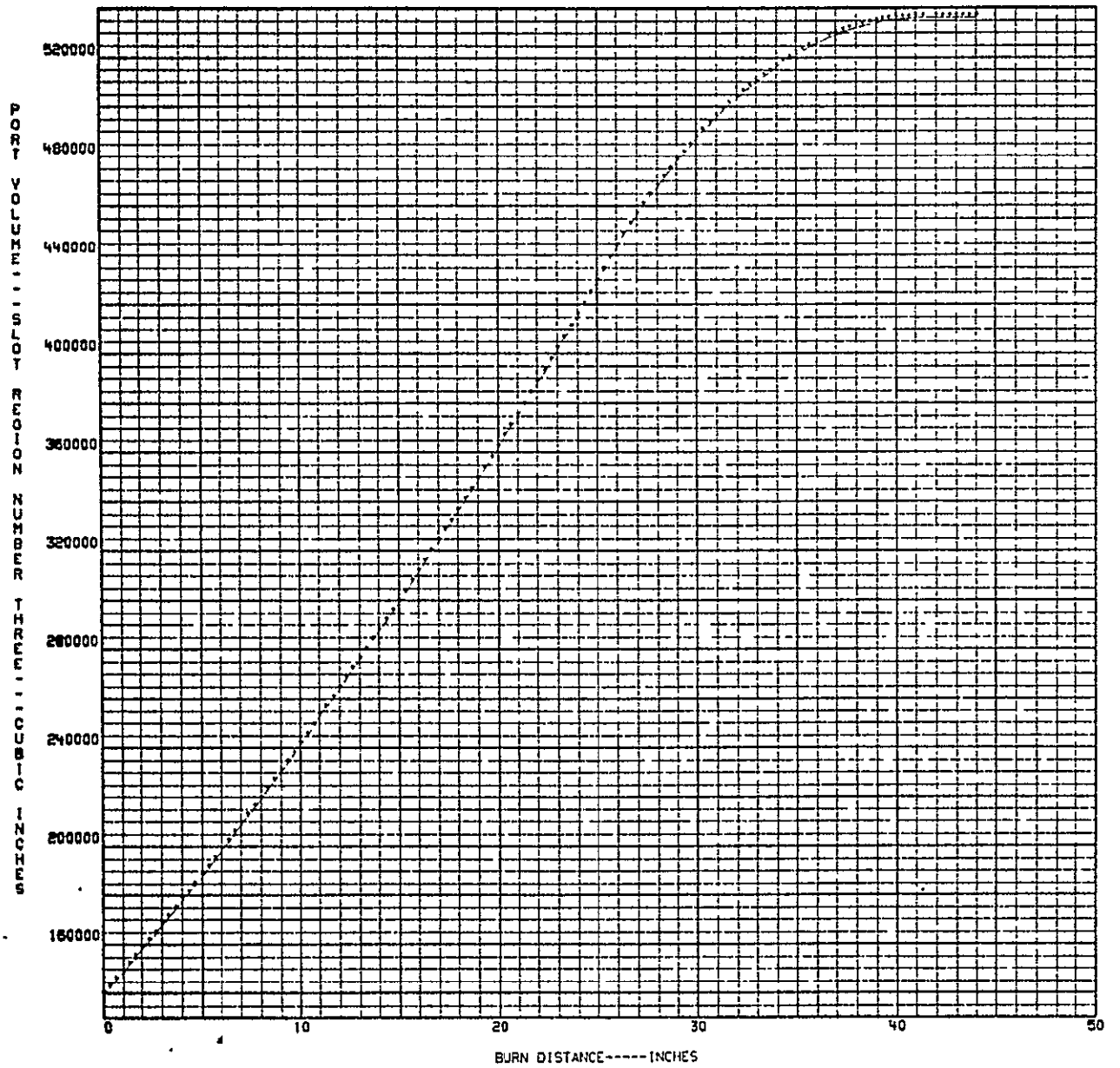
PORT VOLUME--SLOT REGION NUMBER THREE--CUBIC INCHES
520000
480000
440000
400000
360000
320000
280000
240000
200000
160000
0
10
20
30
40
50
BURN DISTANCE-----INCHES

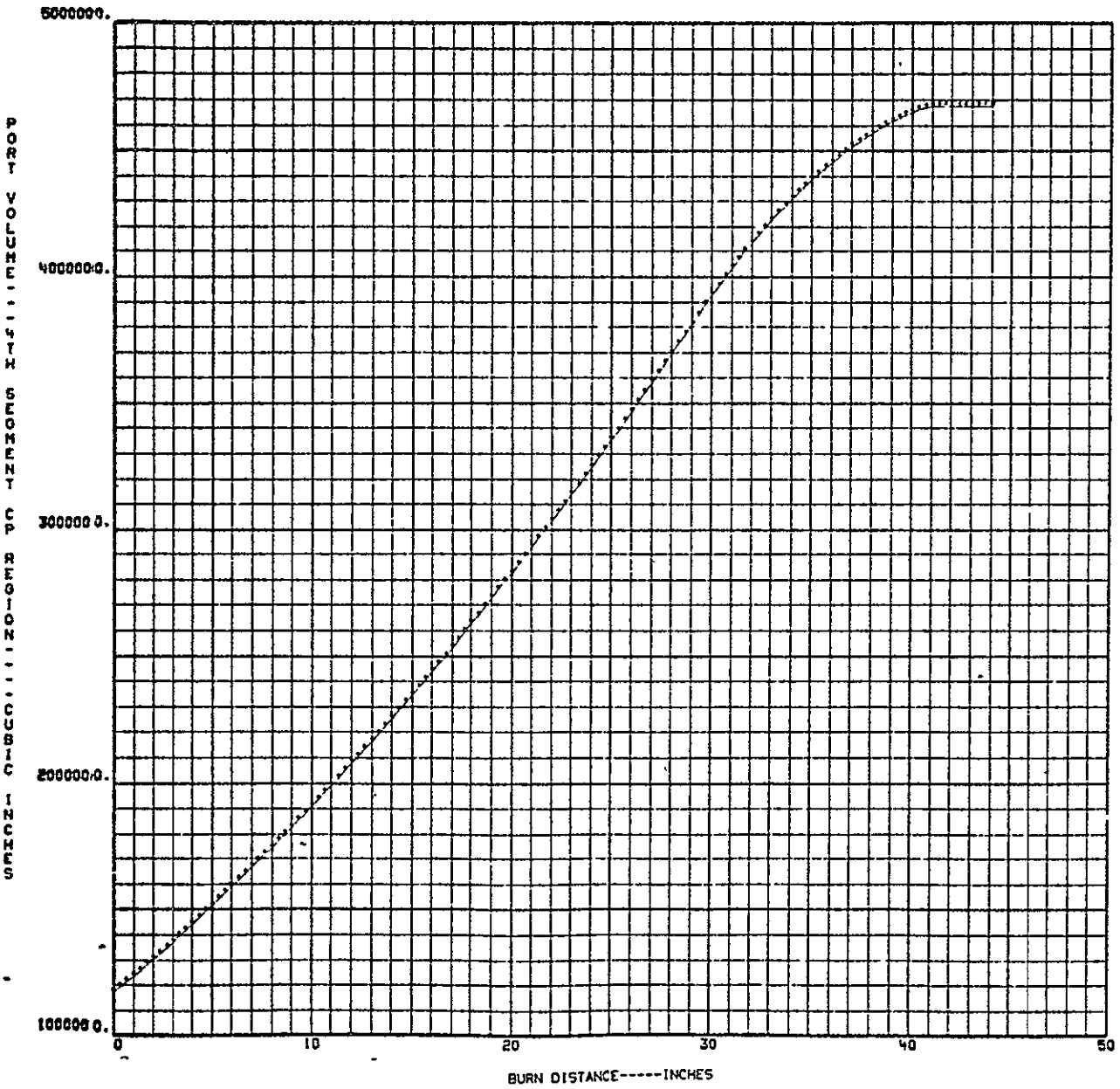
5000000.
4000000.
3000000.
2000000.
1000000.
PORT VOLUME--4TH SEGMENT CP REGION--CUBIC INCHES
0
10
20
30
40
50
BURN DISTANCE-----INCHES

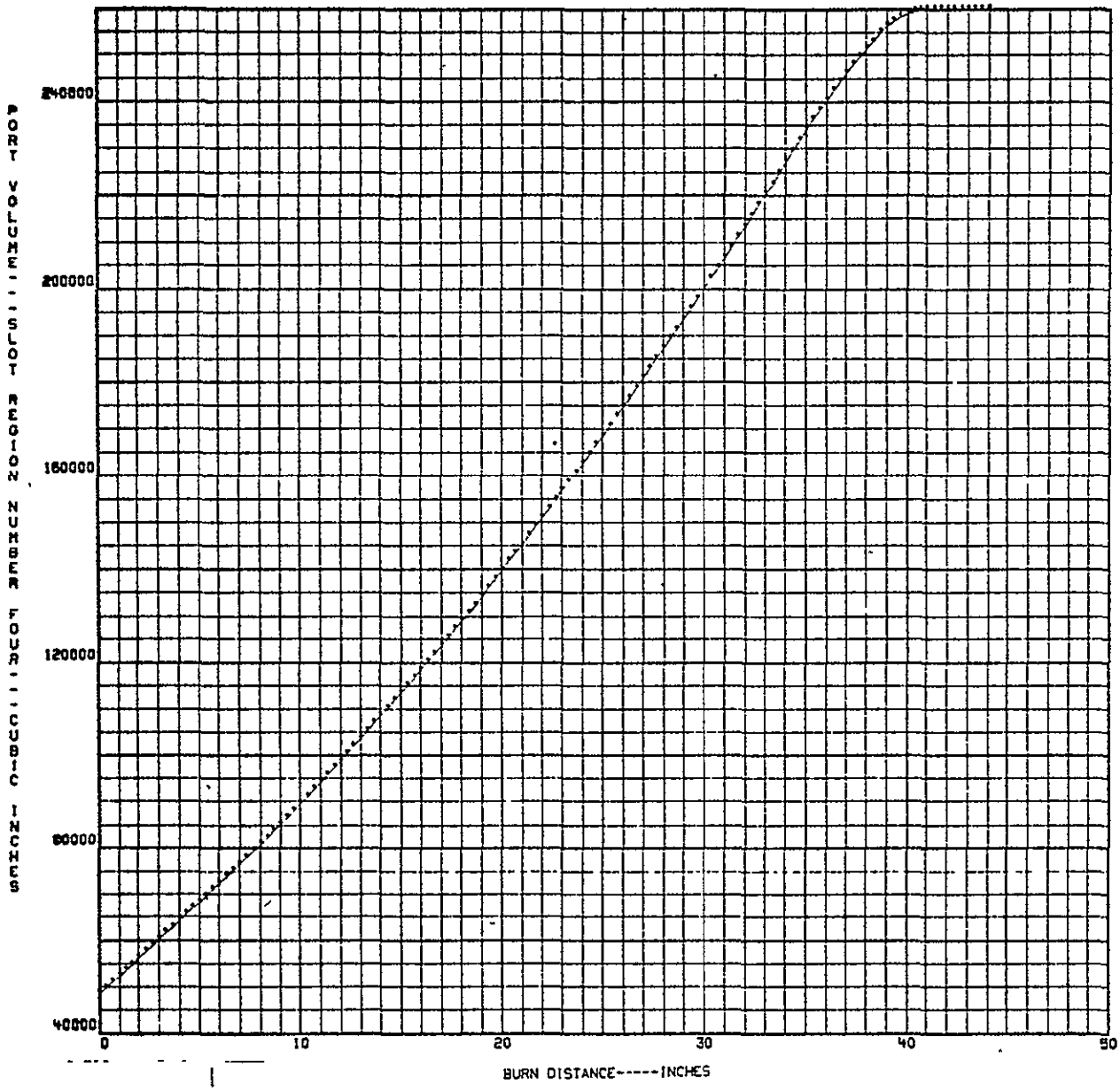

☆U S GOVERNMENT PRINTING OFFICE 1977—740-049/153 REGION NO 4